

Network Coding Design in Wireless Cooperative Networks

Author : Dr. Lili Wei

Advisor : Prof. Wen Chen

Date : January 21, 2012

A dissertation submitted to
Shanghai Jiao Tong University
in partial fulfillment of the requirements for

Chinese PostDoc

Department of Electronic Engineering

Acknowledgment

I would like to express my heartfelt gratitude and appreciation to my Postdoc advisor, Professor Wen Chen, for providing me this great opportunity to continue my research, also the endless encouragement, patience, guidance and research support throughout the postdoc period.

Sincere appreciation goes to all the faculty and staff of Electronic Engineering Department, Shanghai Jiao Tong University (SJTU) for all kinds of academic and administrative helps. As an SJTU alumna who fulfills Bachelor, Master and now Postdoc, I have an abiding love of SJTU for providing first-class education, cutting-edge scientific research and personality nurturing.

My colleagues in Network Coding and Transmission Lab, Haibing Wan, Yang Yu, Chunshu Li, Kun Xie, Xiang Ren, Hai Liu, Xiaoyan Zhou, Sha Wei, Hongying Tang, Feng Wang, Yong Liu and Qingqing Wu, etc, have always been a source of inspiration and support. Their professional stimulation and friendship are cherished.

Finally, I want to express my deepest thanks to my parents, my husband and even my cute baby son for their love, encouragement and invaluable spiritual support that helped me overcome any difficulties through all the years.

Contents

Acknowledgment	i
Abbreviations	v
List of Figures	vii
List of Tables	viii
Abstract	ix
1 Introduction	1
1.1 Research Background	1
1.2 Research Contents of Each Chapter	2
2 Compute-and-Forward Network Coding Design over Multi-Source Multi-Relay Channels	5
2.1 Multi-Source Multi-Relay Channel	5
2.1.1 System Model	5
2.1.2 Compute-and-Forward Scheme	7
2.1.3 Problem Statement	9
2.2 Proposed Strategy	11
2.2.1 Searching Candidate Set Ω_m^{Tmax} for Each Relay	11
2.2.2 Constructing Network Coding Matrix A	18
2.3 Experimental Studies	22
2.3.1 A Transparent Realization	22

2.3.2	Simulation Results	24
2.4	Conclusion	28
3	Efficient Compute-and-Forward Network Codes Search for Two-Way Relay Channel	29
3.1	System Model	29
3.2	Optimal Network Codes Search for TWRC	32
3.2.1	Formulation	32
3.2.2	Searching Algorithm Derivation	34
3.2.3	Optimal Network Codes Search Algorithm for TWRC	35
3.3	Experimental Studies	36
3.4	Conclusions	39
4	Integer-Forcing Linear Receiver Design with Slowest Descent Method	40
4.1	System Model	40
4.2	Integer Forcing Linear Receiver Design	45
4.2.1	Candidate Set Searching Algorithm with Slowest Descent Method	45
4.2.2	Constructing IF Coefficient Matrix \mathbf{A}_{IF}	51
4.3	Experimental Studies	52
4.4	Conclusion	56
4.5	Appendix	58
5	Network Coding in Wireless Cooperative Networks with Multiple Antenna Relays	60
5.1	System Model A: Two Sources Without Direct Links	60
5.1.1	Different Schemes for System Model A	62
5.1.2	Experimental Studies	66
5.2	System Model B: Two Sources With Direct Links	67
5.2.1	Different Schemes for System Model B	67
5.2.2	Experimental Studies	72
5.3	System Model C: Three Sources with Direct Links	73

5.3.1	Different Schemes for System Model C	74
5.3.2	Experimental Studies	81
5.4	System Model D: Four Sources with Direct Links	81
5.4.1	Different Schemes for System Model D	82
5.4.2	Experimental Studies	94
5.5	Conclusions	96
	Bibliography	99
	Publications During Postdoc in SJTU	107
	Research Projects and Patents Information	109

Abbreviations

NC	Network Coding
PLNC	Physical-Layer Network Coding
TWRC	Two Way Relay Channel
MARC	Multiple Access Relay Channel
MSMR	Multiple-Source Multiple-Relay
DT	Direct Transmission
DF	Decode-and-Forward
STDF	Space-Time Decode-and-Forward
ANC	Analog Network Coding
STANC	Space-Time Analog Network Coding
DNC	Digital Network Coding
CPF	Compute-and-forward
IF	Integer Forcing
SDM	Slowest Descent Method
ZF	Zero-Forcing
MMSE	Minimum Mean Square Error
ML	Maximum-Likelihood
FP	Fincke-Pohst

List of Figures

2.1	MSMR model	6
2.2	Time division allocation for one transmission realization	6
2.3	Compute-and-Forward Diagram	9
2.4	Candidate sets and rate tables for all relays	19
2.5	Constructing network coding system matrix \mathbf{A}	20
2.6	Probability of rank failure with local optimization for MSMR	25
2.7	Rate comparisons with $L = 3$ for MSMR	26
2.8	Rate comparisons with $L = 4$ for MSMR	27
3.1	TWRC Model	29
3.2	TWRC Diagram	30
3.3	Probability of zero entry in TWRC	37
3.4	Average rate comparisons for TWRC	38
4.1	MIMO diagram with independent data streams	41
4.2	IF decoder diagram	43
4.3	Creation of one slowest ascent line	46
4.4	The procedure of slowest descent method	47
4.5	IF performance regarding J ($L=8, M=2$)	53
4.6	Probability of successful IF matrix construction regarding J ($L=8, M=2$)	54
4.7	IF performance regarding M ($L=8, J=4$)	55
4.8	Rate comparisons of different linear detectors ($L=4, J=2, M=2$)	56
4.9	Rate comparisons of different linear detectors ($L=6, J=3, M=2$)	57
4.10	Rate comparisons of different linear detectors ($L=8, J=4, M=2$)	58

5.1	System model A	61
5.2	Comparison of four schemes regarding system model A	66
5.3	System model B	67
5.4	Comparison of four schemes regarding system model B	73
5.5	System model C	74
5.6	Sum rate comparison for different schemes regarding system model C . .	82
5.7	BER comparison for different schemes regarding system model C	83
5.8	System Model D	84
5.9	The equivalent two separate MARC with two sources for DF	88
5.10	The equivalent two separate MARC with two sources for DNC	90
5.11	Comparison of five schemes regarding system model D, $\sigma_f^2 = \sigma_h^2 = \sigma_g^2 = 1$	95
5.12	Comparison of five schemes regarding system model D: $\sigma_f^2 = 0.1, \sigma_h^2 =$ $\sigma_g^2 = 1,$	96
5.13	Comparison of five schemes regarding system model D: $\sigma_h^2 = 0.1, \sigma_f^2 =$ $\sigma_g^2 = 1$	97

List of Tables

3.1	Average number of candidate vectors for TWRC	39
5.1	Different Schemes for System Model A	65
5.2	$x_1 \oplus x_2$ for BPSK modulation	70
5.3	Different Schemes for System Model B	72
5.4	Different Schemes for System Model C	81
5.5	Different Schemes for System Model D	94

Abstract

The objective of this work is to investigate network coding design in wireless cooperative networks. Along this line, our work can be divided into following subjects: *(i)* Compute-and-forward strategy is one category of network coding in which a relay will decode and forward a linear combination of source messages according to the observed channel coefficients, based on the algebraic structure of lattice codes. The destination will recover all transmitted messages if enough linear equations are received. For multi-source multi-relay wireless cooperative channels, we design in a system level, the compute-and-forward network coding coefficients by Fincke-Pohst based candidate set searching algorithm and network coding system matrix constructing algorithm, such that by those proposed algorithms, the transmission rate of the multi-source multi-relay system is maximized. Numerical results demonstrate the effectiveness of our proposed algorithms. *(ii)* We consider the two-way relay channel (TWRC) of wireless cooperative system with compute-and-forward network coding strategy. First a new lemma is proposed as network codes search criteria for TWRC. Then, instead of exhaustive search, we present an efficient network codes search algorithm based on modified Fincke-Pohst method. Numerical results demonstrate the effectiveness and complexity reduction of our proposed lemma and algorithm. *(iii)* Based on the idea of compute-and-forward, integer forcing (IF) linear receiver architecture is for MIMO system to recover different integer combinations of lattice codewords for further original message detection. In our work, we consider the problem of IF linear receiver design with respect to the channel conditions. We present practical and efficient algorithms to design the IF coefficient matrix with full rank such that the total achievable rate is maximized, based on the slowest descent method. Numerical results demonstrate the effectiveness of our proposed algorithms. *(iv)* We consider network cod-

ing application in wireless multiple access relay channels with multiple-antenna relays. We investigate several different relay techniques applicable for different system models, including decode-and-forward (DF), space-time decode-and-forward (STDF), analog network coding (ANC), space-time analog network coding (STANC), digital network coding (DNC), etc. We describe in details those different schemes in different system models with transmission time slots constraints, and compare the error rate performance.

Chapter 1

Introduction

1.1 Research Background

In the past decade, network coding [24] has rapidly emerged as a major research area in electrical engineering and computer science. Originally designed for wired networks, network coding is a generalized routing approach that breaks the traditional assumption of simply forwarding data, and allows intermediate nodes to send out functions of their received packets, by which the multicast capacity given by the max-flow min-cut theorem can be achieved. Subsequent works of [25]-[27] made the important observation that, for multicasting, intermediate nodes can simply send out a linear combination of their received packets. Linear network coding with random coefficients is considered in [28]. In order to address the broadcast nature of wireless transmission, physical layer network coding [29] was proposed to embrace interference in wireless networks in which intermediate nodes attempt to decode the modulo-two sum (XOR) of the transmitted messages. Several network coding realizations in wireless networks are discussed in [31]-[30].

There is also a large body of works on lattice codes [36]-[37] and their applications in communications. For many AWGN networks of interest, nested lattice codes [38] can approach the performance of standard random coding arguments. It has been shown that nested lattice codes (combined with lattice decoding) can achieve the capacity of the point-to-point AWGN channel [39]. Subsequent work of [40] showed that nested lattice codes achieve the diversity-multiplexing tradeoff of MIMO channel. In the two-way relay

networks, a nested lattice based strategy has been developed that the achievable rate is near the optimal upper bound [45]-[47]. The nested lattice codes have the linear structure that ensures that integer combinations of codewords are themselves codewords.

Compute-and-forward (CPF) strategy [48]-[49] is a promising new approach to physical-layer network coding for general wireless networks, beneficial from both network coding and lattice codes. The main idea is that a relay will decode a linear function of transmitted messages according to the observed channel coefficients rather than ignoring the interference as noise. Upon utilizing the algebraic structure of lattice codes, i.e., the integer combination of lattice codewords is still a codeword, the intermediate relay node decodes and forwards an integer combination of original messages. With enough linear independent equations, the destination can recover the original messages respectively. Subsequent works for design and analysis of the CPF technique have been given in [50]-[54].

As a research extension from the idea of CPF strategy, a new linear receiver technique called *integer forcing* (IF) receiver for MIMO system has been proposed in [58]-[59]. In MIMO communication, the destination often utilizes linear receiver architecture to reduce implementation complexity with some performance sacrifice compared with maximum-likelihood (ML) receiver. The standard linear detection methods include zero-forcing (ZF) technique and the minimum mean square error (MMSE) technique [56]. In the newly proposed IF linear receiver, instead of attempting to recover a transmitted codeword directly, each IF decoder recovers a different integer combination of the lattice codewords according to a designed IF coefficient matrix. If the IF coefficient matrix is of full rank, these linear equations can be solved for the original messages.

1.2 Research Contents of Each Chapter

In Chapter 2, we consider multi-source multi-relay channels with CPF network coding. Previous works in CPF only consider the integer network coding coefficients optimization of each relay locally/separately. However, for a multi-source multi-relay system with L sources, separate optimizations cannot guarantee the network coding system matrix,

which is constructed by all the integer network coding coefficient vectors, is of rank L such that the destination can decode all messages. In this work, the compute-and-forward network coding strategy is considered in a system level. First, by our proposed Fincke-Pohst [41] based candidate set searching algorithm, instead of one optimal network coding coefficient vector, for each relay we will provide a network coding vector candidate set with corresponding computation rate in descending order. Then, by our proposed network coding system matrix constructing algorithm, we will try to choose network coding vectors from those candidate sets to construct network coding system matrix with rank L , while in the meantime the transmission rate of the multi-source multi-relay system is maximized. The underlying codes are based on lattice codes whose algebraic structure ensures that integer combinations of messages can be decoded reliably. Results from this line of research have been published in [1].

In Chapter 3, we investigate CPF network coding strategy in the two-way relay channel (TWRC) [34], where two sources exchange information through a relay. First we modify the previous general results in [50]-[52], add the no zero entry constraints and propose a new lemma as network codes search criteria for TWRC. Furthermore, we present in detail an optimal network codes search algorithm for TWRC based on Fincke-Pohst method [41], which returns the same solution as exhaustive search with much lower complexity. The proposed new lemma and algorithm lay a solid foundation for CPF network codes search for TWRC. Results from this line of research have been published in [2].

In Chapter 4, we address the problem of IF linear receiver design with respect to the channel conditions. We present practical and efficient algorithms to design the IF coefficient matrix with full rank such that the total achievable rate is maximized, based on the slowest descent method (SDM) [60]. Slowest descent method is a technique to search for discrete points near the continuous-valued slowest descent/ascent lines from the continuous maximizer/minimizer in the Euclidean vector space. This method has been effectively applied to search for binary signatures with quadratic optimization problems in CDMA systems [6]-[7] and MIMO complex discrete signal detection [61]. In this work, to design the IF coefficient matrix with integer elements, first we will generate feasible

searching set instead of the whole integer searching space based on the slowest descent method. Then we try to pick up integer vectors within our searching set to construct the full rank IF coefficient matrix, while in the meantime, the total achievable rate is maximized. Results from this line of research have been published in [11] [16].

In Chapter 5, we carry out a study on network coding in multiple access relay channels (MARC) with multiple antenna relay with different system model setting-ups. Under the same transmission time slots constraint, we investigate several different relay techniques applicable for different system models, including direct transmission (DT), decode-and-forward (DF), space-time decode-and-forward (STDF), analog network coding (ANC), space-time analog network coding (STANC), digital network coding (DNC), etc. We describe in details those different schemes in different system models with transmission time slots constraints, and compare the error rate performance. Results from this line of research have been published in [13] [14] [17].

The notations used in this work are as follows. $\{\cdot\}^T$ denotes the transpose operation, $|\cdot|$ represents the cardinality of a set, \mathbb{Z}^n denotes the n dimensional integer ring, \mathbb{R}^n denotes the n dimensional real field. \mathbb{F}_p denotes a finite field of size p . \mathbf{I}_n denotes the identity matrix of size $n \times n$, and $\mathbf{0}$ denotes the vectors with all zeros elements. $Re(\cdot)$ and $Im(\cdot)$ denote the real part and the imaginary part. $\partial f / \partial(\mathbf{a})$ denotes the partial derivative of function f regarding vector \mathbf{a} . Assume that the log operation is with respect to base 2. We use boldface lowercase letters to denote column vectors and boldface uppercase letters to denote matrices.

Chapter 2

Compute-and-Forward Network Coding Design over Multi-Source Multi-Relay Channels

2.1 Multi-Source Multi-Relay Channel

2.1.1 System Model

We consider the multi-source multi-relay (MSMR) system model as shown in Fig. 2.1, where L sources $\mathcal{S}_1, \mathcal{S}_2, \dots, \mathcal{S}_L$ are communicating to one destination \mathcal{D} through L relays $\mathcal{R}_1, \mathcal{R}_2, \dots, \mathcal{R}_L$. Each node is equipped with a single antenna and works in half-duplex mode. There are no direct links from sources to the destination.

The information transmission, which we call one transmission realization, is performed in two phases. The first phase is for the transmissions from all sources $\mathcal{S}_1, \mathcal{S}_2, \dots, \mathcal{S}_L$ to the relays $\mathcal{R}_1, \mathcal{R}_2, \dots, \mathcal{R}_L$. Each relay will receive signals from all sources due to the wireless medium. In the second phase, assume each relay has a point-to-point AWGN channel or orthogonal access to the destination, for example, in different time slots as shown in Fig. 2.2. Every relay will obtain a linear combination of original messages and forward towards the destination by orthogonal channels. With enough linear combinations, the destination is able to recover the desired original messages from all sources.

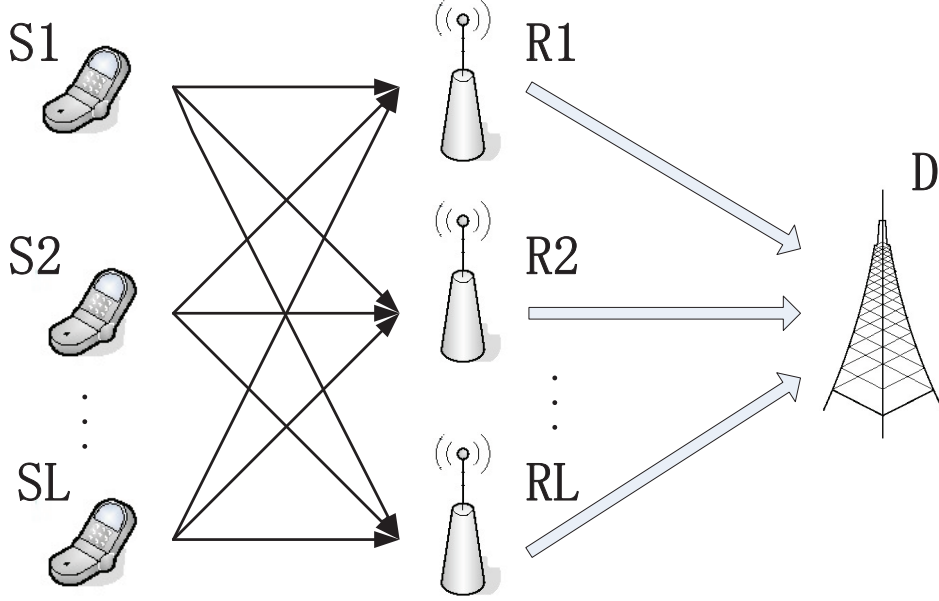


Fig. 2.1: MSMR model

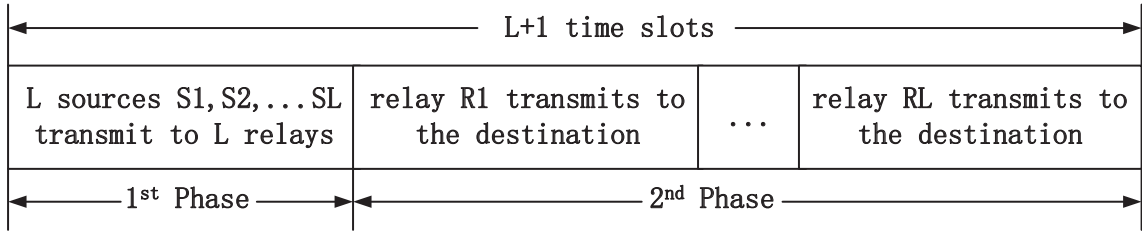


Fig. 2.2: Time division allocation for one transmission realization

Without loss of generality, in one transmission realization, each source has a length- k message vector that is drawn independently and uniformly over a prime size finite field,

$$\mathbf{w}_l \in \mathbb{F}_p^k, \quad l = 1, 2, \dots, L, \quad (2.1)$$

where \mathbb{F}_p denotes the finite field with a set of p elements. Each source is equipped with an encoder

$$\Psi_l : \mathbb{F}_p^k \rightarrow \mathbb{R}^n \quad (2.2)$$

that maps the length- k message \mathbf{w}_l into a length- n real valued lattice codeword $\mathbf{x}_l = \Psi_l(\mathbf{w}_l)$. The lattice codeword \mathbf{x}_l must satisfy the power constraint,

$$\frac{1}{n} \|\mathbf{x}_l\|^2 \leq P \quad (2.3)$$

for $P \geq 0$ and $l = 1, 2, \dots, L$. The message rate, defined as the length of the message measured in bits normalized by the number of channel uses $R = \frac{k}{n} \log p$ [48], is the same for all sources.

After mapping its message $\mathbf{w}_l \in \mathbb{F}_p^k$ into a lattice codeword $\mathbf{x}_l \in \mathbb{R}^n$, the source \mathcal{S}_l will send the codeword \mathbf{x}_l across the channel. Due to the broadcast nature of wireless medium, the m -th relay will observe a noisy combination of the transmitted signals at the end of the first phase,

$$\mathbf{y}_m = \sum_{l=1}^L h_{ml} \mathbf{x}_l + \mathbf{z}_m, \quad m = 1, 2, \dots, L, \quad (2.4)$$

where $h_{ml} \in \mathbb{R}$ denotes real valued fading channel coefficient from \mathcal{S}_l to relay \mathcal{R}_m , generated i.i.d. according to a normal distribution $\mathcal{N}(0, 1)$; $\mathbf{z}_m \in \mathbb{R}^n$ denotes additive Gaussian noise vector, $\mathbf{z}_m \sim \mathcal{N}(\mathbf{0}, \mathbf{I}_n)$. Let

$$\mathbf{h}_m = [h_{m1}, \dots, h_{mL}]^T \quad (2.5)$$

denote the vector of channel coefficients from all sources to the m -th relay. We assume this channel state information \mathbf{h}_m is available at relay m .

2.1.2 Compute-and-Forward Scheme

In a recent work, Nazer and Gastpar propose the *compute-and-forward* approach [48] which exploits the property that any integer combination of lattice points is again a lattice point. After receiving the noisy vector \mathbf{y}_m of (2.4), the m -th relay will first select a scalar $\beta_m \in \mathbb{R}$ and an integer network coding coefficient vector

$$\mathbf{a}_m = [a_{m1}, a_{m2}, \dots, a_{mL}]^T \in \mathbb{Z}^L, \quad (2.6)$$

then attempt to decode the lattice point $\sum_{l=1}^L a_{ml} \mathbf{x}_l$ from

$$\beta_m \mathbf{y}_m = \sum_{l=1}^L \beta_m h_{ml} \mathbf{x}_l + \beta_m \mathbf{z}_m \quad (2.7)$$

$$= \sum_{l=1}^L a_{ml} \mathbf{x}_l + \underbrace{\sum_{l=1}^L (\beta_m h_{ml} - a_{ml}) \mathbf{x}_l + \beta_m \mathbf{z}_m}_{\text{Effective Noise}}. \quad (2.8)$$

Note that we do not need to conduct joint maximum likelihood (ML) decoding to get $(\hat{\mathbf{x}}_1, \hat{\mathbf{x}}_2, \dots, \hat{\mathbf{x}}_L)$ for network coding. Instead we decode $\sum_{l=1}^L a_{ml}\mathbf{x}_l$ as one regular codeword due to the lattice algebraic structure. In other words, the network coded codeword is still in the same field as original source codeword.

In the finite field, it is equivalent that each relay is desired to reliably recover a linear combination of the messages,

$$\mathbf{u}_m = \bigoplus_{l=1}^L q_{ml}\mathbf{w}_l = \left[\sum_{l=1}^L a_{ml}\mathbf{w}_l \right] \text{ mod } p, \quad (2.9)$$

where \bigoplus denotes summation over the finite field, q_{ml} is a coefficient taking values in \mathbb{F}_p and $q_{ml} = a_{ml} \text{ mod } p$.

Each relay is equipped with a decoder,

$$\Pi_m : \mathbb{R}^n \rightarrow \mathbb{F}_p^k, \quad (2.10)$$

that maps the observed channel output $\mathbf{y}_m \in \mathbb{R}^n$ to an estimate

$$\hat{\mathbf{u}}_m = \Pi_m(\mathbf{y}_m) \in \mathbb{F}_p^k \quad (2.11)$$

of the message combination \mathbf{u}_m . The diagram of compute-and-forward scheme is given in Fig. 2.3.

We are interested in the rate of $\sum_{l=1}^L a_{ml}\mathbf{x}_l$ as a whole and will capture the performance of the computation scheme by what we refer to as the *computation rate*, namely, the number of bits of the linear function successfully recovered per channel use. The work of [48] shows that a relay can often recover an equation of messages at a higher rate than any individual message (or subset of message). The rate is highest when the equation coefficients closely approximate the effective channel coefficients. The formal statements are given in the following theorems [48]-[50]. Let $\log^+(x) \triangleq \max(\log(x), 0)$.

Theorem 2.1.1 *For real-valued AWGN networks with channel coefficient vector $\mathbf{h}_m \in \mathbb{R}^L$ and desired network coding coefficient vector $\mathbf{a}_m \in \mathbb{Z}^L$, the following computation rate is achievable*

$$\mathcal{R}_m(\mathbf{a}_m) = \max_{\beta_m \in \mathbb{R}} \frac{1}{2} \log^+ \left(\frac{P}{\beta_m^2 + P \|\beta_m \mathbf{h}_m - \mathbf{a}_m\|^2} \right). \quad (2.12)$$

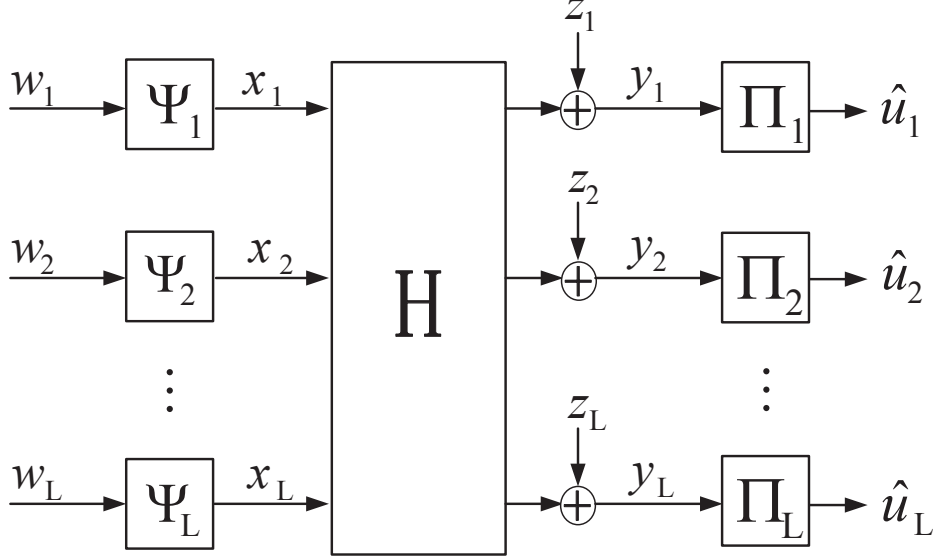


Fig. 2.3: Compute-and-Forward Diagram

Theorem 2.1.2 *The computation rate given in Theorem 2.1.1 is uniquely maximized by choosing β_m to be the MMSE coefficient*

$$\beta_{MMSE} = \frac{P \mathbf{h}_m^T \mathbf{a}_m}{1 + P \|\mathbf{h}_m\|^2}, \quad (2.13)$$

which results in a computation rate of

$$\mathcal{R}_m(\mathbf{a}_m) = \frac{1}{2} \log^+ \left(\|\mathbf{a}_m\|^2 - \frac{P(\mathbf{h}_m^T \mathbf{a}_m)^2}{1 + P \|\mathbf{h}_m\|^2} \right)^{-1}. \quad (2.14)$$

Theorem 2.1.3 *For a given channel coefficient vector $\mathbf{h}_m = [h_{m1}, h_{m2}, \dots, h_{mL}]^T \in \mathbb{R}^L$, $\mathcal{R}_m(\mathbf{a}_m)$ is maximized by choosing the integer network coding coefficient vector $\mathbf{a}_m \in \mathbb{Z}^L$ as*

$$\mathbf{a}_m = \arg \min_{\mathbf{a}_m \in \mathbb{Z}^L, \mathbf{a}_m \neq \mathbf{0}} (\mathbf{a}_m^T \mathbf{G}_m \mathbf{a}_m), \quad (2.15)$$

where

$$\mathbf{G}_m \triangleq \mathbf{I} - \frac{P}{1 + P \|\mathbf{h}_m\|^2} \mathbf{H}_m, \quad (2.16)$$

and $\mathbf{H}_m = [H_{ij}^{(m)}]$, $H_{ij}^{(m)} = h_{mi} h_{mj}$, $1 \leq i, j \leq L$.

2.1.3 Problem Statement

Theorems 2.1.1-2.1.3 only give the optimal network coding integer coefficient vector \mathbf{a}_m and achievable computation rate \mathcal{R}_m for each relay locally/separately and do not take

consideration of the overall system constraints. For the multi-source multi-relay system, at the destination, enough linear combinations of the original messages need to be collected. Let $\mathbf{a}_1, \mathbf{a}_2, \dots, \mathbf{a}_L$ be the integer network coding coefficients vector for each relay, then the network coding system matrix \mathbf{A} at the destination can be denoted as

$$\mathbf{A} = [\mathbf{a}_1, \mathbf{a}_2, \dots, \mathbf{a}_L]^T. \quad (2.17)$$

Hence, the destination can solve for the original packets if the network coding system matrix \mathbf{A} has full rank L , i.e. $|\mathbf{A}| \neq 0$. In which case, as the same rate of source-relay channels in phase I is available for relay-destination channels in phase II, the transmission rate at the destination is dominated/bottlenecked by

$$\mathcal{R}_D = \min \{\mathcal{R}_1, \mathcal{R}_2, \dots, \mathcal{R}_L\}. \quad (2.18)$$

We can easily understand that after calculating the integer network coding coefficient vector \mathbf{a}_m for each relay by theorems 2.1.1-2.1.3 to maximize its own computation rate, the network coding system matrix \mathbf{A} constructed by those integer vectors may not have full rank L , in which case the destination cannot decode the original messages by those linear equations. In other words, we cannot fix the optimal integer network coding vector \mathbf{a}_m for each relay separately, since it cannot guarantee that the system constraint of full rank \mathbf{A} .

Therefore, we need to optimize the integer network coding vectors for L relays in a overall system level. Instead of distributed calculations, to construct the full rank network coding system matrix that maximize the overall message rate at destination, \mathbf{A} will be designed according to the following criteria

$$\begin{aligned} \mathbf{A} &= \arg \max_{|\mathbf{A}| \neq 0} \mathcal{R}_D \\ &= \arg \max_{|\mathbf{A}| \neq 0} (\min \{\mathcal{R}_1, \mathcal{R}_2, \dots, \mathcal{R}_L\}) \\ &= \arg \max_{|\mathbf{A}| \neq 0} \min_{m=1, \dots, L} \left(\frac{1}{2} \log^+ \left(\|\mathbf{a}_m\|^2 - \frac{P(\mathbf{h}_m^T \mathbf{a}_m)^2}{1 + P\|\mathbf{h}_m\|^2} \right)^{-1} \right). \end{aligned} \quad (2.19)$$

In other words, we need to find the integer network coding vectors $\mathbf{a}_1, \mathbf{a}_2, \dots, \mathbf{a}_L$, under

the system level constraint of full rank \mathbf{A} , to maximize the computation rate of each relay $\mathcal{R}_1, \mathcal{R}_2, \dots, \mathcal{R}_L$ jointly, such that the minimum value of $\mathcal{R}_1, \mathcal{R}_2, \dots, \mathcal{R}_L$ is maximized.

Equivalently, the optimum network coding system matrix \mathbf{A} should be

$$\mathbf{A} = \arg \min_{|\mathbf{A}| \neq 0} \max_{m=1, \dots, L} \mathbf{a}_m^T \mathbf{G}_m \mathbf{a}_m, \quad (2.20)$$

where \mathbf{G}_m is defined in (2.16).

2.2 Proposed Strategy

In this work, to approach the overall system optimization of (2.19)-(2.20), we propose the following novel strategy which includes two steps. In the first step, for relay m , instead of finding one optimal network coding coefficient vector \mathbf{a}_m to maximize its own computation rate, we are trying to find a candidate set

$$\Omega_m^{T_{max}} = \{\mathbf{a}_m^{(1)}, \mathbf{a}_m^{(2)}, \dots, \mathbf{a}_m^{(T_{max})}\}, \quad (2.21)$$

with $|\Omega_m^{T_{max}}| = T_{max}$. The network coding coefficient vectors with the top T_{max} maximum computation rates for relay m are within the candidate set $\Omega_m^{T_{max}}$. Note that T_{max} is a parameter to control the candidate set length for each relay and currently set by experience/simulation. We will propose an algorithm based on Fincke-Pohst Method [41] to find the network coding coefficient vector candidate set for each relay.

After we get all the candidate vector sets $\Omega_1^{T_{max}}, \Omega_2^{T_{max}}, \dots, \Omega_L^{T_{max}}$, in the second step, we will try to pick up $\mathbf{a}_1 \in \Omega_1^{T_{max}}, \mathbf{a}_2 \in \Omega_2^{T_{max}}, \dots, \mathbf{a}_L \in \Omega_L^{T_{max}}$, to construct the full rank network coding coefficient matrix $\mathbf{A} = [\mathbf{a}_1, \mathbf{a}_2, \dots, \mathbf{a}_L]^T$, while in the meantime, the minimum value of corresponding $\mathcal{R}_1(\mathbf{a}_1), \mathcal{R}_2(\mathbf{a}_2), \dots, \mathcal{R}_L(\mathbf{a}_L)$ is maximized.

2.2.1 Searching Candidate Set $\Omega_m^{T_{max}}$ for Each Relay

For relay m , we are trying to find the candidate set $\Omega_m^{T_{max}} = \{\mathbf{a}_m^{(1)}, \mathbf{a}_m^{(2)}, \dots, \mathbf{a}_m^{(T_{max})}\}$ with $|\Omega_m^{T_{max}}| = T_{max}$, such that the network coding coefficient vectors with the top T_{max} maximum computation rate for relay m are within. According to Theorem 2.1.3, it is

equivalent to find the set $\Omega_m^{T_{max}}$ with T_{max} vectors, such that those vectors give the bottom T_{max} minimum $\mathbf{a}_m^T \mathbf{G}_m \mathbf{a}_m$ values, where \mathbf{G}_m is defined in (2.16).

The searching of candidate set Ω_m^{max} with fixed length T_{max} can be decomposed into following steps.

- (1) Enumerate all vectors $\mathbf{t} \in \mathbb{Z}^L$ ($\mathbf{t} \neq \mathbf{0}$) in Ω_m , such that $\mathbf{t}^T \mathbf{G}_m \mathbf{t} \leq C$ for a given positive constant C , i.e.,

$$\Omega_m = \{\mathbf{t} : \mathbf{t}^T \mathbf{G}_m \mathbf{t} \leq C, \mathbf{t} \neq \mathbf{0}, \mathbf{t} \in \mathbb{Z}^L\}. \quad (2.22)$$

- (2) Adjust the constant C to guarantee that $|\Omega_m| \geq T_{max}$.
- (3) Sort all the vectors $\mathbf{t}_1, \mathbf{t}_2, \dots, \mathbf{t}_{|\Omega_m|}$ in Ω_m in descending order corresponding to the computation rate value \mathcal{R}_m in (2.14), such that

$$\mathcal{R}_m(\mathbf{t}_1) \geq \mathcal{R}_m(\mathbf{t}_2) \geq \dots \geq \mathcal{R}_m(\mathbf{t}_{|\Omega_m|}). \quad (2.23)$$

- (4) Pick the first T_{max} vectors of Ω_m to form the set $\Omega_m^{T_{max}}$.

The procedure of enumerating all vectors $\mathbf{t} \in \mathbb{Z}^L$ ($\mathbf{t} \neq \mathbf{0}$) in Ω_m , such that $\mathbf{t}^T \mathbf{G}_m \mathbf{t} \leq C$ for a given positive constant C is based on the Fincke-Pohst Method and derived as follows.

We operate Cholesky's factorization of matrix \mathbf{G}_m ,

$$\mathbf{G}_m = \mathbf{U}^T \mathbf{U}, \quad (2.24)$$

where \mathbf{U} is an upper triangular matrix. Denote $\|\cdot\|_F$ for the Frobenius norm. Let u_{ij} , $i, j = 1, 2, \dots, L$, be the entries of the upper triangular matrix \mathbf{U} and

$$\mathbf{t} = [t_1, t_2, \dots, t_L]^T. \quad (2.25)$$

Then, the searching vector \mathbf{t} that makes $\mathbf{t}^T \mathbf{G}_m \mathbf{t} \leq C$ can be expressed as

$$\begin{aligned}
\mathbf{t}^T \mathbf{G}_m \mathbf{t} &= \|\mathbf{U} \mathbf{t}\|_F^2 = \sum_{i=1}^L \left(u_{ii} t_i + \sum_{j=i+1}^L u_{ij} t_j \right)^2 \\
&= \sum_{i=1}^L g_{ii} \left(t_i + \sum_{j=i+1}^L g_{ij} t_j \right)^2 \\
&= \sum_{i=k}^L g_{ii} \left(t_i + \sum_{j=i+1}^L g_{ij} t_j \right)^2 + \sum_{i=1}^{k-1} g_{ii} \left(t_i + \sum_{j=i+1}^L g_{ij} t_j \right)^2 \\
&\leq C
\end{aligned} \tag{2.26}$$

where $g_{ii} = u_{ii}^2$ and $g_{ij} = u_{ij}/u_{ii}$ for $i = 1, 2, \dots, L$, $j = i + 1, \dots, L$. Obviously the second term of (2.26) is non-negative, hence, to satisfy (2.26), it is equivalent to consider for every $k = L, L - 1, \dots, 1$,

$$\sum_{i=k}^L g_{ii} \left(t_i + \sum_{j=i+1}^L g_{ij} t_j \right)^2 \leq C. \tag{2.27}$$

Then, we can start work backwards to find the bounds for vector entries t_L, t_{L-1}, \dots, t_1 one by one.

We begin to evaluate the last element t_L of the searching vector \mathbf{t} . Referring to (2.27) and let $k = L$, we have

$$g_{LL} t_L^2 \leq C. \tag{2.28}$$

Set $\Delta_L = 0$, $C_L = C$, and we will get

$$LB_L \leq t_L \leq UB_L, \tag{2.29}$$

with

$$UB_L = \left\lceil \sqrt{\frac{C_L}{g_{LL}}} - \Delta_L \right\rceil, LB_L = \left\lfloor -\sqrt{\frac{C_L}{g_{LL}}} - \Delta_L \right\rfloor, \tag{2.30}$$

where $\lceil x \rceil$ is the smallest integer no less than x and $\lfloor x \rfloor$ is the greatest integer no bigger than x .

Next, we evaluate the element t_{L-1} of the searching vector \mathbf{t} . Referring to (2.27) and let $k = L - 1$, we have

$$g_{LL} t_L^2 + g_{L-1,L-1} (t_{L-1} + g_{L-1,L} t_L)^2 \leq C, \tag{2.31}$$

which leads to

$$\left[-\sqrt{\frac{C - g_{LL}t_L^2}{g_{L-1,L-1}}} - g_{L-1,L}t_L \right] \leq t_{L-1} \leq \left[\sqrt{\frac{C - g_{LL}t_L^2}{g_{L-1,L-1}}} - g_{L-1,L}t_L \right]. \quad (2.32)$$

If we denote $\Delta_{L-1} = g_{L-1,L}t_L$, $C_{L-1} = C - g_{LL}t_L^2$, the bounds for s_{L-1} can be expressed as

$$LB_{L-1} \leq t_{L-1} \leq UB_{L-1}, \quad (2.33)$$

where

$$UB_{L-1} = \left[\sqrt{\frac{C_{L-1}}{g_{L-1,L-1}}} - \Delta_{L-1} \right], LB_{L-1} = \left[-\sqrt{\frac{C_{L-1}}{g_{L-1,L-1}}} - \Delta_{L-1} \right]. \quad (2.34)$$

We can see that given radius \sqrt{C} and matrix \mathbf{U} , the bounds for t_{L-1} only depends on the previous evaluated t_L , and not correlated with $t_{L-2}, t_{L-3}, \dots, t_1$.

In a similar fashion, we can proceed for t_{L-2} evaluation, and so on.

To evaluate the element t_k of the searching vector \mathbf{t} , referring to (2.27) we will have

$$\sum_{i=k}^L g_{ii} \left(t_i + \sum_{j=i+1}^L g_{ij}t_j \right)^2 \leq C, \quad (2.35)$$

which leads to

$$\begin{aligned} & \left[-\sqrt{\frac{1}{g_{kk}} \left(C - \sum_{i=k+1}^L g_{ii} \left(t_i + \sum_{j=i+1}^L g_{ij}t_j \right)^2 \right)} - \sum_{j=k+1}^L g_{kj}t_j \right] \\ & \leq t_k \leq \left[\sqrt{\frac{1}{g_{kk}} \left(C - \sum_{i=k+1}^L g_{ii} \left(t_i + \sum_{j=i+1}^L g_{ij}t_j \right)^2 \right)} - \sum_{j=k+1}^L g_{kj}t_j \right]. \end{aligned}$$

If we denote

$$\begin{aligned} \Delta_k &= \sum_{j=k+1}^L g_{kj}t_j, \\ C_k &= C - \sum_{i=k+1}^L g_{ii} \left(t_i + \sum_{j=i+1}^L g_{ij}t_j \right)^2, \end{aligned} \quad (2.36)$$

the bounds for s_k can be expressed as

$$LB_k \leq t_k \leq UB_k, \quad (2.37)$$

where

$$UB_k = \left[\sqrt{\frac{C_k}{g_{kk}}} - \Delta_k \right], LB_k = \left[-\sqrt{\frac{C_k}{g_{kk}}} - \Delta_k \right]. \quad (2.38)$$

Note that for given radius \sqrt{C} and matrix \mathbf{U} , the bounds for t_k only depends on the previous evaluated $t_{k+1}, t_{k+2}, \dots, t_L$.

Finally, we evaluate the element t_1 of the searching vector \mathbf{t} . Referring to (2.27) and let $k = 1$, we will have

$$\sum_{i=1}^L g_{ii} \left(t_i + \sum_{j=i+1}^L g_{ij} t_j \right)^2 \leq C, \quad (2.39)$$

which leads to

$$\begin{aligned} & \left[-\sqrt{\frac{1}{g_{11}} \left(C - \sum_{i=2}^L g_{ii} \left(t_i + \sum_{j=i+1}^L g_{ij} t_j \right)^2 \right)} - \sum_{j=2}^L g_{1j} t_j \right] \\ \leq t_1 & \leq \left[\sqrt{\frac{1}{g_{11}} \left(C - \sum_{i=2}^L g_{ii} \left(t_i + \sum_{j=i+1}^L g_{ij} t_j \right)^2 \right)} - \sum_{j=2}^L g_{1j} t_j \right]. \end{aligned} \quad (2.40)$$

If we denote

$$\begin{aligned} \Delta_1 &= \sum_{j=2}^L g_{1j} t_j, \\ C_1 &= C - \sum_{i=2}^L g_{ii} \left(t_i + \sum_{j=i+1}^L g_{ij} t_j \right)^2, \end{aligned} \quad (2.41)$$

the bounds for t_1 can be expressed as

$$LB_1 \leq t_1 \leq UB_1, \quad (2.42)$$

where

$$UB_1 = \left[\sqrt{\frac{C_1}{g_{11}}} - \Delta_1 \right], \quad LB_1 = \left[-\sqrt{\frac{C_1}{g_{11}}} - \Delta_1 \right]. \quad (2.43)$$

In practice, C_L, C_{L-1}, \dots, C_1 can be updated recursively by the following equations

$$\Delta_k = \sum_{j=k+1}^L g_{kj} t_j, \quad (2.44)$$

$$\begin{aligned} C_k &= C - \sum_{i=k+1}^L g_{ii} \left(t_i + \sum_{j=i+1}^L g_{ij} t_j \right)^2 \\ &= C_{k+1} - g_{k+1,k+1} (\Delta_{k+1} + t_{k+1})^2, \end{aligned} \quad (2.45)$$

for $k = L - 1, L - 2, \dots, 1$ and $\Delta_L = 0$, $C_L = C$.

The entries t_L, t_{L-1}, \dots, t_1 are chosen as follows: for a chosen candidate of t_L satisfying the bounds (2.29)-(2.30), we can choose a candidate for t_{L-1} satisfying the bounds (2.33)-(2.34). If a candidate value for t_{L-1} does not exist, we go back to (2.29)-(2.30) and choose other candidate value t_L . Then search for t_{L-1} that meets the bounds (2.33)-(2.34) for the given t_L . If t_L and t_{L-1} are chosen as candidates, we follow the same procedure to choose t_{L-2} , and so on. When a set of t_L, t_{L-1}, \dots, t_1 is chosen and satisfies all corresponding bounds requirements, one candidate vector $\mathbf{t} = [t_1, t_2, \dots, t_L]^T$ is obtained. We record all the candidate vectors satisfying their bounds requirements, such that all vectors meet $\mathbf{t}^T \mathbf{G}_m \mathbf{t} \leq C$ will be in Ω_m .

Regarding the setting of positive constant C , we will set it based on the binary vector obtained by applying the direct sign operator of the real minimum-eigenvalue eigenvector of \mathbf{G}_m , denoted as \mathbf{t}_{quant} , such that

$$C = \mathbf{t}_{quant}^T \mathbf{G}_m \mathbf{t}_{quant}. \quad (2.46)$$

By setting the searching sphere radius this way, it is big enough to have at least one searching vector \mathbf{t}_{quant} falls inside, while in the meantime small enough to have not too many searching vectors within.

Note that this searching procedure will return *all* candidates that satisfy $\mathbf{t}^T \mathbf{G}_m \mathbf{t} \leq C$. There is at least one candidate vector \mathbf{t}_{quant} such that its entries satisfy all the bounds requirements. On the other hand, the maximum likelihood (ML) exhaustive search among all $\mathbf{t} \in \mathbb{Z}^L$, with optimal result \mathbf{t}_{ML} that returns the minimum metric $\mathbf{t}^T \mathbf{G}_m \mathbf{t}$, or equivalently maximum the computation rate for one relay, will also fall inside the search bounds, since

$$\mathbf{t}_{ML}^T \mathbf{G}_m \mathbf{t}_{ML} \leq \mathbf{t}_{quant}^T \mathbf{G}_m \mathbf{t}_{quant} = C. \quad (2.47)$$

Hence, we are guaranteed to include the local optimal network coding coefficient vector, which maximizes the computation rate for one relay m , in Ω_m^{Tmax} .

We summarize our proposed algorithm for the searching candidate set Ω_m^{Tmax} for relay m based on Fincke-Pohst method as follows.

Algorithm 2.1 FP Based Candidate Set Searching Algorithm

Input: Matrix \mathbf{G}_m , $T_{max} = |\Omega_m^{T_{max}}|$.

Output: The candidate vector set $\Omega_m^{T_{max}}$ and corresponding computation rate set $\Gamma_m^{T_{max}}$.

Step 1: Calculate the binary quantized vector obtained by applying the direct sign operator of the real minimum-eigenvalue eigenvector of \mathbf{G}_m , denoted as \mathbf{t}_{quant} , and set C as

$$C = \mathbf{t}_{quant}^T \mathbf{G}_m \mathbf{t}_{quant}. \quad (2.48)$$

Step 2: Operate Cholesky's factorization of matrix \mathbf{G}_m , $\mathbf{G}_m = \mathbf{U}^T \mathbf{U}$, where \mathbf{U} is an upper triangular matrix. Let u_{ij} , $i, j = 1, 2, \dots, L$ denote the entries of matrix \mathbf{U} . Set

$$g_{ii} = u_{ii}^2, \quad g_{ij} = u_{ij}/u_{ii},$$

for $i = 1, 2, \dots, L$, $j = i + 1, \dots, L$.

Step 3: Search set $\Omega_m = \{\mathbf{t} : \mathbf{t}^T \mathbf{G}_m \mathbf{t} \leq C, \mathbf{t} \neq \mathbf{0}, \mathbf{t} \in \mathbb{Z}^L\}$ according to the following Fincke-Pohst procedure.

(i) Start from $\Delta_L = 0$, $C_L = C$, $k = L$ and $\Omega_m = \emptyset$.

(ii) Set the upper bound UB_k and the lower bound LB_k as follows

$$UB_k = \left\lceil \sqrt{\frac{C_k}{g_{kk}}} - \Delta_k \right\rceil, LB_k = \left\lfloor -\sqrt{\frac{C_k}{g_{kk}}} - \Delta_k \right\rfloor,$$

and $t_k = LB_k - 1$.

(iii) Set $t_k = t_k + 1$. For $t_k \leq UB_k$, go to (v); else go to (iv).

(iv) If $k = L$, terminate and output Ω_m ; else set $k = k + 1$ and go to (iii).

(v) For $k = 1$, go to (vi); else set $k = k - 1$, and

$$\begin{aligned} \Delta_k &= \sum_{j=k+1}^L g_{kj} t_j, \\ C_k &= C_{k+1} - g_{k+1,k+1} (\Delta_{k+1} + t_{k+1})^2, \end{aligned}$$

then go to (ii).

(vi) If $\mathbf{t} = \mathbf{0}$ terminate, else we get a candidate vector $\mathbf{t} \neq \mathbf{0}$ that satisfies all the bounds requirements and put it inside Ω_m , i.e. $\Omega_m = \{\Omega_m, \mathbf{t}\}$. Go to (iii).

Step 4: If $|\Omega_m| < T_{max}$, set $C = 2C$ and repeat Step 3.

Step 5: Sort all the vectors $\mathbf{t}_1, \mathbf{t}_2, \dots, \mathbf{t}_{|\Omega_m|}$ in Ω_m in descending order corresponding to the computation rate value \mathcal{R}_m in (2.14), such that

$$\mathcal{R}_m(\mathbf{t}_1) \geq \mathcal{R}_m(\mathbf{t}_2) \geq \dots \geq \mathcal{R}_m(\mathbf{t}_{|\Omega_m|}). \quad (2.49)$$

Pick the first T_{max} vectors of Ω_m to form the set $\Omega_m^{T_{max}}$ and construct the corresponding computation rate $\Gamma_m^{T_{max}}$ as

$$\begin{cases} \Omega_m^{T_{max}} &= \{\mathbf{t}_1, \mathbf{t}_2, \dots, \mathbf{t}_{T_{max}}\}, \\ \Gamma_m^{T_{max}} &= \{\mathcal{R}_m(\mathbf{t}_1), \mathcal{R}_m(\mathbf{t}_2), \dots, \mathcal{R}_m(\mathbf{t}_{T_{max}})\}. \end{cases} \quad (2.50)$$

2.2.2 Constructing Network Coding Matrix A

According to our proposed FP Based Candidate Set $\Omega_m^{T_{max}}$ Searching Algorithm 1, for relay m , we get the candidate set $\Omega_m^{T_{max}}$ for integer network coding coefficient vector \mathbf{a}_m . The set $\Omega_m^{T_{max}}$ consists T_{max} candidates vectors $\Omega_m^{T_{max}} = \{\mathbf{a}_m^{(1)}, \mathbf{a}_m^{(2)}, \dots, \mathbf{a}_m^{(T_{max})}\}$, in which $\mathbf{a}_m^{(1)}, \mathbf{a}_m^{(2)}, \dots, \mathbf{a}_m^{(T_{max})}$ have been sorted such that $\mathcal{R}_m(\mathbf{a}_m^{(1)}) \geq \mathcal{R}_m(\mathbf{a}_m^{(2)}) \geq \dots \geq \mathcal{R}_m(\mathbf{a}_m^{(T_{max})})$. Denote $\mathcal{R}_m^{(i)} = \mathcal{R}_m(\mathbf{a}_m^{(i)})$, $i = 1, 2, \dots, T_{max}$. Then for each relay we can have two length- T_{max} tables as shown in Fig. 2.4,

$$\text{Table 1: } \Gamma_m^{T_{max}} = \{\mathcal{R}_m^{(1)}, \mathcal{R}_m^{(2)}, \dots, \mathcal{R}_m^{(T_{max})}\}, \quad (2.51)$$

$$\text{Table 2: } \Omega_m^{T_{max}} = \{\mathbf{a}_m^{(1)}, \mathbf{a}_m^{(2)}, \dots, \mathbf{a}_m^{(T_{max})}\}. \quad (2.52)$$

The second table consists the sorted candidate vector set $\Omega_m^{T_{max}}$, while the first one consists the corresponding computation rate set $\Gamma_m^{T_{max}}$ with elements $\mathcal{R}_m^{(1)} \geq \mathcal{R}_m^{(2)} \geq \dots \geq \mathcal{R}_m^{(T_{max})}$.

After we get all the candidate vector sets $\Omega_1^{T_{max}}, \Omega_2^{T_{max}}, \dots, \Omega_L^{T_{max}}$ and computation rate sets $\Gamma_1^{T_{max}}, \Gamma_2^{T_{max}}, \dots, \Gamma_L^{T_{max}}$, we will try to pick up $\mathbf{a}_1 \in \Omega_1^{T_{max}}, \mathbf{a}_2 \in \Omega_2^{T_{max}}, \dots,$

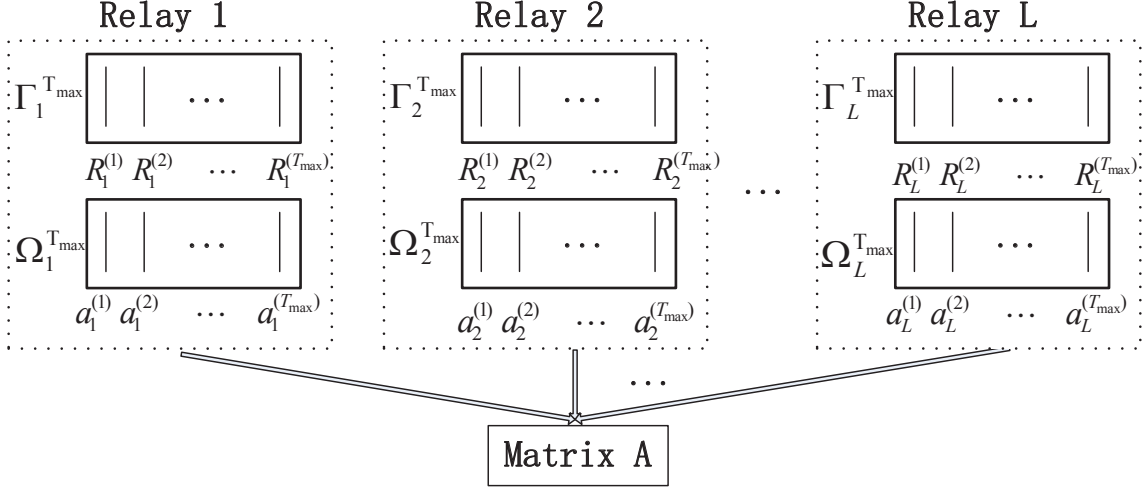


Fig. 2.4: Candidate sets and rate tables for all relays

$\mathbf{a}_L \in \Omega_L^{T_{max}}$, to construct the network coding system matrix $\mathbf{A} = [\mathbf{a}_1, \mathbf{a}_2, \dots, \mathbf{a}_L]^T$ with full rank, while at the same time, the minimum corresponding rate $\mathcal{R}_1(\mathbf{a}_1), \mathcal{R}_2(\mathbf{a}_2), \dots, \mathcal{R}_L(\mathbf{a}_L)$ is maximized.

Regarding this problem, first, we will sort the overall computation rate set for all relays $\{\Gamma_1^{T_{max}}, \Gamma_2^{T_{max}}, \dots, \Gamma_L^{T_{max}}\}$ in a descending order into

$$\{\gamma_1, \gamma_2, \dots, \gamma_{L \times T_{max}}\}, \quad (2.53)$$

such that

$$\gamma_1 \geq \gamma_2 \geq \dots \geq \gamma_{L \times T_{max}}. \quad (2.54)$$

Then, starting from the largest possible achievable rate γ_{index} with $index = L$ (the first $L - 1$ rates are obviously not achievable), we will check one by one whether the rate γ_{index} is achievable, which means we can find L vectors $\mathbf{a}_1 \in \Omega_1^{T_{max}}, \mathbf{a}_2 \in \Omega_2^{T_{max}}, \dots, \mathbf{a}_L \in \Omega_L^{T_{max}}$, such that the following two constraints are satisfied:

- (i) The system network coding coefficient matrix \mathbf{A} is of full rank;
- (ii) $\mathcal{R}_1(\mathbf{a}_1), \mathcal{R}_2(\mathbf{a}_2), \dots, \mathcal{R}_L(\mathbf{a}_L)$ all greater or equal to γ_{index} .

If not, we move to the next largest possible achievable rate $\gamma_{index+1}$ and check in the same way, until the first achievable rate is found.

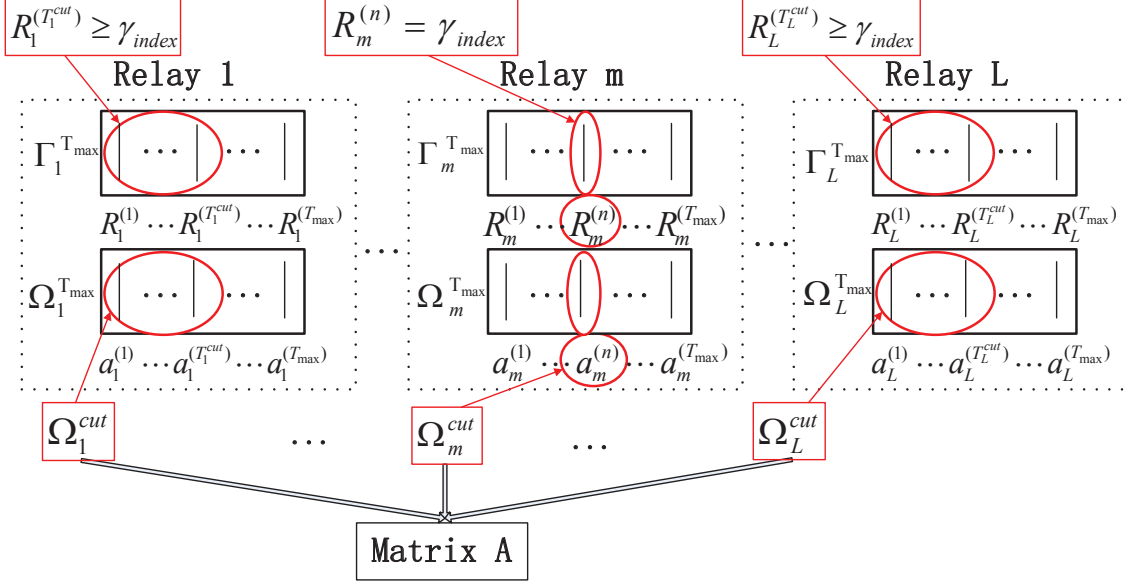


Fig. 2.5: Constructing network coding system matrix \mathbf{A}

When we are checking one possible achievable rate γ_{index} , we will reduce/cut the network coding candidate set $\Omega_m^{T_{max}}$ into Ω_m^{cut} such that any $\mathbf{a}_m \in \Omega_m^{cut}$ will satisfy that $\mathcal{R}_m(\mathbf{a}_m)$ greater or equal to γ_{index} . In other words, the sets of Ω_1^{cut} , Ω_2^{cut} , \dots , Ω_L^{cut} are constructed such that the constraint (ii) will definitely be satisfied if $\mathbf{a}_1 \in \Omega_1^{cut}$, $\mathbf{a}_2 \in \Omega_2^{cut}$, \dots , $\mathbf{a}_L \in \Omega_L^{cut}$.

Suppose $\gamma_{index} = \mathcal{R}_m^{(n)} \in \Gamma_m^{T_{max}}$, i.e. γ_{index} is taken from Table 1 of relay m with table index n , then the network coding vector $\mathbf{a}_m^{(n)}$ is taken from Table 2 with the same index n , i.e. $\mathbf{a}_m^{(n)} \in \Omega_m^{max}$ is fixed for that relay and $\Omega_m^{cut} = \{\mathbf{a}_m^{(n)}\}$. For other relays $i \neq m$, the candidate set will reduce/cut to length T_i^{cut} such that $\mathcal{R}_i^{(1)}$, $\mathcal{R}_i^{(2)}$, \dots , $\mathcal{R}_i^{(T_i^{cut})}$ all greater or equal to γ_{index} .

Denote

$$\Omega_i^{cut} = \{\mathbf{a}_i^{(1)}, \mathbf{a}_i^{(2)}, \dots, \mathbf{a}_i^{(T_i^{cut})}\}. \quad (2.55)$$

We can start to check the constraint (i) of the system network coding matrix \mathbf{A} constructed by any

$$\mathbf{a}_1 \in \Omega_1^{cut}, \mathbf{a}_2 \in \Omega_2^{cut}, \dots, \mathbf{a}_L \in \Omega_L^{cut}. \quad (2.56)$$

If there exists one constructed \mathbf{A} with full rank, then this rate γ_{index} is achievable. The procedure is shown in Fig. 2.5.

We summarize this procedure to constructing the full rank network coding system matrix \mathbf{A} with candidate sets $\Omega_1^{T_{max}}, \Omega_2^{T_{max}}, \dots, \Omega_L^{T_{max}}$ and the corresponding computation rate sets $\Gamma_1^{T_{max}}, \Gamma_2^{T_{max}}, \dots, \Gamma_L^{T_{max}}$ as follows.

Algorithm 2.2 Network Coding System Matrix Constructing Algorithm

Input: Candidate vector sets $\Omega_1^{T_{max}}, \Omega_2^{T_{max}}, \dots, \Omega_L^{T_{max}}$;

Computation rate sets $\Gamma_1^{T_{max}}, \Gamma_2^{T_{max}}, \dots, \Gamma_L^{T_{max}}$.

Output: The network coding system matrix \mathbf{A} constructed from $\mathbf{a}_1 \in \Omega_1^{T_{max}}, \mathbf{a}_2 \in \Omega_2^{T_{max}}, \dots, \mathbf{a}_L \in \Omega_L^{T_{max}}$ with full rank that gives the maximum transmission rate \mathcal{R}_D^{max} .

Step 1: Sort the overall computation rate set for all relays $\{\Gamma_1^{T_{max}}, \Gamma_2^{T_{max}}, \dots, \Gamma_L^{T_{max}}\}$ in a descending order into $\{\gamma_1, \gamma_2, \dots, \gamma_{L \times T_{max}}\}$, such that $\gamma_1 \geq \gamma_2 \geq \dots \geq \gamma_{L \times T_{max}}$. Initialize $index = L$.

Step 2: Check whether the rate of γ_{index} is achievable by the following procedure. Suppose $\gamma_{index} = \mathcal{R}_m^{(n)} \in \Gamma_m^{T_{max}}$. Then, for relay i , the reduced candidate set $\Omega_i^{cut}, i = 1, 2, \dots, L$ will be constructed as follows.

(i) For relay m , set $\Omega_m^{cut} = \{\mathbf{a}_m^{(n)}\}$.

(ii) For relay $i \neq m$, compare the value of γ_{index} and the sorted descending set $\Gamma_i^{T_{max}} = \{\mathcal{R}_i^{(1)}, \mathcal{R}_i^{(2)}, \dots, \mathcal{R}_i^{(T_{max})}\}$. Find all $\{\mathcal{R}_i^{(1)}, \mathcal{R}_i^{(2)}, \dots, \mathcal{R}_i^{(T_i^{cut})}\}$ greater or equal to γ_{index} . Set $\Omega_i^{cut} = \{\mathbf{a}_i^{(1)}, \mathbf{a}_i^{(2)}, \dots, \mathbf{a}_i^{(T_i^{cut})}\}$.

Step 3: Check every $\mathbf{a}_1 \in \Omega_1^{cut}, \mathbf{a}_2 \in \Omega_2^{cut}, \dots, \mathbf{a}_L \in \Omega_L^{cut}$, until we find one network coding system matrix $\mathbf{A} = [\mathbf{a}_1, \mathbf{a}_2, \dots, \mathbf{a}_L]^T$ has full rank, i.e. $|\mathbf{A}| \neq 0$. If so, terminate and output the network coding system matrix \mathbf{A} and the maximum transmission rate $\mathcal{R}_D^{max} = \gamma_{index}$.

Step 4: If for any $\mathbf{a}_1 \in \Omega_1^{cut}, \mathbf{a}_2 \in \Omega_2^{cut}, \dots, \mathbf{a}_L \in \Omega_L^{cut}$, we cannot construct a full rank network coding system matrix \mathbf{A} , then set $index = index + 1$, go to Step 2.

One possible implementation of the whole system will let relays calculate the candi-

date sets and corresponding computation rate sets, construct the optimal network coding system matrix \mathbf{A} , then transmit the $L \times L$ integers matrix \mathbf{A} to the destination. Another possible implementation is to allow the destination work as processing center, that does all calculations, including candidate sets, corresponding computation rate sets, and the optimal network coding system matrix \mathbf{A} construction. The destination will then feedback the optimal network coding vector $\mathbf{a}_m \in \mathbb{Z}^L$ to relay m for $m = 1, 2, \dots, L$. After system initialization, these optimal network coding vectors can be used for the system when the channels are stationary.

2.3 Experimental Studies

2.3.1 A Transparent Realization

In this subsection, we will give a detailed experimental example to show our proposed algorithms in a transparent way. For a three-source three-relay system with $L = 3$, we set the power constraints $P = 10dB$ and $T_{max} = 5$. The channel coefficient vector \mathbf{h}_m for each relay is generated as

$$\begin{aligned}\mathbf{h}_1 &= [0.9730, 0.4674, 0.5103]^T, \\ \mathbf{h}_2 &= [-1.7291, 0.7166, -0.5856]^T, \\ \mathbf{h}_3 &= [-0.3912, 1.4407, -0.8115]^T.\end{aligned}$$

After calculating \mathbf{G}_m , $m = 1, 2, 3$ and running our proposed FP based candidate set searching algorithm for each relay, we will get the network coding candidate vector sets $\Omega_1^{T_{max}}$, $\Omega_2^{T_{max}}$, $\Omega_3^{T_{max}}$ and corresponding computation rate sets $\Gamma_1^{T_{max}}$, $\Gamma_2^{T_{max}}$, $\Gamma_3^{T_{max}}$ as follows

$$\begin{aligned}\Omega_1^{T_{max}} &= \begin{bmatrix} 1 & 2 & 1 & 1 & 1 \\ 0 & 1 & 1 & 0 & 1 \\ 0 & 1 & 1 & 1 & 0 \end{bmatrix}, \\ \Gamma_1^{T_{max}} &= [0.4846, 0.4620, 0.3408, 0.2918, 0.2231];\end{aligned}$$

$$\begin{aligned}\Omega_2^{T_{max}} &= \begin{bmatrix} 1 & 2 & 3 & -1 & -2 \\ 0 & -1 & -1 & 1 & 1 \\ 0 & 1 & 1 & 0 & 0 \end{bmatrix}, \\ \Gamma_2^{T_{max}} &= [0.7087, 0.6785, 0.5572, 0.3625, 0.2694]; \\ \\ \Omega_3^{T_{max}} &= \begin{bmatrix} 0 & 0 & 1 & 0 & 1 \\ -1 & 1 & -2 & -2 & -3 \\ 1 & 0 & 1 & 1 & 2 \end{bmatrix}, \\ \Gamma_3^{T_{max}} &= [0.5987, 0.5935, 0.4384, 0.4165, 0.2902].\end{aligned}$$

We can see that the computation rate set $\Gamma_m^{T_{max}}$, $m = 1, 2, 3$ has elements sorted in descending order where the first element is the maximum computation rate for relay m . The n -th column in $\Omega_m^{T_{max}}$ is a candidate network coding vector $\mathbf{a}_m^{(n)}$ for relay m , while the corresponding computation rate is the n -th element in $\Gamma_m^{T_{max}}$. Note that if we optimize the network coding coefficients separately, which means each relay will use network coding vector that maximizes its own computation rate, \mathbf{a}_m is taken from the first column of $\Omega_m^{T_{max}}$, $m = 1, 2, 3$ and the constructed network coding system matrix

$$\mathbf{A}_{local} = \begin{bmatrix} 1 & 1 & 0 \\ 0 & 0 & -1 \\ 0 & 0 & 1 \end{bmatrix}^T$$

is obviously not of full rank. In this case, the destination actually cannot decode all the messages efficiently.

Then we go forward to run our proposed network coding system matrix constructing algorithm. We sort the computation rates for all relays in a descending order,

$$\{\underbrace{0.7087}_{\gamma_1}, \underbrace{0.6785}_{\gamma_2}, \underbrace{0.5987}_{\gamma_3}, \underbrace{0.5935}_{\gamma_4}, \underbrace{0.5572}_{\gamma_5}, \underbrace{0.4846}_{\gamma_6}, \dots\}.$$

and start to check the rate from the third maximum value, $\gamma_3 = 0.5987$, then $\gamma_4 = 0.5935$, then $\gamma_5 = 0.5572, \dots$, to see whether it is achievable. If so, terminate and output; if not, move to the next rate.

For example, when we are checking $\gamma_4 = 0.5935 = \mathcal{R}_3^{(2)}$, which is taken from the second element of Γ_3^{Tmax} , the reduced candidate sets Ω_1^{cut} , Ω_2^{cut} , Ω_3^{cut} with all corresponding rates greater or equal to $\gamma_4 = 0.5935$ can be constructed as

$$\Omega_1^{cut} = \emptyset, \quad \Omega_2^{cut} = \begin{bmatrix} 1 & 2 \\ 0 & -1 \\ 0 & 1 \end{bmatrix}, \quad \Omega_3^{cut} = \begin{bmatrix} 0 \\ 1 \\ 0 \end{bmatrix}.$$

We can easily see that no full rank network coding system matrix \mathbf{A} can be constructed with $\mathbf{a}_1 \in \Omega_1^{cut}$, $\mathbf{a}_2 \in \Omega_2^{cut}$, $\mathbf{a}_3 \in \Omega_3^{cut}$. Hence the rate of $\gamma_4 = 0.5935$ is not achievable. We will move to $\gamma_5 = 0.5572$ and check in the same way.

After running our proposed Network Coding System Matrix \mathbf{A} Constructing Algorithm 2, the network coding system matrix $\mathbf{A} = [\mathbf{a}_1, \mathbf{a}_2, \mathbf{a}_3]^T$ is finally constructed as

$$\mathbf{A}_{proposed} = \begin{bmatrix} 1 & 2 & 0 \\ 0 & -1 & 1 \\ 0 & 1 & 0 \end{bmatrix}^T$$

and the maximum transmission rate $\mathcal{R}_D^{max} = 0.4846$.

2.3.2 Simulation Results

We present numerical results to evaluate the performance of our proposed algorithms. First, we show that if network coding integer coefficient vector is optimized separately/locally at each relay, the probability that the network coding system matrix \mathbf{A} is not of full rank, i.e. $|\mathbf{A}| = 0$, in which case the destination actually cannot decode the original messages efficiently. With the average of 10000 randomly generated channel realizations, it can be observed from Fig. 2.6 the severity of this issue. For example, when $L = 3$ and $P = 1\text{dB}-8\text{dB}$, the probability of rank failure with local optimized network coding vectors is always beyond 0.4. This further assures the importance and necessity of our proposed algorithms.

In Fig. 2.7, we compare the overall transmission rate \mathcal{R}_D at destination, with the average of 10000 randomly generated channel realizations, of several different strategies

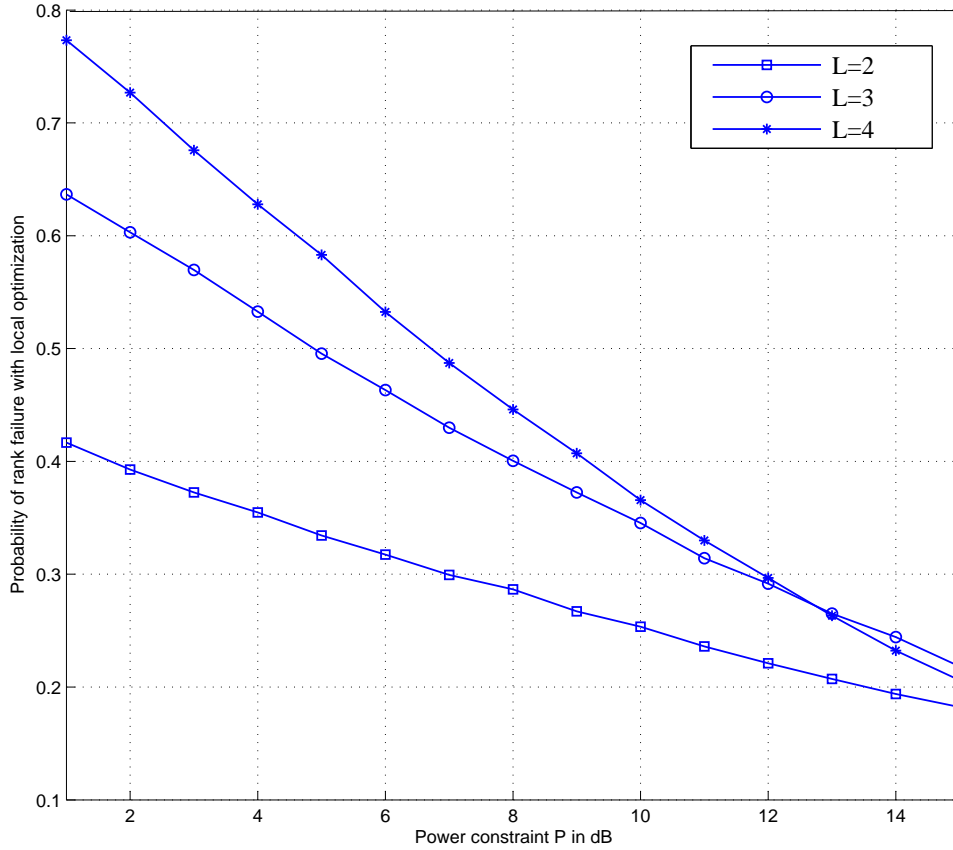


Fig. 2.6: Probability of rank failure with local optimization for MSMR

in multi-source multi-relay channels with $L = 3$ and $T_{max} = 5$. (i) The “*DF with interference as noise*” is a strategy in which relay m is trying to decode one message from source m and treat other messages as noise. In this special case, the system matrix $\mathbf{A} = \mathbf{I}_L$. (ii) The “*CPF NC with Round-H*” is a strategy that each relay decodes a linear integer combination of transmitted messages, while the network coding coefficients are set by a simplified method, i.e. rounding the channel coefficients directly to the nearest integers. (iii) The “*CPF NC with local optimization*” is a strategy that each relay also decodes a linear integer combination of transmitted messages, while the network coding coefficients are optimized locally/separately. Due to the rank failure issue of network coding system matrix, in which case the destination cannot decode all messages, the rate is decreased. Finally, (iv) the “*CPF NC with proposed algorithms*” is the strategy

that each relay decodes a linear integer combination of transmitted messages with our proposed FP based candidate set searching algorithm and network coding system matrix constructing algorithm.

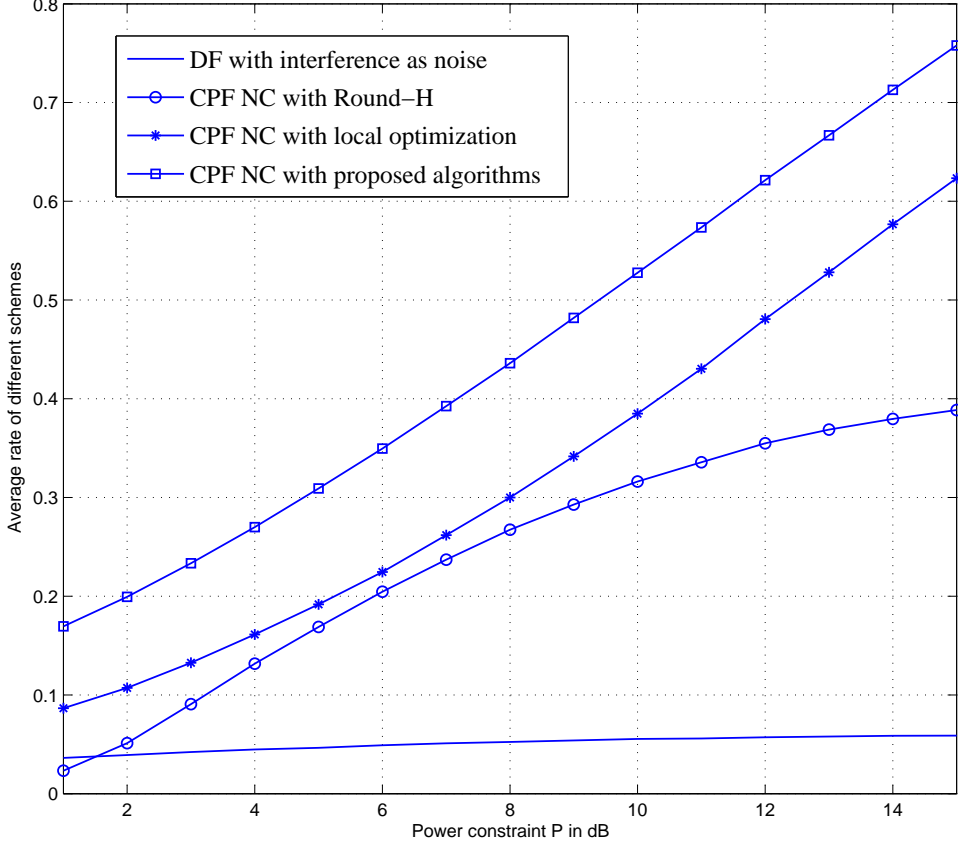


Fig. 2.7: Rate comparisons with $L = 3$ for MSMR

As shown in Fig. 2.7, the performance differences are significant. “*DF with interference as noise*” gives very poor result. Furthermore, increasing power constraint has not much effect on this strategy since as the power increases for the interested message, the corresponding interference power is also raised. The “*CPF NC with Round-H*” strategy works a little better since it somehow takes advantage of network coding to improve the rate, but the coefficients are chosen in a simplified way and not optimal. The “*CPF NC with proposed algorithms*” strategy, in which case the network coding coefficients are optimized systematically, performs superior to all other strategies and has about 3dB

gain compared with the “*CPF NC with local optimization*”.

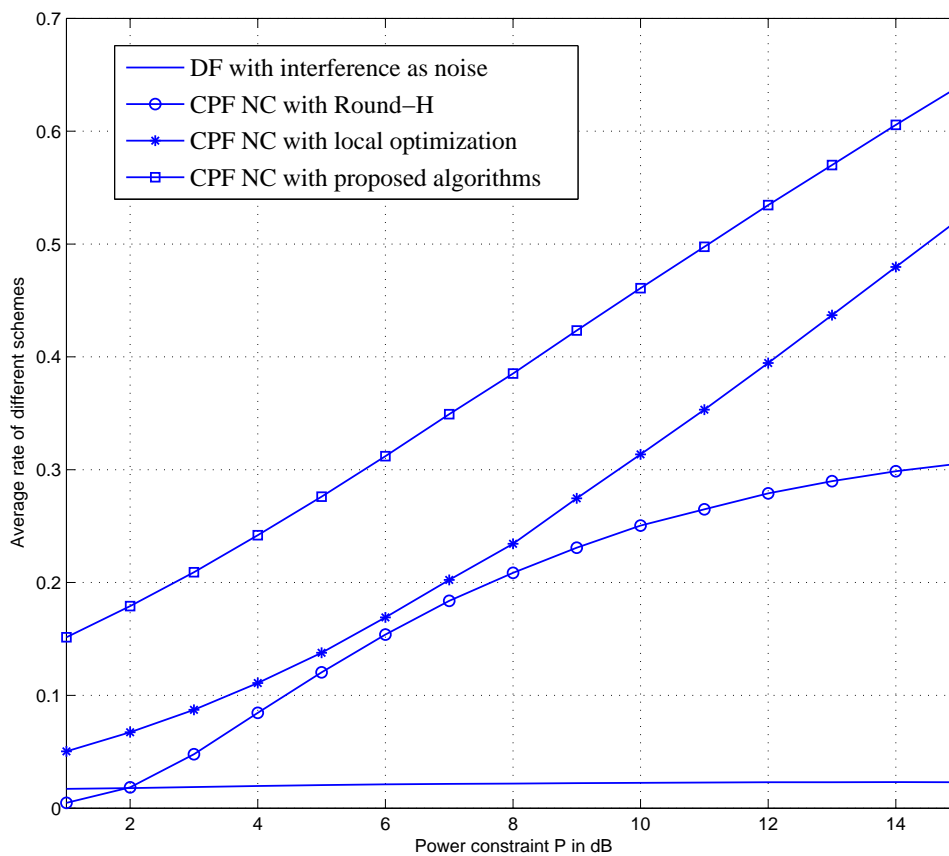


Fig. 2.8: Rate comparisons with $L = 4$ for MSMR

We repeat our experiment with multi-source multi-relay channels of $L = 4$ and present the average rate comparisons of different schemes with respect to the power constraint. Similar results are shown as in Fig. 2.8. “*CPF NC with proposed algorithms*” strategy still gives the best performance and further demonstrates the effectiveness of our proposed algorithms.

2.4 Conclusion

In this work, we consider the problem of integer network coding coefficients design in a system level over a compute-and-forward multi-source multi-relay system. Instead of optimizing network coding vector of each relay separately, we propose the Fincke-Pohst based candidate set searching algorithm, to provide a network coding vector candidate set for each relay with corresponding computation rate in descending order. Then, with our proposed network coding system matrix constructing algorithm, we choose network coding vectors from candidate sets to construct network coding system matrix with full rank, while in the meantime the transmission rate of the overall system is maximized. Numerical results give the performance comparisons of our proposed compute-and-forward network coding algorithms and other strategies.

Chapter 3

Efficient Compute-and-Forward Network Codes Search for Two-Way Relay Channel

3.1 System Model

Consider the classic TWRC with two sources \mathcal{S}_1 , \mathcal{S}_2 attempting to exchange information with each other through a relay \mathcal{R} as in Fig. 3.1. There is no direct link between two sources and each node is equipped with one antenna.

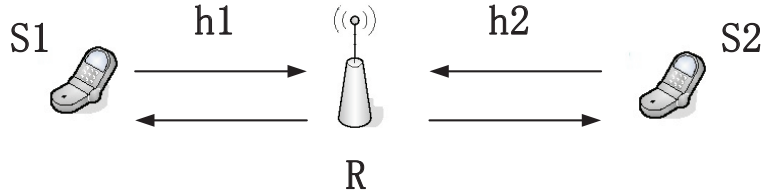


Fig. 3.1: TWRC Model

Without loss of generality, in one information codeword transmission, each source has a length- k information vector

$$\mathbf{w}_m \in \mathbb{F}_p^k, \quad (3.1)$$

$m = 1, 2$, where $\mathbb{F}_p = \{0, 1, \dots, p-1\}$ is a prime size finite field. Each source is equipped with an encoder

$$\mathcal{E}_m : \mathbb{F}_p^k \rightarrow \mathbb{R}^n \quad (3.2)$$

that maps the length- k message \mathbf{w}_m into a length- n lattice codeword

$$\mathbf{x}_m \in \mathbb{R}^n. \quad (3.3)$$

The codeword satisfies the power constraint of

$$\frac{1}{n} \|\mathbf{x}_m\|^2 \leq P. \quad (3.4)$$

The information transmission includes two phases. In the first phase, two sources \mathcal{S}_1 , \mathcal{S}_2 transmit simultaneously to relay \mathcal{R} , which can be modeled by a *multiple-access channel* with inputs \mathbf{x}_1 , \mathbf{x}_2 and output \mathbf{y}_R . In the second phase, relay \mathcal{R} broadcast to \mathcal{S}_1 and \mathcal{S}_2 , which can be modeled by a *broadcast channel* with input \mathbf{x}_R and outputs \mathbf{y}_1 and \mathbf{y}_2 . The transmission diagram of TWRC is shown in Fig. 3.2.

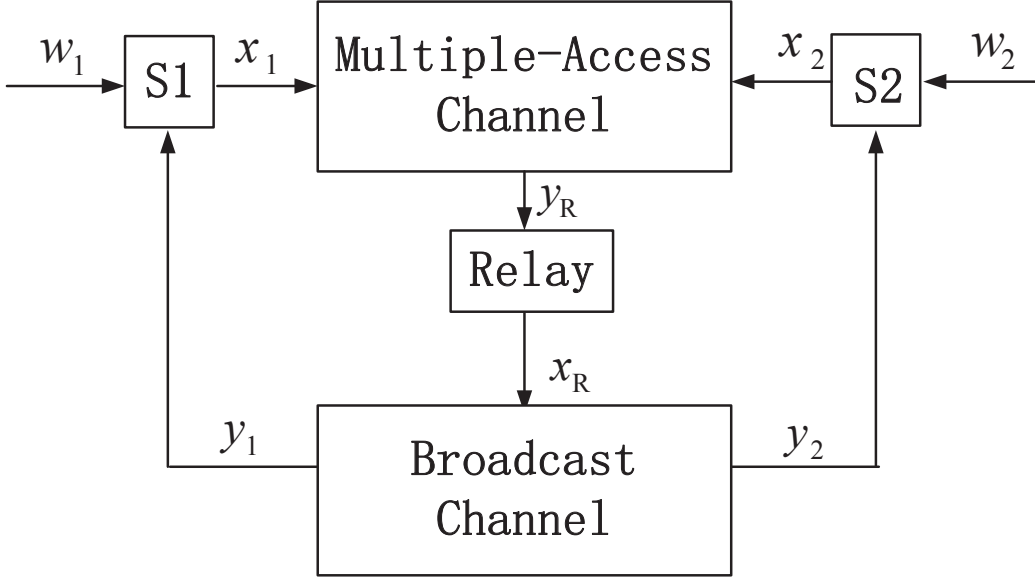


Fig. 3.2: TWRC Diagram

At the end of first phase, relay \mathcal{R} will receive

$$\mathbf{y}_R = h_1 \mathbf{x}_1 + h_2 \mathbf{x}_2 + \mathbf{z}_R, \quad (3.5)$$

where $h_1, h_2 \in \mathbb{R}$ are real valued fading channel coefficient from \mathcal{S}_1 and \mathcal{S}_1 to relay \mathcal{R} respectively and $\mathbf{z}_R \in \mathbb{R}^n$ is additive Gaussian noise. All channel coefficients are generated i.i.d. according to a normal distribution $\mathcal{N}(0, 1)$.

In the framework of CPF [50], the property that any integer combination of lattice codewords is again a lattice codeword is exploited. After receiving the noisy vector \mathbf{y}_R , relay \mathcal{R} will select a scalar $\beta \in \mathbb{R}$ and an integer network coding vector $\mathbf{a} = [a_1, a_2]^T \in \mathbb{Z}^2$, and attempts to decode

$$\mathbf{x}_R = a_1 \mathbf{x}_1 + a_2 \mathbf{x}_2 \quad (3.6)$$

from

$$\begin{aligned} \beta \mathbf{y}_R &= \beta h_1 \mathbf{x}_1 + \beta h_2 \mathbf{x}_2 + \beta \mathbf{z}_R \\ &= a_1 \mathbf{x}_1 + a_2 \mathbf{x}_2 + \underbrace{\sum_{m=1}^2 (\beta h_m - a_m) \mathbf{x}_m}_{\text{Effective Noise}} + \beta \mathbf{z}_R. \end{aligned} \quad (3.7)$$

At the end of second phase, $\mathcal{S}_1, \mathcal{S}_2$ will receive respectively

$$\mathbf{y}_1 = h_1(a_1 \mathbf{x}_1 + a_2 \mathbf{x}_2) + \mathbf{z}_1 \quad (3.8)$$

$$\mathbf{y}_2 = h_2(a_1 \mathbf{x}_1 + a_2 \mathbf{x}_2) + \mathbf{z}_2. \quad (3.9)$$

Then, each source can subtract its own signal and attempt to decode for the other source.

At the relay, we are interested in the rate of $a_1 \mathbf{x}_1 + a_2 \mathbf{x}_2$ as a whole and capture the performance by what refer to as the *computation rate*, namely, the number of bits of the integer linear function successfully recovered per channel use. The role of β can be thought as trying to move the channel coefficients toward integers [51]. We conclude the results regarding CPF network coding in [50]-[52] in the following theorems. Denote channel vector $\mathbf{h} = [h_1, h_2]^T$ and $\log^+(x) \triangleq \max(\log(x), 0)$.

Theorem 3.1.1 For real-valued AWGN network with channel vector \mathbf{h} and network coding vector \mathbf{a} , the following computation rate is achievable

$$\mathcal{R}(\mathbf{a}) = \max_{\beta \in \mathbb{R}} \frac{1}{2} \log^+ \left(\frac{P}{\beta^2 + P \|\beta \mathbf{h} - \mathbf{a}\|^2} \right). \quad (3.10)$$

Theorem 3.1.2 The computation rate given in Theorem 3.1.1 is uniquely maximized by choosing β to be the MMSE coefficient

$$\beta_{MMSE} = \frac{P \mathbf{h}^T \mathbf{a}}{1 + P \|\mathbf{h}\|^2}, \quad (3.11)$$

which results in

$$\mathcal{R}(\mathbf{a}) = \frac{1}{2} \log^+ \left(\|\mathbf{a}\|^2 - \frac{P(\mathbf{h}^T \mathbf{a})^2}{1 + P\|\mathbf{h}\|^2} \right)^{-1}. \quad (3.12)$$

Theorem 3.1.3 For a given channel vector \mathbf{h} , $\mathcal{R}(\mathbf{a})$ is maximized by choosing the integer network coding vector \mathbf{a} as

$$\mathbf{a} = \arg \min_{\mathbf{a} \in \mathbb{Z}^2, \mathbf{a} \neq \mathbf{0}} (\mathbf{a}^T \mathbf{G} \mathbf{a}), \quad (3.13)$$

with constraint $\|\mathbf{a}\|^2 \leq 1 + P\|\mathbf{h}\|^2$ and $\mathbf{G} \triangleq \mathbf{I} - \frac{P(\mathbf{h}\mathbf{h}^T)}{1 + P\|\mathbf{h}\|^2}$.

3.2 Optimal Network Codes Search for TWRC

3.2.1 Formulation

Theorems 3.1.1-3.1.3 only give the general criteria to search the optimal network coding integer vector \mathbf{a} at relay \mathcal{R} and do not take consideration of the specific system constraints. For TWRC, in order to let each source receive signals from the other one through relay \mathcal{R} , there should be no zero entry in network coding vector $\mathbf{a} = [a_1, a_2]^T$, i.e. $a_1 \neq 0$ and $a_2 \neq 0$ must be satisfied at the same time. In other words, network coding vector in form of $[a_1, 0]^T$ or $[0, a_2]^T$ will fail the information transmission for TWRC.

Hence, we modify theorem 3.1.3 and propose a new network coding vector search criteria for TWRC as follows.

Lemma 3.2.1 In TWRC, for a given channel vector \mathbf{h} , $\mathcal{R}(\mathbf{a})$ is maximized by choosing the integer network coding vector \mathbf{a} as

$$\mathbf{a} = \arg \min_{\mathbf{a} \in \mathbb{Z}^2, a_1 \neq 0, a_2 \neq 0} (\mathbf{a}^T \mathbf{G} \mathbf{a}), \quad (3.14)$$

with constraint $\|\mathbf{a}\|^2 \leq 1 + P\|\mathbf{h}\|^2$ and $\mathbf{G} \triangleq \mathbf{I} - \frac{P(\mathbf{h}\mathbf{h}^T)}{1 + P\|\mathbf{h}\|^2}$.

A direct approach to this optimization problem in Lemma 3.2.1 will be exhaustive search among all integer vectors satisfying

$$\|\mathbf{a}\|^2 \leq 1 + P\|\mathbf{h}\|^2. \quad (3.15)$$

However, as the power constraint P gets larger, the number of candidate vectors increases dramatically. In this work, we will propose an algorithm based on modified Finche-Pohst (FP) method, to searching within a much smaller candidate set with the optimal solution included.

Operate Cholesky's factorization of matrix \mathbf{G} ,

$$\mathbf{G} = \mathbf{U}^T \mathbf{U}, \quad (3.16)$$

where \mathbf{U} is an upper triangular matrix. Then, the optimization of (3.14) becomes

$$\mathbf{a} = \arg \min_{\mathbf{a} \in \mathbb{Z}^2, a_1 \neq 0, a_2 \neq 0} \|\mathbf{U} \mathbf{a}\|_F^2. \quad (3.17)$$

The original FP method [41] searches through the integer points \mathbf{a} in Euclidean space, which make the corresponding vectors $\mathbf{z} \triangleq \mathbf{U} \mathbf{a}$ inside a sphere of given radius \sqrt{C} centered at the origin point, i.e. $\|\mathbf{U} \mathbf{a}\|_F^2 = \|\mathbf{z}\|_F^2 \leq C$. This guarantees that only the points that make the corresponding vectors \mathbf{z} within the square distance C from the origin point are considered in the metric minimization.

Compared with the original FP algorithm, we have two main modifications: (i) We add two constraints: the no zero entry constraint and $\|\mathbf{a}\|^2 \leq 1 + P\|\mathbf{h}\|^2$ constraint to search for the optimal network coding vector in TWRC. (ii) According to the binary vector obtained by applying the direct sign operator on the real minimum-eigenvalue eigenvector of \mathbf{G} , denoted as \mathbf{a}_{quant} , we can have a very proper square distance setting as

$$C = \mathbf{a}_{quant}^T \mathbf{G} \mathbf{a}_{quant}, \quad (3.18)$$

such that the searching sphere radius is big enough to have at least one searching point fall inside, while in the meantime small enough to have only a few within. We calculate the $\mathbf{a}^T \mathbf{G} \mathbf{a}$ metric for every candidate vector that satisfies $\|\mathbf{U} \mathbf{a}\|_F^2 \leq C$, such that the optimal network coding vector with minimum $\mathbf{a}^T \mathbf{G} \mathbf{a}$ metric (maximizing the computation rate for relay \mathcal{R} equivalently) is obtained from the modified FP algorithm directly.

Since the radius is fixed for our modified FP algorithm, the complexity uncertainty due to the radius update, which means that the radius need to be expanded if no points found in the sphere and the radius need to be reduced if too many points found within as shown in the literature of sphere decoding, is not a question in this optimization.

3.2.2 Searching Algorithm Derivation

Let u_{ij} , $i, j = 1, 2$, be entries of matrix \mathbf{U} . Then, the searching vector \mathbf{a} that makes $\mathbf{a}^T \mathbf{G} \mathbf{a} \leq C$ can be expressed as

$$\begin{aligned} \mathbf{a}^T \mathbf{G} \mathbf{a} = \|\mathbf{U} \mathbf{a}\|_F^2 &= (u_{11}a_1 + u_{12}a_2)^2 + (u_{22}a_2)^2 \\ &= g_{11}(a_1 + g_{12}a_2)^2 + g_{22}a_2^2 \leq C \end{aligned} \quad (3.19)$$

where $g_{ii} = u_{ii}^2$ for $i = 1, 2$ and $g_{12} = u_{12}/u_{11}$. To satisfy (3.19), it is equivalent to consider,

$$\begin{cases} g_{22}a_2^2 \leq C \\ g_{11}(a_1 + g_{12}a_2)^2 + g_{22}a_2^2 \leq C \end{cases} \quad (3.20)$$

We begin with evaluation of the entry a_2 . Set $\Delta_2 = 0$, $C_2 = C$. Referring to (3.20), we get

$$LB_2 \leq a_2 \leq UB_2, \quad (3.21)$$

and

$$UB_2 = \left\lceil \sqrt{\frac{C_2}{g_{22}}} - \Delta_2 \right\rceil, \quad LB_2 = \left\lfloor -\sqrt{\frac{C_2}{g_{22}}} - \Delta_2 \right\rfloor. \quad (3.22)$$

where $\lceil x \rceil$ is the smallest integer no less than x and $\lfloor x \rfloor$ is the greatest integer no bigger than x . The candidate for a_2 is chosen as an integer inside its bound requirement (3.21)-(3.22) and excludes zero.

To evaluate a_1 , set $\Delta_1 = g_{12}a_2$, $C_1 = C - g_{22}a_2^2$. Referring to (3.20) we will have

$$LB_1 \leq a_1 \leq UB_1, \quad (3.23)$$

and

$$UB_1 = \left\lceil \sqrt{\frac{C_1}{g_{11}}} - \Delta_1 \right\rceil, \quad LB_1 = \left\lfloor -\sqrt{\frac{C_1}{g_{11}}} - \Delta_1 \right\rfloor. \quad (3.24)$$

Then a_1 is chosen as an integer inside its bound requirement (3.23)-(3.24) and excludes zero.

The entries a_2, a_1 are chosen as follows: for a chosen a_2 that satisfies its bound requirement (3.21)-(3.22) and $a_2 \neq 0$, we can choose a_1 satisfying its bounds requirements (3.23)-(3.24) and $a_1 \neq 0$. If such a_1 does not exist, we go back and choose other a_2 . Then search for a_1 that meets its bounds requirement for this new a_2 and $a_1 \neq 0$. When a set of a_2, a_1 is chosen, we test the $\|\mathbf{a}\|^2 \leq 1 + P\|\mathbf{h}\|^2$ constraint. If satisfied, one candidate network coding vector $\mathbf{a} = [a_1, a_2]^T$ is obtained. We choose the one among all network coding candidate vectors that gives the smallest $\mathbf{a}^T \mathbf{G} \mathbf{a}$ metric, which equivalently maximizes the computation rate at relay \mathcal{R} .

Note that this searching procedure will return *all* candidates that satisfy $\mathbf{a}^T \mathbf{G} \mathbf{a} \leq C$, and gives the one with minimum value. There is at least one candidate vector \mathbf{a}_{quant} such that its entries satisfy all the bounds requirements, since that is how we set the radius value in (3.18). On the other hand, the exhaustive search result $\mathbf{a}_{exhaustive}$ that returns the minimum metric will also fall inside the search bounds, since

$$\mathbf{a}_{exhaustive}^T \mathbf{G} \mathbf{a}_{exhaustive} \leq \mathbf{a}_{quant}^T \mathbf{G} \mathbf{a}_{quant} = C. \quad (3.25)$$

Hence, we are guaranteed to find the optimal exhaustive search result by the proposed algorithm. Simulation results in Section IV also demonstrate this optimality.

3.2.3 Optimal Network Codes Search Algorithm for TWRC

We summarize our proposed algorithm to search the optimal network coding vector for TWRC as follows.

Algorithm 3.1 Optimal Network Codes Search Algorithm for TWRC

Input: Channel coefficient vector \mathbf{h} .

Output: The optimal network coding vector \mathbf{a}_{min} for TWRC.

Step 1: Based on the channel coefficient vector \mathbf{h} , construct matrix \mathbf{G} as $\mathbf{G} = \mathbf{I} - \frac{P(\mathbf{h}\mathbf{h}^T)}{1+P\|\mathbf{h}\|^2}$.

Step 2: Calculate the binary quantized vector obtained by applying the direct sign op-

erator of the real minimum-eigenvalue eigenvector of \mathbf{G} , denoted as \mathbf{a}_{quant} , and set C as

$$C = \mathbf{a}_{quant}^T \mathbf{G} \mathbf{a}_{quant}. \quad (3.26)$$

Step 3: Operate Cholesky's factorization of matrix \mathbf{G} , $\mathbf{G} = \mathbf{U}^T \mathbf{U}$. Let u_{ij} , $i, j = 1, 2$ denote the entries of matrix \mathbf{U} . Set $g_{ii} = u_{ii}^2$ for $i = 1, 2$ and $g_{12} = u_{12}/u_{11}$.

Step 4: Search the candidate vector $\mathbf{a} = [a_1, a_2]^T$ according to the following procedure.

(i) Initialize $\Delta_2 = 0$, $C_2 = C$, $metric = C$, $\mathbf{a}_{min} = \mathbf{a}_{quant}$ and $k = 2$.

(ii) Set the upper bound UB_k and the lower bound LB_k as follows

$$UB_k = \left[\sqrt{\frac{C_k}{g_{kk}}} - \Delta_k \right], \quad LB_k = \left[-\sqrt{\frac{C_k}{g_{kk}}} - \Delta_k \right]$$

and $a_k = LB_k - 1$.

(iii) Set $a_k = a_k + 1$. If $a_k = 0$, move to $a_k = 1$. For $a_k \leq UB_k$, go to (v); else go to (iv).

(iv) If $k = 2$, terminate and output the searching result \mathbf{a}_{min} ; else set $k = k + 1$ and go to (iii).

(v) For $k = 1$, go to (vi); else set $k = k - 1$, and

$$\Delta_1 = g_{12}a_2, \quad C_1 = C - g_{22}a_2^2,$$

then go to (ii).

(vi) Test for $\|\mathbf{a}\|^2 \leq 1 + P\|\mathbf{h}\|^2$ constraint to get a candidate vector \mathbf{a} . If $\mathbf{a}^T \mathbf{G} \mathbf{a} \leq metric$, update $\mathbf{a}_{min} = \mathbf{a}$ and $metric = \mathbf{a}^T \mathbf{G} \mathbf{a}$. Go to (iii).

3.3 Experimental Studies

We present experimental studies to demonstrate the effectiveness of our proposed lemma and algorithm. First, with the average of 10000 randomly generated channel realizations,

we show in Fig. 3.3 that if network coding vector is searched based on general criteria of theorem 2.3 without our lemma, the probability that the resulting vector will have at least one zero entry and fails the TWRC system. It can be observed that this issue is actually very severe. For example, with $P \leq 15dB$, the probability of zero entry is always beyond $1/2$.

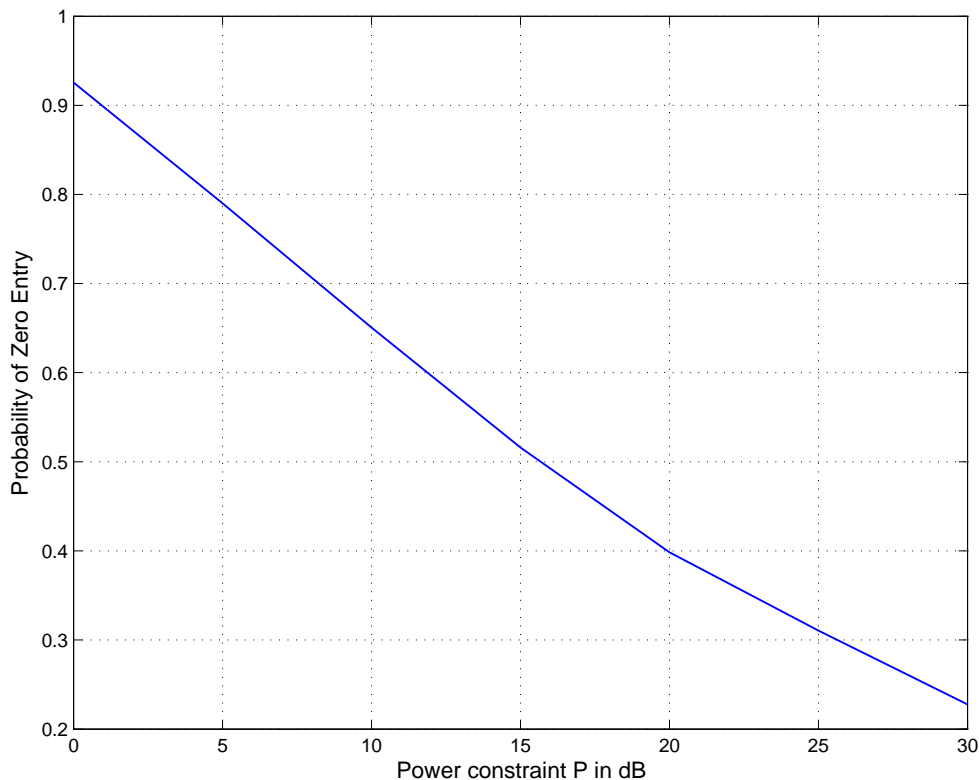


Fig. 3.3: Probability of zero entry in TWRC

In Fig. 3.4. we compare the average rate of several strategies under TWRC model. (i) Relay \mathcal{R} decode and transmit $\mathbf{x}_1 + \mathbf{x}_2$ to both sources, which we denote as “DF-NC”. This strategy can be seen as *static* network coding as it does not consider the channel variations. (ii) Relay \mathcal{R} decode a linear integer combination of both sources, while the network coding vector are set by simply rounding channel vector \mathbf{h} directly, denoted as “HNC”. (iii) The general CPF scheme while the network coding vector is optimized without our proposed lemma. We denote as “CPF without zero entry constraints”.

(iv) The CPF scheme under our proposed lemma and algorithm for TWRC, denoted as “CPF with proposed algorithm”. (v) The CPF scheme under our proposed lemma and exhaustive search, denoted as “CPF with exhaustive search”. (vi) The “Upper Bound” on the computation rate, $\mathcal{R}_{Upper} = \min_{m=1,2} \frac{1}{2} \log(1 + |h_m|^2 P)$ [50].

As show in Fig. 3.4, the performance differences are apparent. “DF-NC” gives very poor result compared with other strategies since the network coding vector is not adaptive to the changing channel. “HNC” strategy somehow consider network coding adaptively, but the network coding vector is chosen in a simplified way and not optimal. “CPF with proposed algorithm” performs superior to other practical strategies and actually overlaps with the “CPF with exhaustive search” curve. It further verifies the optimality of our proposed algorithm which produces the same solution as exhaustive search.

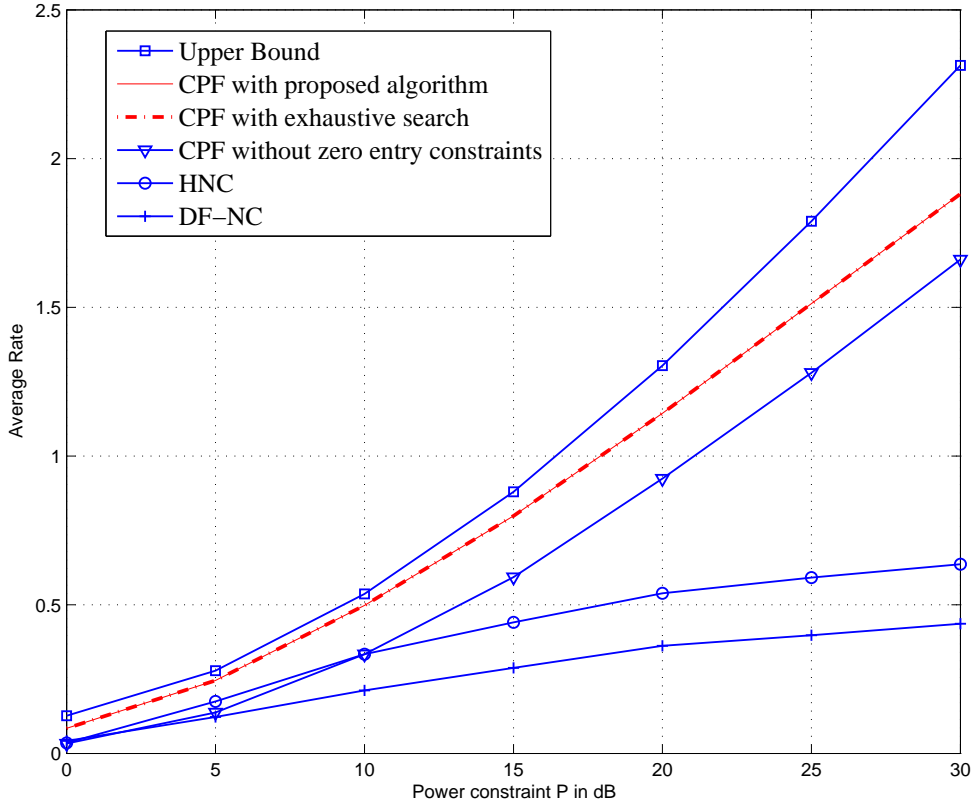


Fig. 3.4: Average rate comparisons for TWRC

Finally, to demonstrate the complexity reduction of proposed algorithm with exhaus-

P	0dB	5dB	10dB	15dB	20dB	25dB	30dB
Proposed	1.1970	1.9388	3.1606	5.5110	10.3098	20.0808	38.6586
Exhaustive	1.8188	7.1324	25.7178	86.7106	287.6744	957.2552	3073.03

Table 3.1: Average number of candidate vectors for TWRC

tive search, in Table 3.1 we show, over 10000 randomly generated channel realizations, the statistical average number of network coding candidate vectors need to be searched to find the optimum solution. We can see that the candidate set is reduced significantly by our proposed algorithm hence lower the complexity dramatically. For example, when $P = 15dB$, there are in average 86.7106 integer vectors need to considered for $\mathbf{a}^T \mathbf{G} \mathbf{a}$ calculation to get the optimal network coding vector for exhaustive search, while with our proposed algorithm, we only need to consider in average 5.5110 integer vectors. Hence, our proposed algorithm has the same optimal solution as exhaustive search with much lower complexity.

3.4 Conclusions

We consider the two-way relay channel (TWRC) with compute-and-forward network coding strategy. First a new lemma is proposed as network codes search criteria for TWRC. Then, instead of exhaustive search, we present an efficient network codes search algorithm based on modified Fincke-Pohst method. Numerical results demonstrate the effectiveness and complexity reduction of our proposed lemma and algorithm.

Chapter 4

Integer-Forcing Linear Receiver Design with Slowest Descent Method

4.1 System Model

First we note that it is straightforward that a general complex MIMO system $\mathbf{y} = \mathbf{H}\mathbf{x} + \mathbf{z}$ can be easily converted into an equivalent real system [62] as

$$\begin{bmatrix} \text{Re}(\mathbf{y}) \\ \text{Im}(\mathbf{y}) \end{bmatrix} = \begin{bmatrix} \text{Re}(\mathbf{H}) & -\text{Im}(\mathbf{H}) \\ \text{Im}(\mathbf{H}) & \text{Re}(\mathbf{H}) \end{bmatrix} \begin{bmatrix} \text{Re}(\mathbf{x}) \\ \text{Im}(\mathbf{x}) \end{bmatrix} + \begin{bmatrix} \text{Re}(\mathbf{z}) \\ \text{Im}(\mathbf{z}) \end{bmatrix}. \quad (4.1)$$

Hence, we will focus on the real MIMO system for analysis convenience.

We consider the classic MIMO channels with L transmit antennas and N receive antennas. Each transmit antenna delivers an independent data stream which is encoded separately to form the transmitted codewords. We assume that the channel state information is only available at the receiver during each transmission. Let $L = N$ for analysis simplicity.

Without loss of generality, in one transmission realization, each antenna has a length- k information vectors \mathbf{w}_m that is drawn independently and uniformly over a prime-size finite field $\mathbb{F}_p = \{0, 1, \dots, p-1\}$, i.e.,

$$\mathbf{w}_m \in \mathbb{F}_p^k, \quad m = 1, 2, \dots, L. \quad (4.2)$$

Each antenna is equipped with an encoder Ψ_m , that maps the length- k messages \mathbf{w}_m

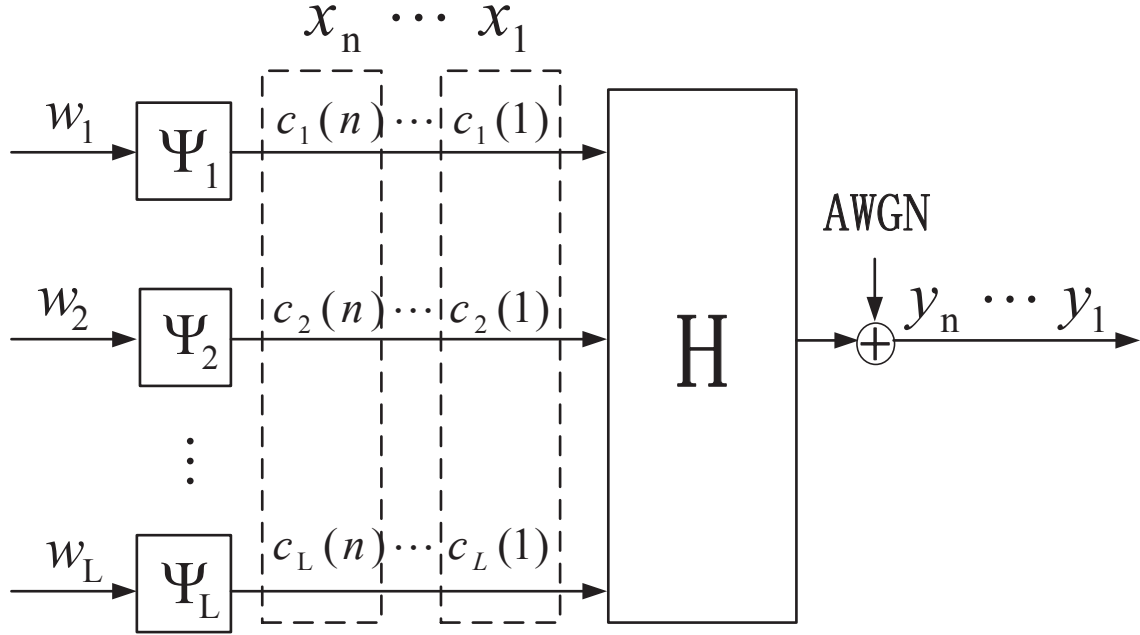


Fig. 4.1: MIMO diagram with independent data streams

into the length- n lattice codewords $\mathbf{c}_m \in \mathbb{R}^n$,

$$\Psi_m : \mathbb{F}_p^k \rightarrow \mathbb{R}^n. \quad (4.3)$$

The codeword satisfies the power constraint of $\frac{1}{n} \|\mathbf{c}_m\|^2 \leq P$, $m = 1, \dots, L$.

After mapping message \mathbf{w}_m into a lattice codeword \mathbf{c}_m with

$$\mathbf{c}_m = [c_m(1), c_m(2), \dots, c_m(n)]^T, \quad m = 1, \dots, L, \quad (4.4)$$

antenna m will transmit one information codeword \mathbf{c}_m in one transmission realization with a total of n time slots. In the i -th time slot, the transmitted signal vector $\mathbf{x}_i \in \mathbb{R}^L$ over L transmit antennas is

$$\mathbf{x}_i = [c_1(i), c_2(i), \dots, c_L(i)]^T, \quad i = 1, \dots, n. \quad (4.5)$$

The MIMO system diagram with independent data streams is shown in Fig. 4.1.

Assume a slow fading model where the channel remains constant over the entire codeword transmission. During one transmission realization, at the i th time slot, $i = 1, \dots, n$, the received vector $\mathbf{y}_i \in \mathbb{R}^L$ is,

$$\mathbf{y}_i = \mathbf{H}\mathbf{x}_i + \mathbf{z}_i, \quad (4.6)$$

where \mathbf{H} denotes the $L \times L$ channel matrix, with $\mathbf{H} = [h_{mj}]$ and h_{mj} is the real valued fading channel coefficient from transmit antenna j to receive antenna m , and $\mathbf{z}_i \in \mathbb{R}^L$ is the additive Gaussian noise. The entries of the channel matrix and the additive noise vector are generated i.i.d. according to a normal distribution $\mathcal{N}(0, 1)$.

To facilitate the detection of desired signals from each antenna, in a linear receiver architecture, the receiver will project the received vector \mathbf{y}_i with some matrix $\mathbf{B} \in \mathbb{R}^{L \times L}$ to get the effective received vector for further decoding,

$$\mathbf{d}_i = \mathbf{B}\mathbf{y}_i = \mathbf{B}\mathbf{H}\mathbf{x}_i + \mathbf{B}\mathbf{z}_i = \mathbf{A}\mathbf{x}_i + \mathbf{n}_i, \quad (4.7)$$

where $\mathbf{A} \triangleq \mathbf{B}\mathbf{H}$ and $\mathbf{n}_i \triangleq \mathbf{B}\mathbf{z}_i$.

The standard suboptimal linear detection methods include the zero-forcing (ZF) receiver and the minimum mean square error (MMSE) receiver,

$$\mathbf{B}_{ZF} = (\mathbf{H}^T\mathbf{H})^{-1}\mathbf{H}^T, \quad (4.8)$$

$$\mathbf{B}_{MMSE} = (\mathbf{H}^T\mathbf{H} + \frac{1}{P}\mathbf{I}_L)^{-1}\mathbf{H}^T, \quad (4.9)$$

where $(\cdot)^T$ denotes transpose operation and \mathbf{I}_L is the $L \times L$ identity matrix. The ZF technique nullifies the interference such that $\mathbf{A}_{ZF} = \mathbf{I}_L$ with the effect of noise enhancement. The MMSE receiver maximizes the post-detection signal-to-interference plus noise ratio (SINR) and mitigates the noise enhancement effects. However, both ZF and MMSE receiver have been proved to be largely suboptimal in terms of diversity-multiplexing tradeoff [63].

We recall the important algebraic structure of lattice codes, that the integer combination of lattice codewords is still a codeword. Instead of restricting matrix \mathbf{A} to be identity, we may allow \mathbf{A} to be some full rank matrix with integer coefficients, i.e.

$$\mathbf{A}_{IF} \in \mathbb{Z}^{L \times L}. \quad (4.10)$$

Then we can first separately recover linear combinations of transmitted lattice codewords with coefficients drawn from matrix \mathbf{A}_{IF} , which can be easily solved for the original messages. Specifically, if

$$\mathbf{d}_i = [d_1(i), d_2(i), \dots, d_L(i)]^T, \quad (4.11)$$

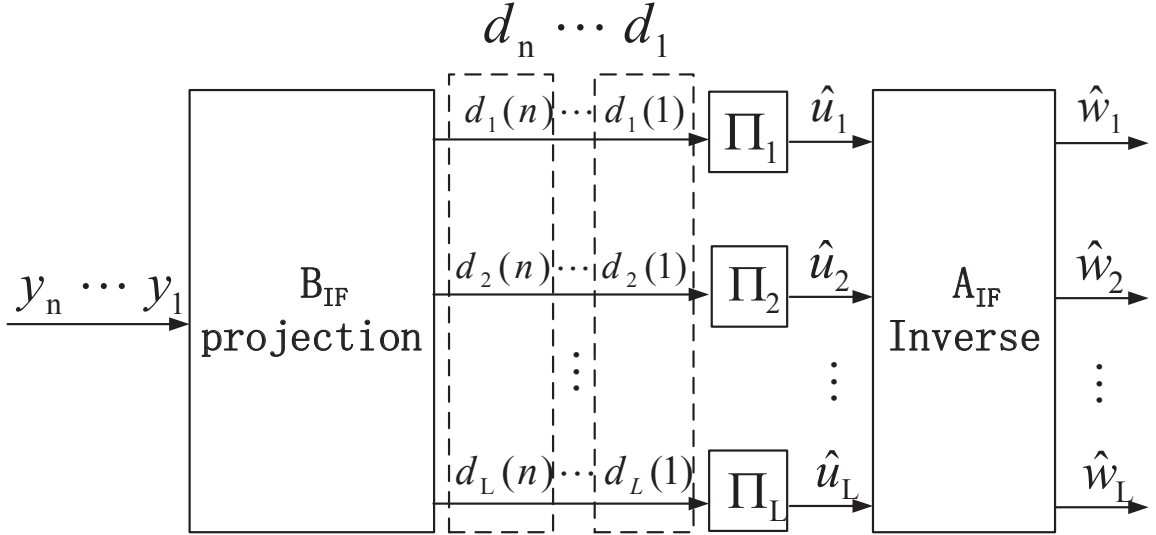


Fig. 4.2: IF decoder diagram

then each post-processed output $d_m(i)$ is passed into a separate decoder Π_m . After one transmission realization with n time slots, at one decoder,

$$\Pi_m : \mathbb{R}^n \rightarrow \mathbb{F}_p^k, \quad (4.12)$$

it maps the post-processed output $d_m(1), d_m(2), \dots, d_m(n)$ to an estimate $\hat{\mathbf{u}}_m \in \mathbb{F}_p^k$ of the linear message combination \mathbf{u}_m , where

$$\mathbf{u}_m = \bigoplus_{l=1}^L q_{ml} \mathbf{w}_l = \left[\sum_{l=1}^L a_{ml} \mathbf{w}_l \right] \text{ mod } p, \quad (4.13)$$

where \bigoplus denotes summation over the finite field, q_{ml} is a coefficient taking values in \mathbb{F}_p and $q_{ml} = a_{ml} \text{ mod } p$. The original messages can be recovered from the set of linear equations by a simple inverse operation,

$$[\hat{\mathbf{w}}_1, \hat{\mathbf{w}}_2, \dots, \hat{\mathbf{w}}_L]^T = \mathbf{A}_{\text{IF}}^{-1} [\hat{\mathbf{u}}_1, \hat{\mathbf{u}}_2, \dots, \hat{\mathbf{u}}_L]^T. \quad (4.14)$$

The diagram of IF decoder is shown in Fig. 4.2.

Hence, with integer forcing (IF) technique, the receiver will try to design a projection matrix $\mathbf{B}_{\text{IF}} \in \mathbb{R}^{L \times L}$, such that after the projection process of (4.7), the resulting full rank IF matrix \mathbf{A}_{IF} satisfies that $\mathbf{A}_{\text{IF}} \in \mathbb{Z}^{L \times L}$ and the achievable rate is maximized. We summarize the results regarding IF receiver in [58]-[59] in the following theorem.

Theorem 4.1.1 Let $\mathbf{A}_{IF} = [\mathbf{a}_1, \mathbf{a}_2, \dots, \mathbf{a}_L]^T$ and $\mathbf{B}_{IF} = [\mathbf{b}_1, \mathbf{b}_2, \dots, \mathbf{b}_L]^T$. For each pair of $(\mathbf{a}_m, \mathbf{b}_m)$, the following computation rate is achievable,

$$\mathcal{R}_m = \frac{1}{2} \log \left(\frac{P}{\|\mathbf{b}_m\|^2 + P\|\mathbf{H}^T \mathbf{b}_m - \mathbf{a}_m\|^2} \right). \quad (4.15)$$

For a fixed IF coefficient matrix \mathbf{A}_{IF} , the computation rate is maximized by choosing¹

$$\mathbf{b}_m^T = \mathbf{a}_m^T \mathbf{H}^T \left(\mathbf{H} \mathbf{H}^T + \frac{1}{P} \mathbf{I}_L \right)^{-1}. \quad (4.16)$$

□

According to Theorem 4.1.1, we plug in the optimal \mathbf{b}_m of (4.16) into the computation rate \mathcal{R}_m of (4.15), which will result in

$$\mathcal{R}_m = \frac{1}{2} \log \left(\frac{1}{\mathbf{a}_m^T \mathbf{Q} \mathbf{a}_m} \right), \quad (4.17)$$

where

$$\mathbf{Q} \triangleq \mathbf{I}_L - \mathbf{H}^T \left(\mathbf{H} \mathbf{H}^T + \frac{1}{P} \mathbf{I}_L \right)^{-1} \mathbf{H}. \quad (4.18)$$

The proof of equation (4.17)-(4.18) is in Appendix A. Then, the total achievable rate of the IF receiver is

$$\begin{aligned} \mathcal{R}_{total} &\triangleq \max_{|\mathbf{A}| \neq 0} L \min_m \mathcal{R}_m \\ &= \max_{|\mathbf{A}| \neq 0} \min_m L \log \left(\frac{1}{\mathbf{a}_m^T \mathbf{Q} \mathbf{a}_m} \right), \end{aligned} \quad (4.19)$$

Hence, the design criteria for optimal IF coefficient matrix \mathbf{A}_{IF} is

$$\begin{aligned} \mathbf{A}_{IF} &= \arg \max_{|\mathbf{A}| \neq 0} \min_m L \log \left(\frac{1}{\mathbf{a}_m^T \mathbf{Q} \mathbf{a}_m} \right) \\ &= \arg \min_{|\mathbf{A}| \neq 0} \max_m \mathbf{a}_m^T \mathbf{Q} \mathbf{a}_m. \end{aligned} \quad (4.20)$$

It means that we need to find integer vectors $\mathbf{a}_1, \mathbf{a}_2, \dots, \mathbf{a}_L$ to construct a full rank matrix \mathbf{A}_{IF} , such that the maximum value of $\mathbf{a}_m^T \mathbf{Q} \mathbf{a}_m$ is minimized.

Solving this optimization problem is critical as it dominates the total achievable rate of the desired IF receiver that sources can reliably communicate with the destination. As it need to return L integer vectors to construct the IF coefficient matrix \mathbf{A}_{IF} with full rank, no explicit solution is presented in the previous works. In this manuscript, we will propose efficient and practical algorithms to design this optimal \mathbf{A}_{IF} .

¹The optimal projection matrix is $\mathbf{B}_{IF} = \mathbf{A}_{IF} \mathbf{H}^T (\mathbf{H} \mathbf{H}^T + \frac{1}{P} \mathbf{I}_L)^{-1}$.

4.2 Integer Forcing Linear Receiver Design

To approach the optimization problem of (4.20), first we need to generate some feasible searching set $\Omega \subset \mathbb{Z}^L$ for $\mathbf{a}_m \in \Omega$, $m = 1, 2, \dots, L$, instead of the whole searching space $\mathbf{a}_m \in \mathbb{Z}^L$. Then, we will find L linearly independent vectors within this searching set Ω to construct the optimal IF coefficient matrix \mathbf{A}_{IF} .

Accordingly, we propose the following strategy with two steps. In the first step, we generate the searching set Ω based on slowest descent method [60], which first obtains the optimal minimizer within the continuous domain, and then finds discrete integer points with closest Euclidean distance from slowest ascent lines passing through the optimal continuous minimizer, such that the “good points” with small $\mathbf{a}^T \mathbf{Q} \mathbf{a}$ values are within the candidate set Ω .

In the second step, we pick up $\mathbf{a}_1, \mathbf{a}_2, \dots, \mathbf{a}_L \in \Omega$, to construct the full rank IF coefficient matrix $\mathbf{A}_{IF} = [\mathbf{a}_1, \mathbf{a}_2, \dots, \mathbf{a}_L]^T$, while in the meantime, the maximum value of $\mathbf{a}_m^T \mathbf{Q} \mathbf{a}_m$ is minimized. Then, equivalently, this optimal \mathbf{A}_{IF} will maximize the total achievable rate.

4.2.1 Candidate Set Searching Algorithm with Slowest Descent Method

We attempt to find the candidate vector set Ω for $\mathbf{a} \in \mathbb{Z}^L$, $\mathbf{a} \neq \mathbf{0}$, with small $\mathbf{a}^T \mathbf{Q} \mathbf{a}$ values based on slowest descent method. Note that originally slowest descent method [60] is presented for maximization problem with “slowest descent” from continuous maximizer. It can be symmetrically applied to minimization problem with “slowest ascent” from continuous minimizer. We keep the expression of “slowest descent method” for both cases.

First, we relax the constraint of $\mathbf{a} \in \mathbb{Z}^L$, $\mathbf{a} \neq \mathbf{0}$, and assume, instead, that \mathbf{a} can be continuous, real-valued ($\mathbf{a} \in \mathbb{R}^L$) with norm constraint² $\|\mathbf{a}\| \geq 1$, then the corresponding

²The integer constraint $\mathbf{a} \in \mathbb{Z}^L$, $\mathbf{a} \neq \mathbf{0}$ is equivalent to the constraint $\mathbf{a} \in \mathbb{Z}^L$, $\|\mathbf{a}\| \geq 1$.

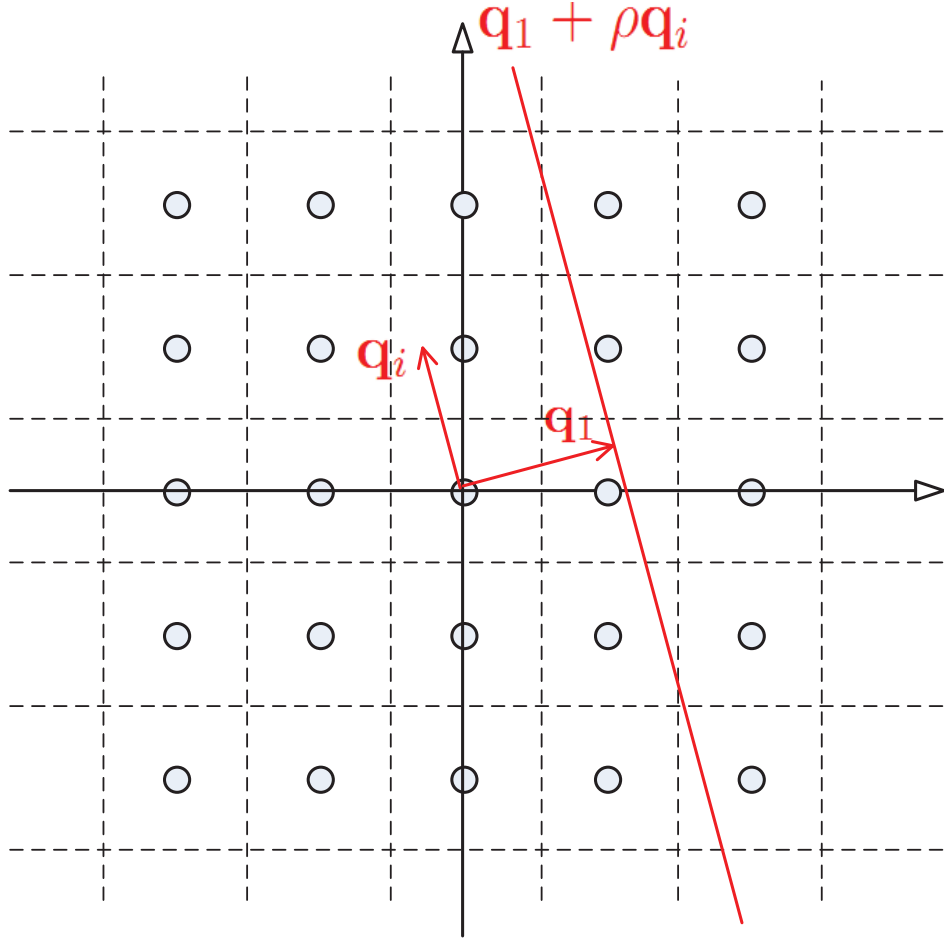


Fig. 4.3: Creation of one slowest ascent line

optimization problem becomes,

$$\mathbf{a}_c = \arg \min_{\mathbf{a} \in \mathbb{R}^L, \|\mathbf{a}\| \geq 1} \mathbf{a}^T \mathbf{Q} \mathbf{a}. \quad (4.21)$$

Denote $f(\mathbf{a})$ as the cost function, i.e.,

$$f(\mathbf{a}) \triangleq \mathbf{a}^T \mathbf{Q} \mathbf{a}. \quad (4.22)$$

Let $\mathbf{q}_1, \mathbf{q}_2, \dots, \mathbf{q}_L$ be the L normalized eigenvectors of \mathbf{Q} with corresponding eigenvalues $\lambda_1 \leq \lambda_2 \leq \dots \leq \lambda_L$. The real-valued vector for the optimization of (4.21) is well known and equal to the eigenvector that corresponds to the minimum eigenvalue of matrix \mathbf{Q} , i.e.,

$$\mathbf{a}_c = \arg \min_{\mathbf{a} \in \mathbb{R}^{2L}, \|\mathbf{a}\| \geq 1} f(\mathbf{a}) = \mathbf{q}_1. \quad (4.23)$$

The Hessian of $f(\mathbf{a})$, which is defined as $\mathbf{H}_{es}^f(\mathbf{a}) \triangleq (\partial^2 f(\mathbf{a})) / (\partial \mathbf{a} \partial \mathbf{a}^T)$ is

$$\mathbf{H}_{es}^f(\mathbf{a}) = (\partial^2 f(\mathbf{a})) / (\partial \mathbf{a} \partial \mathbf{a}^T) = \mathbf{Q}, \quad (4.24)$$

and well defined at the continuous minimizer vector \mathbf{q}_1 .

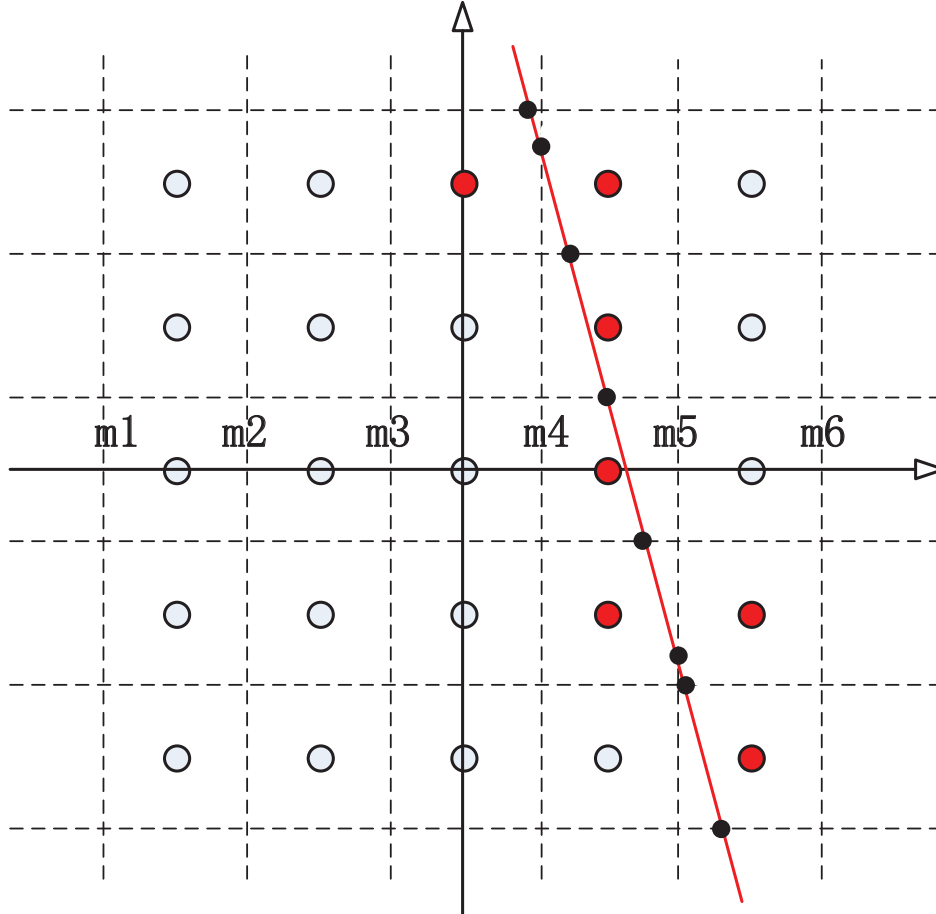


Fig. 4.4: The procedure of slowest descent method

Then, the eigenvectors $\mathbf{q}_2, \mathbf{q}_3, \dots, \mathbf{q}_L$ of the Hessian $\mathbf{H}_{es}^f(\mathbf{a}) = \mathbf{Q}$ defines mutually orthogonal directions of the least ascent in $f(\mathbf{a})$ from the continuous minimizer $\mathbf{a}_c = \mathbf{q}_1$ [60]. Accordingly, we can construct the slowest ascent lines as

$$L(\rho, i) = \mathbf{q}_1 + \rho \mathbf{q}_i, \quad \rho \in \mathbb{R}, \quad i = 2, \dots, L, \quad (4.25)$$

which pass through the real minimizer $\mathbf{a}_c = \mathbf{q}_1$ with the direction of \mathbf{q}_i .

The creation of one slowest ascent line $\mathbf{q}_1 + \rho \mathbf{q}_i$ is shown in Fig. 4.3. We can see that

when ρ takes values from $(-\infty, \infty)$, $\rho \mathbf{q}_i$ is a line in the direction of \mathbf{q}_i , hence $\mathbf{q}_1 + \rho \mathbf{q}_i$ is a line passing through \mathbf{q}_1 and parallel with the direction of \mathbf{q}_i .

Those ‘‘good’’ vectors $\mathbf{a} \in \mathbb{Z}^{2L}$, $\mathbf{a} \neq \mathbf{0}$ that have small $f(\mathbf{a})$ values stays close to those slowest ascent lines. Thus, we are trying to identify those vectors that are closest in Euclidean distance to the above slowest ascent lines, which are the set of candidate vectors

$$\Omega = \{\mathbf{a}(\rho, i) : \rho \in \mathbb{R}, i = 2, \dots, L\}, \quad (4.26)$$

with

$$\mathbf{a}(\rho, i) = \arg \min_{\mathbf{a} \in \mathbb{Z}^L, \mathbf{a} \neq \mathbf{0}} \|\mathbf{a} - L(\rho, i)\|. \quad (4.27)$$

Let M be the bound for searching vector $\mathbf{a} \in \mathbb{Z}^L$ in each coordinate, i.e., each coordinate of \mathbf{a} takes integer value form $[-M, M]$. Denote m_j , $j = 1, 2, \dots, 2M + 2$ as the midpoints of adjacent discrete points and the bounds of edge points, i.e., m_j takes value from $[-M - \frac{1}{2}, M + \frac{1}{2}]$ with increasing step equal to one. In other words, $m_j \in \Lambda$, where

$$\Lambda = \{-M - \frac{3}{2} + j, j = 1, 2, \dots, 2M + 2\}. \quad (4.28)$$

For one slowest ascent line $\mathbf{q}_1 + \rho \mathbf{q}_i$, the closest points to this line changes as ρ varies. To determine those points, it suffices to find the value of ρ for which $\mathbf{a}(\rho, i)$ exhibits a jump. We may partition the real axis as

$$(-\infty, \rho_1], (\rho_1, \rho_2], \dots, (\rho_{T-1}, \rho_T], (\rho_T, +\infty), \quad (4.29)$$

such that within each interval $(\rho_i, \rho_{i+1}]$, $i = 1, \dots, T$, there exists exactly one discrete point \mathbf{a} closest to the slowest ascent line.

Denote $\mathbf{q}_1 = [q_{11}, q_{12}, \dots, q_{1,L}]^T$ and $\mathbf{q}_i = [q_{i1}, q_{i2}, \dots, q_{i,L}]^T$. Then a jump in one component of $\mathbf{a}(\rho, i)$ occurs when ρ takes the following value,

$$\rho'_{(j-1)*L+k} = \frac{m_j - q_{1k}}{q_{ik}}, \quad (4.30)$$

with $k = 1, \dots, L$, and $j = 1, \dots, 2M + 2$.

After sorting the $\rho'_{1,1}, \rho'_{1,2}, \dots, \rho'_{(2M+2) \times 2L}$ calculated from (4.30) in ascending order, we will get the $\rho_1, \rho_2, \dots, \rho_T$ for the partition of (4.29) with $T \leq (2M + 2) \times 2L$.

Now that we have those intervals for ρ , we are ready to find the points closest to the slowest ascent line $\mathbf{q}_1 + \rho\mathbf{q}_i$. For one interval $(\rho_j, \rho_{j+1}]$, $j = 1, \dots, T - 1$, we can let ρ take the value of

$$\rho = \frac{1}{2}(\rho_j + \rho_{j+1}), \quad (4.31)$$

and calculate the closest point $\mathbf{a}_{(\rho_j, \rho_{j+1}], i}$ by rounding to the closest integer point as

$$\mathbf{a}_{(\rho_j, \rho_{j+1}], i} = \text{round} \left(\mathbf{q}_1 + \frac{1}{2}(\rho_j + \rho_{j+1})\mathbf{q}_i \right). \quad (4.32)$$

After searching through all $T - 1$ intervals of ρ , we clear the points beyond the bounds $[-M, M]$ in any coordinate, excludes the zero vector³ and put all the final validate points that closest to one slowest ascent line $\mathbf{q}_1 + \rho\mathbf{q}_i$ in the set of Ω_{i-1} , $i \in \{2, \dots, L\}$.

Finally, for J slowest ascent lines, $1 \leq J \leq L - 1$, we obtain the candidate vector set

$$\Omega = \Omega_1 \cup \Omega_2 \cup \dots \cup \Omega_J. \quad (4.33)$$

The procedure of slowest descent method is shown in Fig. 4.4. In this example, the bound for searching vector \mathbf{a} in each coordinate is $M = 2$, i.e., each coordinate takes value from $[-2, -1, 0, 1, 2]$. m_j , $j = 1, 2, \dots, 6$ is among $\Lambda = [-2.5, -1.5, -0.5, 0.5, 1.5, 2.5]$. There exists a jump in one component of searching vector \mathbf{a} when ρ takes value in some interval edge such that the slowest ascent line $\mathbf{q}_1 + \rho\mathbf{q}_i$ passes the dark solid dots. Within two dark solid dots, there exists only one point closest to the slowest ascent line. After proceeding the described slowest descent method, the outcome candidate points are shown with red solid points.

The complexity reduction of our proposed algorithm for candidate vector set algorithm based on slowest descent method with direct exhaustive search is remarkable. Even when we restrict the direct exhaustive search among the same bound $[-M, M]$ in every coordinate for the searching vector, the direct exhaustive search will need to consider $(2M + 1)^L$ searching vectors, which is exponential to L . While with our proposed algorithm with slowest descent method, we only need to consider $T \leq (2M + 2) \times L$ points for each slowest ascent line. For J slowest ascent lines, the total vectors considered will

³We add the zero points to facilitate the searching. At the end of the procedure, the vector with all-zero coordinates will exclude.

be less than $(2M + 2)J \times L$. Simulation will show that only a few slowest descent lines need to be considered. Hence, the total complexity of proposed algorithm for candidate vector set algorithm based on slowest descent method will be polynomial to L .

We summarize our proposed algorithm for candidate vector set Ω search based on slowest descent method as follows.

Algorithm 4.1 Candidate Set Search Algorithm with Slowest Descent Method

Input: Matrix \mathbf{Q} , the bound for each coordinate M , and the number of slowest descent lines J .

Output: The searching vector candidate set Ω .

Step 1: Calculate the eigenvectors $\mathbf{q}_1, \mathbf{q}_2, \dots, \mathbf{q}_L$ of matrix \mathbf{Q} with corresponding eigenvalues $\lambda_1 \leq \lambda_2 \leq \dots \leq \lambda_L$.

Step 2: Compute the set of Λ which $m_j, j = 1, 2, \dots, 2M + 2$ takes value from,

$$\Lambda = \left\{ -M - \frac{3}{2} + j, j = 1, 2, \dots, 2M + 2 \right\}. \quad (4.34)$$

Step 3: For $i = 2, \dots, J + 1$ ($1 \leq J \leq L - 1$), do

(i) Obtain the jumping points where ρ takes value as

$$\rho'_{(j-1)*L+k} = \frac{m_j - q_{1k}}{q_{ik}},$$

with $k = 1, \dots, L, j = 1, \dots, 2M + 2$.

(ii) Sort $\rho'_1, \rho'_2, \dots, \rho'_{(2M+2) \times L}$ in ascending order into $\rho_1, \rho_2, \dots, \rho_T$.

(iii) For each interval $(\rho_j, \rho_{j+1}]$, $j = 1, \dots, T - 1$, we take the value of ρ as

$$\rho = \frac{1}{2}(\rho_j + \rho_{j+1}),$$

and calculate the closest point $\mathbf{a}_{(\rho_j, \rho_{j+1}], i}$ as

$$\mathbf{a}_{(\rho_j, \rho_{j+1}], i} = \text{round} \left(\mathbf{q}_1 + \frac{1}{2}(\rho_j + \rho_{j+1})\mathbf{q}_i \right).$$

(iv) Clear the points beyond the bounds $[-M, M]$ in any coordinate, excludes the zero vector and put all the final validate points that closest to one slowest ascent line $\mathbf{q}_1 + \rho\mathbf{q}_i$ in set Ω_{i-1} .

Step 3: After searching along J slowest ascent lines, we obtain

$$\Omega = \Omega_1 \cup \Omega_2 \cup \dots \cup \Omega_J. \quad (4.35)$$

4.2.2 Constructing IF Coefficient Matrix \mathbf{A}_{IF}

According to our proposed candidate set search algorithm with slowest descent method, we get the feasible searching set Ω for IF vectors $\mathbf{a}_1, \mathbf{a}_2, \dots, \mathbf{a}_L$. With function $f(\cdot)$ defined in (4.22), we sort all vectors within the candidate set Ω such that

$$\Omega = \{\mathbf{t}_1, \mathbf{t}_2, \dots, \mathbf{t}_{|\Omega|} : f(\mathbf{t}_1) \leq f(\mathbf{t}_2) \leq \dots \leq f(\mathbf{t}_{|\Omega|})\}. \quad (4.36)$$

We are trying to choose L linear independent vectors within this sorted set by

$$\mathbf{a}_1 = \mathbf{t}_{i_1}, \mathbf{a}_2 = \mathbf{t}_{i_2}, \dots, \mathbf{a}_L = \mathbf{t}_{i_L}, \text{ for some } i_1 < i_2 < \dots < i_L, \quad (4.37)$$

then the constructed IF coefficient matrix \mathbf{A}_{IF} has full rank L . We will select $\mathbf{a}_1, \mathbf{a}_2, \dots, \mathbf{a}_L$ in Ω based on the greedy search algorithm [53].

The procedure try to find $\mathbf{a}_1, \mathbf{a}_2, \dots, \mathbf{a}_L$ sequentially and is described as follows,

$$\begin{aligned} \mathbf{a}_1 &= \mathbf{t}_1 \\ \mathbf{a}_2 &= \arg \min_{\mathbf{t} \in \Omega} \{f(\mathbf{t}) \mid \mathbf{t}, \mathbf{a}_1 \text{ are linearly independent}\} \\ \mathbf{a}_3 &= \arg \min_{\mathbf{t} \in \Omega} \{f(\mathbf{t}) \mid \mathbf{t}, \mathbf{a}_1, \mathbf{a}_2 \text{ are linearly independent}\} \\ &\vdots \\ \mathbf{a}_L &= \arg \min_{\mathbf{t} \in \Omega} \{f(\mathbf{t}) \mid \mathbf{t}, \mathbf{a}_1, \dots, \mathbf{a}_{L-1} \text{ are linearly independent}\} \end{aligned}$$

We summarize this procedure to constructing the full rank optimal matrix \mathbf{A}_{IF} with candidate vector set Ω as follows.

Algorithm 4.2 IF Coefficient Matrix Constructing with Greedy Search Algorithm

Input: Searching set Ω , Matrix \mathbf{Q} .

Output: The IF coefficient matrix \mathbf{A}_{IF} with full rank that gives

the maximum total achievable rate \mathcal{R}_{total} .

Step 1: Let $f(\mathbf{t}) = \mathbf{t}^T \mathbf{Q} \mathbf{t}$ and sort all vectors in the searching candidate set Ω such that

$$\Omega = \{\mathbf{t}_1, \mathbf{t}_2, \dots, \mathbf{t}_{|\Omega|} : f(\mathbf{t}_1) \leq f(\mathbf{t}_2) \leq \dots \leq f(\mathbf{t}_{|\Omega|})\}.$$

Set $\mathbf{a}_1 = \mathbf{t}_1$. Initialize $i = 1$ and $j = 1$.

Step 2: While $i < |\Omega|$ and $j < L$, do

(i) Set $i = i + 1$.

(ii) If $\mathbf{t}_i, \mathbf{a}_1, \dots, \mathbf{a}_j$ are linearly independent, then:

Set $j = j + 1$,

$\mathbf{a}_j = \mathbf{t}_i$.

Else goto Step 2.

Step 3: Construct the full rank IF coefficient matrix \mathbf{A} as $\mathbf{A} = [\mathbf{a}_1, \mathbf{a}_2, \dots, \mathbf{a}_L]^T$.

4.3 Experimental Studies

We present numerical results to evaluate the performance of our proposed algorithm for IF receiver design. First, we discuss the IF performance with respect to some parameters. One of them is J , which represents how many slowest ascent lines are chosen during the candidate set search procedure. For an example setting with $L = 8$, which J can take values in $[1, 2, \dots, 7]$, we average over 10000 randomly generated channel realizations and show the average rate in Fig. 4.5. The bound for each coordinate of searching vector is $M = 2$. We can see that as J increases, since the candidate set $\Omega = \Omega_1 \cup \Omega_2 \dots \cup \Omega_J$ will expand, the performance is getting better as expected. However, we do not need to span

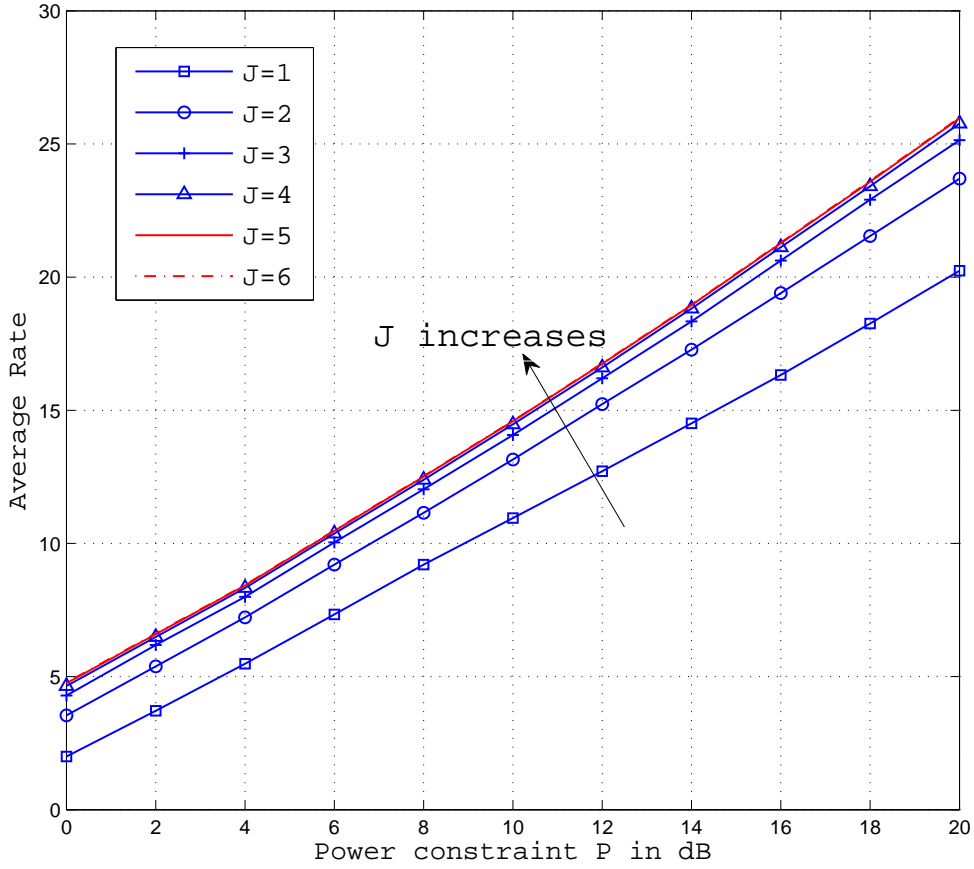


Fig. 4.5: IF performance regarding J ($L=8, M=2$)

all slowest ascent lines since the performance improvements are becoming indifferent as J becomes larger, for example, $J \geq 4$, which means further increase of J will not have much effect on the performance.

With the same simulation settings, in Fig. 4.6, we show the probability of successful construction of IF matrix after running the proposed candidate set search algorithm with slowest descent method and IF coefficient matrix constructing with greedy search algorithm. When the candidate set Ω is too small, there are chances that we could not construct a full rank IF coefficient matrix with those vectors in Ω . Since the candidate set Ω is expanding with regarding to the setting of J , the successful construction probability will raise as J increases, which we can observe in Fig. 4.6. On the other hand, when

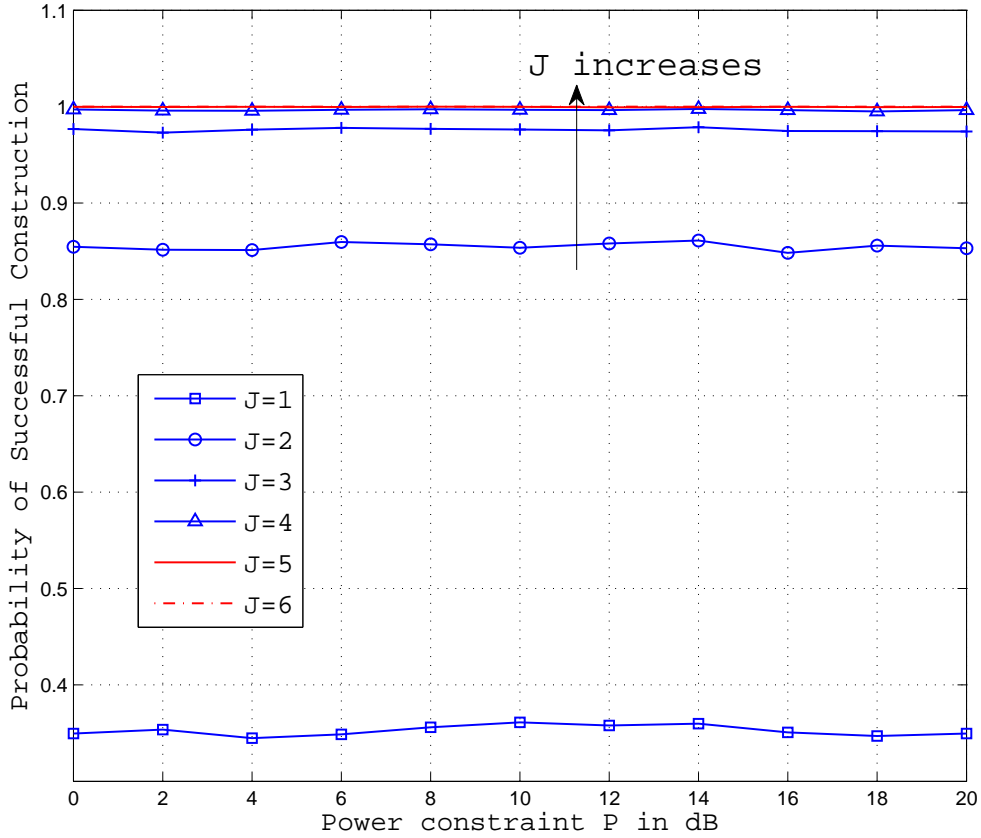


Fig. 4.6: Probability of successful IF matrix construction regarding J ($L=8, M=2$)

$J \geq 4$, the successful probability of IF integer matrix is almost equal to 1, which means we do not need to consider all $L - 1$ slowest ascent lines.

Next, we investigate the IF performance regarding the parameter of M , which is the bound for each coordinate of searching vector. In other words, for searching vector $\mathbf{a} = [a_1, a_2, \dots, a_L]$, the bound M restrict $a_i \in \mathbb{Z}$ and $|a_i| \leq M$. Obviously when M is expanding, the IF performance is getting improved since we are searching among a broader space. In Fig. 4.7, we show the average rate with respect to the setting example of M with $L = 8$ and $J = 4$ over 10000 randomly generated channel realizations. $M = 1$ means each coordinate of the searching vector takes value within $[-1, 0, 1]$; $M = 2$ means each coordinate of the searching vector takes value within $[-2, -1, 0, 1, 2]$, and so on. We can observe that when $M \geq 2$, further expanding of M actually does not help improving

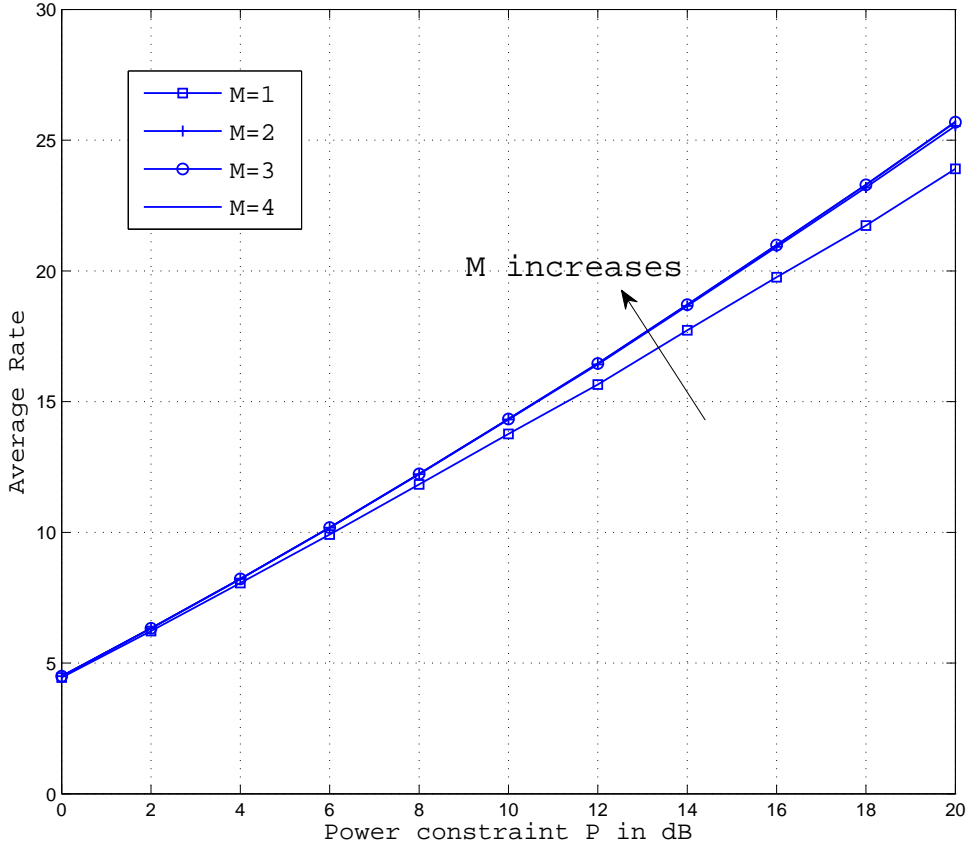


Fig. 4.7: IF performance regarding M ($L=8, J=4$)

the performance any more. This is because those “good” vectors $\mathbf{a} \in \mathbb{Z}^L$, $\mathbf{a} \neq \mathbf{0}$ that have small $\mathbf{a}^T \mathbf{Q} \mathbf{a}$ values stay close to the continuous minimizer (4.23) and tends to have small coordinates. As shown in Fig. 4.7, $M = 2$ is good enough for this setting example. Hence, for different settings, we can investigate and decide the proper J and M parameters for further realizations.

After the parameters setting discussion, we are ready to compare the performance of different linear detection methods. The standard linear detection methods of ZF and MMSE are included for comparisons. We also take account in the channel capacity of $C = \frac{1}{2} \log \det(\mathbf{I}_L + P\mathbf{H}\mathbf{H}^T)$, which represents the upper bound for all receiver structures, linear or non-linear including joint ML. In Fig. 4.8, we show the rate comparisons over MIMO channels with $L = 4$, $J = 2$, $M = 2$ and average of 10000 randomly generated

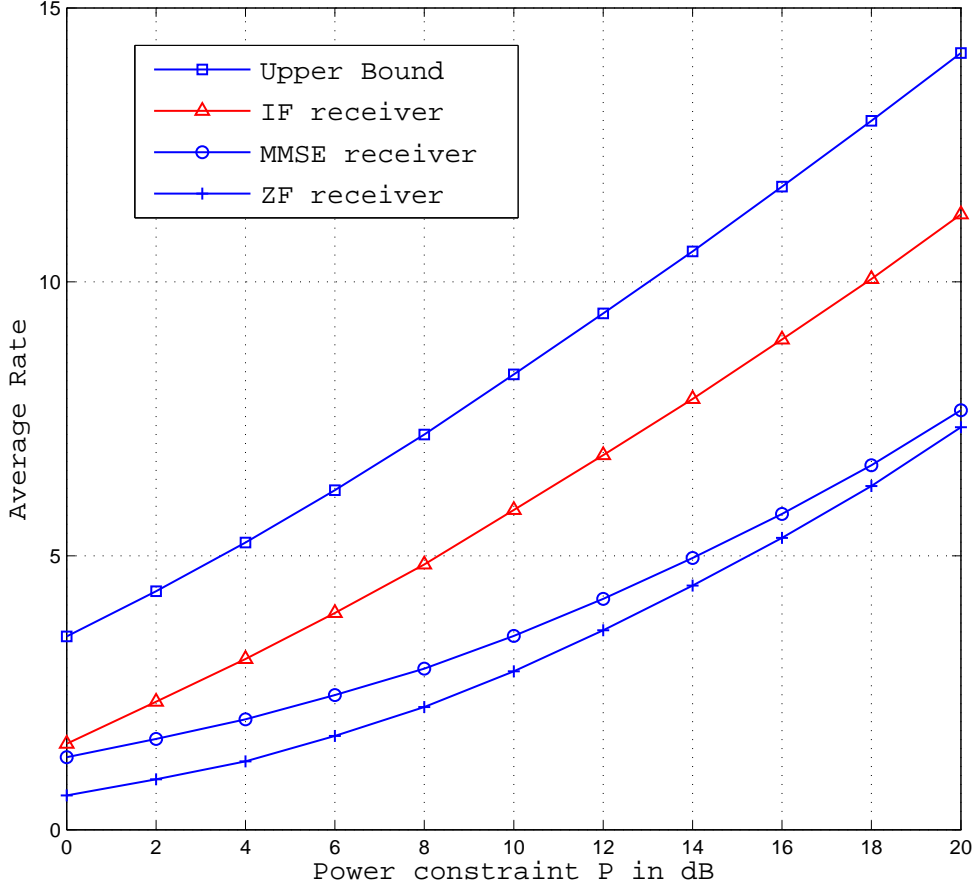


Fig. 4.8: Rate comparisons of different linear detectors ($L=4, J=2, M=2$)

channel realizations. The designed IF linear receiver with IF coefficient matrix \mathbf{A}_{IF} obtained by our proposed algorithms, the average rate is significantly improved compared to ZF and MMSE linear receiver. We repeat our experimental in Fig. 4.9 with $L = 6$, $J = 3$, $M = 2$, in Fig. 4.10 with $L = 8$, $J = 4$, $M = 2$. Similar conclusions can be drawn.

4.4 Conclusion

Motivated by recently presented integer-forcing linear receiver architecture, in this paper, we consider the problem of IF linear receiver design with respect to the channel condi-

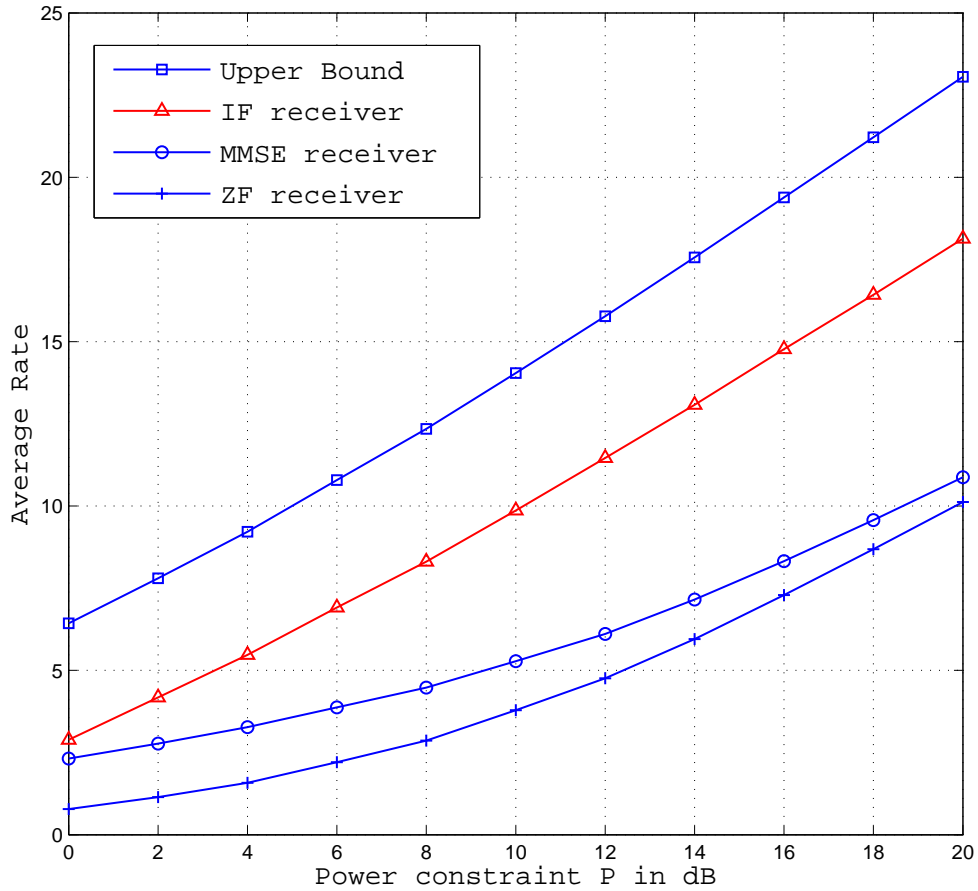


Fig. 4.9: Rate comparisons of different linear detectors ($L=6, J=3, M=2$)

tions. We present practical and efficient algorithms to design the IF full rank coefficient matrix with integer elements, such that the total achievable rate is maximized, based on the slowest descent method. First we will generate feasible searching set with integer vector search near the continuous-valued lines of least metric increase from the continuous minimizer in the Euclidean vector space. Then we try to pick up integer vectors within our searching set to construct the full rank IF coefficient matrix, while in the meantime, the total achievable rate is maximized. Numerical studies discuss the parameter settings and comparisons of other traditional linear receivers.

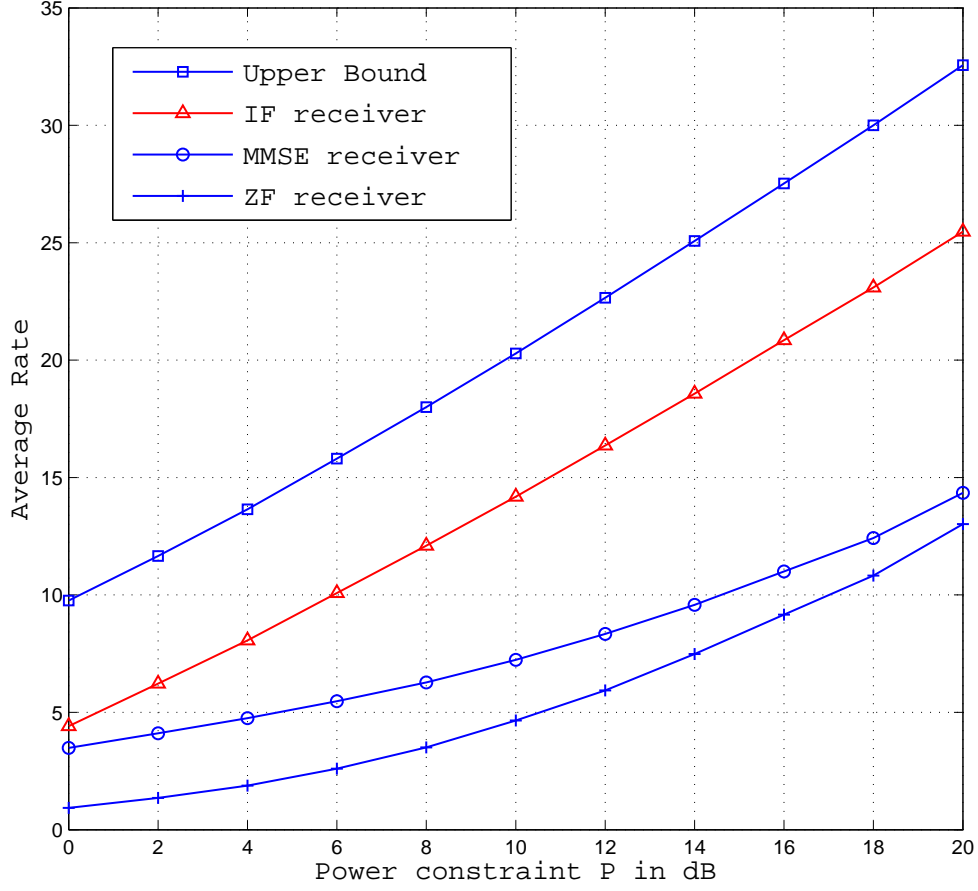


Fig. 4.10: Rate comparisons of different linear detectors ($L=8, J=4, M=2$)

4.5 Appendix

Proof of Equations (4.17)-(4.18)

Denote $\mathcal{L} \triangleq \frac{1}{P} \|\mathbf{b}_m\|^2 + \|\mathbf{H}^T \mathbf{b}_m - \mathbf{a}_m\|^2$, then

$$\mathcal{L} = \frac{1}{P} \mathbf{b}_m^T \mathbf{b}_m + \mathbf{b}_m^T \mathbf{H} \mathbf{H}^T \mathbf{b}_m - \mathbf{a}_m^T \mathbf{H}^T \mathbf{b}_m - \mathbf{b}_m^T \mathbf{H} \mathbf{a}_m + \mathbf{a}_m^T \mathbf{a}_m.$$

Let $\mathcal{F} \triangleq \mathbf{H} \mathbf{H}^T + \frac{1}{P} \mathbf{I}_L$. Accordingly the optimal \mathbf{b}_m^T can be written as

$$\begin{aligned} \mathbf{b}_m^T &= \mathbf{a}_m^T \mathbf{H}^T \left(\mathbf{H} \mathbf{H}^T + \frac{1}{P} \mathbf{I}_L \right)^{-1} \\ &= \mathbf{a}_m^T \mathbf{H}^T \mathcal{F}^{-1}. \end{aligned}$$

Plug in this optimal \mathbf{b}_m^T in \mathcal{L} , we have

$$\begin{aligned}
\mathcal{L} &= \mathbf{a}_m^T \frac{\mathbf{H}^T \mathcal{F}^{-1}}{P} \mathbf{b}_m + \mathbf{a}_m^T \mathbf{H}^T \mathcal{F}^{-1} \mathbf{H} \mathbf{H}^T \mathbf{b}_m - \mathbf{a}_m^T \mathbf{H}^T \mathbf{b}_m \\
&\quad - \mathbf{a}_m^T \mathbf{H}^T \mathcal{F}^{-1} \mathbf{H} \mathbf{a}_m + \mathbf{a}_m^T \mathbf{a}_m \\
&= \mathbf{a}_m^T \mathbf{H}^T \mathcal{F}^{-1} \underbrace{\left(\frac{1}{P} \mathbf{I}_L + \mathbf{H} \mathbf{H}^T \right)}_{\mathcal{F}} \mathbf{b}_m - \mathbf{a}_m^T \mathbf{H}^T \mathbf{b}_m \\
&\quad - \mathbf{a}_m^T \mathbf{H}^T \mathcal{F}^{-1} \mathbf{H} \mathbf{a}_m + \mathbf{a}_m^T \mathbf{a}_m \\
&= \mathbf{a}_m^T \mathbf{a}_m - \mathbf{a}_m^T \mathbf{H}^T \mathcal{F}^{-1} \mathbf{H} \mathbf{a}_m \\
&= \mathbf{a}_m^T \underbrace{(\mathbf{I}_L - \mathbf{H}^T \mathcal{F}^{-1} \mathbf{H})}_{\mathbf{Q}} \mathbf{a}_m.
\end{aligned}$$

Hence, the computation rate

$$\begin{aligned}
\mathcal{R}_m &= \frac{1}{2} \log \left(\frac{P}{\|\mathbf{b}_m\|^2 + P \|\mathbf{H}^T \mathbf{b}_m - \mathbf{a}_m\|^2} \right) \\
&= \frac{1}{2} \log \left(\frac{1}{\mathcal{L}} \right) \\
&= \frac{1}{2} \log \left(\frac{1}{\mathbf{a}_m^T \mathbf{Q} \mathbf{a}_m} \right),
\end{aligned}$$

where

$$\begin{aligned}
\mathbf{Q} &= \mathbf{I}_L - \mathbf{H}^T \mathcal{F}^{-1} \mathbf{H} \\
&= \mathbf{I}_L - \mathbf{H}^T \left(\mathbf{H} \mathbf{H}^T + \frac{1}{P} \mathbf{I}_L \right)^{-1} \mathbf{H}.
\end{aligned}$$

□

Chapter 5

Network Coding in Wireless Cooperative Networks with Multiple Antenna Relays

In this Chapter, we consider network coding application in wireless multiple access relay channels. Four system models are considered:

- (i) System model A: Two sources without direct links;
- (ii) System model B: Two sources with direct links;
- (iii) System model C: Three sources with direct links;
- (iv) System model D: Four sources with direct links.

5.1 System Model A: Two Sources Without Direct Links

Consider cooperative system with two sources: multiple access relay channels without direct links. Two sources \mathcal{S}_1 , \mathcal{S}_2 communicate with destination \mathcal{D} via a relay \mathcal{R} without direct links from sources to destination, as shown in Fig. 5.1. We assume the sources \mathcal{S}_1 , \mathcal{S}_2 and the destination \mathcal{D} are equipped with single antenna, while relay \mathcal{R} is equipped with two antennas.

The information transmission is performed in two phases with three time slots in total. In the first phase two source nodes transmit simultaneously to relay \mathcal{R} in one time

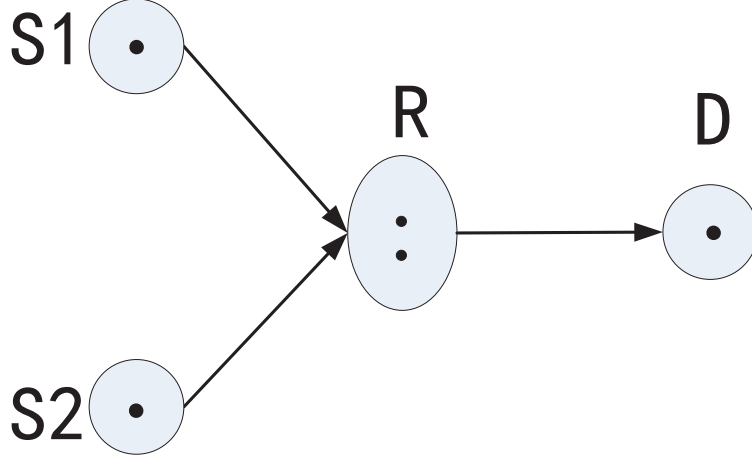


Fig. 5.1: System model A

slot; while in the second phase relay \mathcal{R} transmits to destination \mathcal{D} in the remaining two time slots.

The received signal at relay \mathcal{R} at the end of first phase is

$$\mathbf{y}_R = \begin{bmatrix} y_{R1} \\ y_{R2} \end{bmatrix} = \sqrt{E_x} \underbrace{\begin{bmatrix} h_{11} & h_{12} \\ h_{21} & h_{22} \end{bmatrix}}_{\mathbf{H}} \underbrace{\begin{bmatrix} x_1 \\ x_2 \end{bmatrix}}_{\mathbf{x}} + \mathbf{n}_R, \quad (5.1)$$

where $\mathbf{y}_R = [y_{R1}, y_{R2}]^T$ is the received vector at relay with two antennas; x_i is the transmit data symbol¹ from node \mathcal{S}_i which has been normalized to $E\{|x_i|^2\} = 1$; E_x is the power constraint for data symbol transmission. The transmitting data vector of two sources is denoted as

$$\mathbf{x} = [x_1, x_2]^T, \quad (5.2)$$

and $\mathbf{x} \in \Omega_{\mathbf{x}}$, where $\Omega_{\mathbf{x}}$ is the data vector alphabet set; $\mathbf{n}_R = [n_{R1}, n_{R2}]^T$ is the additive Gaussian noise vector at relay; h_{ri} is the channel coefficient between source node \mathcal{S}_i and relay antenna r and we define

$$\mathbf{h}_r \triangleq [h_{r1}, h_{r2}]^T. \quad (5.3)$$

All channel coefficients and additive noise elements are generated i.i.d. according to a normal distribution $\mathbb{CN}(0, 1)$.

¹For source \mathcal{S}_i , x_i is the transmitted symbol after modulation based on the transmitted bit b_i .

In the second phase, relay \mathcal{R} will transmit to the destination \mathcal{D} according to different schemes. As no direct links exist in system model A, physical layer network coding (PLNC) cannot be applied in system model A directly. Note that all schemes take three time slots for one transmission realization.

5.1.1 Different Schemes for System Model A

(i) System Model A Scheme 1: Decode-and-Forward (DF)

With this scheme, after receiving \mathbf{y}_R in (5.1), relay \mathcal{R} will first decode for two sources

$$\hat{\mathbf{x}}_R = \begin{bmatrix} \hat{x}_{R1} \\ \hat{x}_{R2} \end{bmatrix} = \arg \min_{\mathbf{x} \in \Omega_{\mathbf{x}}} \|\mathbf{y}_R - \sqrt{E_x} \mathbf{H} \mathbf{x}\|^2. \quad (5.4)$$

Then, relay \mathcal{R} will transmit \hat{x}_{R1} and \hat{x}_{R2} in two time slots as follows,

$$\begin{aligned} \mathbf{y}_D &= \sqrt{E_R} \begin{bmatrix} \hat{x}_{R1} & 0 \\ 0 & \hat{x}_{R2} \end{bmatrix} \begin{bmatrix} g_1 \\ g_2 \end{bmatrix} + \mathbf{n}_D \\ &= \sqrt{E_R} \underbrace{\begin{bmatrix} g_1 & 0 \\ 0 & g_2 \end{bmatrix}}_{\mathbf{G}_1} \begin{bmatrix} \hat{x}_{R1} \\ \hat{x}_{R2} \end{bmatrix} + \mathbf{n}_D, \end{aligned} \quad (5.5)$$

which is equivalent to

$$\mathbf{y}_D = \sqrt{E_R} \mathbf{G}_1 \hat{\mathbf{x}}_R + \mathbf{n}_D, \quad (5.6)$$

where g_r , $r = 1, 2$ is the channel coefficient between relay antenna r and destination \mathcal{D} .

The decoding procedure at destination \mathcal{D} will be

$$\hat{\mathbf{x}} = \arg \min_{\mathbf{x} \in \Omega_{\mathbf{x}}} \|\mathbf{y}_D - \sqrt{E_R} \mathbf{G}_1 \mathbf{x}\|^2. \quad (5.7)$$

(ii) System Model A Scheme 2: Space Time Decode-and-Forward (STDF)

In this scheme, relay \mathcal{R} will first decode for two sources the same way as scheme 1, equation (5.4), then transmit \hat{x}_{R1} and \hat{x}_{R2} according to Alamouti space time coding [68].

In the second time slot, the relay will transmit $[\hat{x}_{R1}, \hat{x}_{R2}]^T$ and in the third time slot, the relay will transmit $[-\hat{x}_{R2}^*, \hat{x}_{R1}^*]^T$. Denote the corresponding received signals at destination \mathcal{D} in the second phase (with two time slots) as y_{D1} and y_{D2} , then

$$[y_{D1}, y_{D2}] = \sqrt{E_R} [g_1, g_2] \begin{bmatrix} \hat{x}_{R1} & -\hat{x}_{R2}^* \\ \hat{x}_{R2} & \hat{x}_{R1}^* \end{bmatrix} + [n_{D1}, n_{D2}]. \quad (5.8)$$

After receiving signals from relay \mathcal{R} in the second phase, destination \mathcal{D} arranges the received signals into a vector $\mathbf{y}_D = [y_{D1}, -y_{D2}^*]^T$, which can be rewritten as

$$\begin{aligned} \mathbf{y}_D &= \begin{bmatrix} y_{D1} \\ -y_{D2}^* \end{bmatrix} \\ &= \sqrt{E_R} \underbrace{\begin{bmatrix} g_1 & g_2 \\ -g_2^* & g_1^* \end{bmatrix}}_{\mathbf{G}_2} \begin{bmatrix} \hat{x}_{R1} \\ \hat{x}_{R2} \end{bmatrix} + \mathbf{n}_D \\ &= \sqrt{E_R} \mathbf{G}_2 \hat{\mathbf{x}}_R + \mathbf{n}_D, \end{aligned} \quad (5.9)$$

where $\mathbf{n}_D = [n_{D1}, -n_{D2}^*]^T$.

The decoding procedure at destination \mathcal{D} will be

$$\hat{\mathbf{x}} = \arg \min_{\mathbf{x} \in \Omega_{\mathbf{x}}} \|\mathbf{y}_D - \sqrt{E_R} \mathbf{G}_2 \mathbf{x}\|^2. \quad (5.10)$$

(iii) System Model A Scheme 3: Analog Network Coding (ANC)

In this scheme, relay \mathcal{R} will utilize analog network coding to process the received signals. First, after receiving \mathbf{y}_R of (5.1), relay \mathcal{R} constructs the following signal vector $\mathbf{t} = [t_1, t_2]^T$ based on the received signals on each antenna

$$\mathbf{t} = \begin{bmatrix} \beta_1 y_{R1} \\ \beta_2 y_{R2} \end{bmatrix} = \underbrace{\begin{bmatrix} \beta_1 & 0 \\ 0 & \beta_2 \end{bmatrix}}_{\mathbf{B}} (\sqrt{E_x} \mathbf{H} \mathbf{x} + \mathbf{n}_R), \quad (5.11)$$

where β_r , $r = 1, 2$ is the scaling factor to meet the per-antenna power constraint P_R at relay \mathcal{R} given by

$$\beta_r = \sqrt{\frac{1}{E\{|y_{Rr}|^2\}}} = \sqrt{\frac{1}{E_x \|\mathbf{h}_r\|^2 + 1}}. \quad (5.12)$$

Then, relay \mathcal{R} will transmit t_1 and t_2 in two time slots as follows,

$$\begin{aligned}
\mathbf{y}_D &= \sqrt{E_R} \begin{bmatrix} t_1 & 0 \\ 0 & t_2 \end{bmatrix} \begin{bmatrix} g_1 \\ g_2 \end{bmatrix} + \mathbf{n}_D \\
&= \sqrt{E_R} \underbrace{\begin{bmatrix} g_1 & 0 \\ 0 & g_2 \end{bmatrix}}_{\mathbf{G}_1} \begin{bmatrix} t_1 \\ t_2 \end{bmatrix} + \mathbf{n}_D \\
&= \sqrt{E_R} \sqrt{E_x} \mathbf{G}_1 \mathbf{B} \mathbf{H} \mathbf{x} + \sqrt{E_R} \mathbf{G}_1 \mathbf{B} \mathbf{n}_R + \mathbf{n}_D.
\end{aligned} \tag{5.13}$$

The decoding procedure at destination \mathcal{D} will be

$$\hat{\mathbf{x}} = \arg \min_{\mathbf{x} \in \Omega_{\mathbf{x}}} \|\mathbf{y}_D - \sqrt{E_R} \sqrt{E_x} \mathbf{G}_1 \mathbf{B} \mathbf{H} \mathbf{x}\|^2. \tag{5.14}$$

(iv) System Model A Scheme 4: Space Time Analog Network Coding (S-TANC)

In this scheme, we consider combine analog network coding with Alamouti space time coding. After constructing $\mathbf{t} = [t_1, t_2]^T$ as equation (5.11), relay \mathcal{R} will transmit $[t_1, t_2]^T$ in the second time slot and $[-t_2^*, t_1^*]^T$ in the third time slot. Denote the corresponding received signals at destination \mathcal{D} in the second phase (with two time slots) as y_{D1} and y_{D2} , then

$$[y_{D1}, y_{D2}] = \sqrt{E_R} [g_1, g_2] \begin{bmatrix} t_1 & -t_2^* \\ t_2 & t_1^* \end{bmatrix} + [n_{D1}, n_{D2}], \tag{5.15}$$

where g_r , $r = 1, 2$ is the channel coefficient between relay antenna r and destination \mathcal{D} .

After receiving signals from relay \mathcal{R} in the second phase, destination \mathcal{D} arranges the received signals into a vector $\mathbf{y}_D = [y_{D1}, -y_{D2}^*]^T$, which can be rewritten as

$$\begin{aligned}
\mathbf{y}_D &= \begin{bmatrix} y_{D1} \\ -y_{D2}^* \end{bmatrix} \\
&= \sqrt{E_R} \underbrace{\begin{bmatrix} g_1 & g_2 \\ -g_2^* & g_1^* \end{bmatrix}}_{\mathbf{G}_2} \begin{bmatrix} t_1 \\ t_2 \end{bmatrix} + \mathbf{n}_D \\
&= \sqrt{E_R} \sqrt{E_x} \mathbf{G}_2 \mathbf{B} \mathbf{H} \mathbf{x} + \sqrt{E_R} \mathbf{G}_2 \mathbf{B} \mathbf{n}_R + \mathbf{n}_D,
\end{aligned} \tag{5.16}$$

Model A	Time Slot 1	Time Slot 2	Time Slot 3
DF	$S1 : x_1$ $S2 : x_2$	$R : \begin{bmatrix} \hat{x}_{R1} \\ 0 \end{bmatrix}$	$R : \begin{bmatrix} 0 \\ \hat{x}_{R2} \end{bmatrix}$
STDF	$S1 : x_1$ $S2 : x_2$	$R : \begin{bmatrix} \hat{x}_{R1} \\ \hat{x}_{R2} \end{bmatrix}$	$R : \begin{bmatrix} -\hat{x}_{R2}^* \\ \hat{x}_{R1}^* \end{bmatrix}$
ANC	$S1 : x_1$ $S2 : x_2$	$R : \begin{bmatrix} t_1 \\ 0 \end{bmatrix}$	$R : \begin{bmatrix} 0 \\ t_2 \end{bmatrix}$
STANC	$S1 : x_1$ $S2 : x_2$	$R : \begin{bmatrix} t_1 \\ t_2 \end{bmatrix}$	$R : \begin{bmatrix} -t_2^* \\ t_1^* \end{bmatrix}$

Table 5.1: Different Schemes for System Model A

where $\mathbf{n}_D = [n_{D1}, -n_{D2}^*]^T$.

The decoding procedure at destination \mathcal{D} will be

$$\hat{\mathbf{x}} = \arg \min_{\mathbf{x} \in \Omega_{\mathbf{x}}} \|\mathbf{y}_D - \sqrt{E_R} \sqrt{E_x} \mathbf{G}_2 \mathbf{B} \mathbf{H} \mathbf{x}\|^2. \quad (5.17)$$

The comparison of four schemes for system model A in three slots are shown in Table 5.1.

5.1.2 Experimental Studies

We present numerical results to evaluate the performance of all possible schemes for system model A. Let $E_x = E_R$, i.e., the transmission power constraint at sources and relay are equivalent. With the average of 100000 randomly generated channel realizations, we show in Fig. 5.3 the error rate comparisons of four possible schemes for system model A (multiple access relay channel without direct links). The error rate is for the transmission signal vector \mathbf{x} defined in (5.2). All schemes are under three time slots constraint.

We can observe that space time coding technique improves the performance, i.e., STDF scheme outperforms DF scheme and STANC scheme outperforms ANC scheme. Also, the STDF scheme gives the best performance, which means, if the relay has the ability to decode, then, using STDF is a better choice among other schemes.

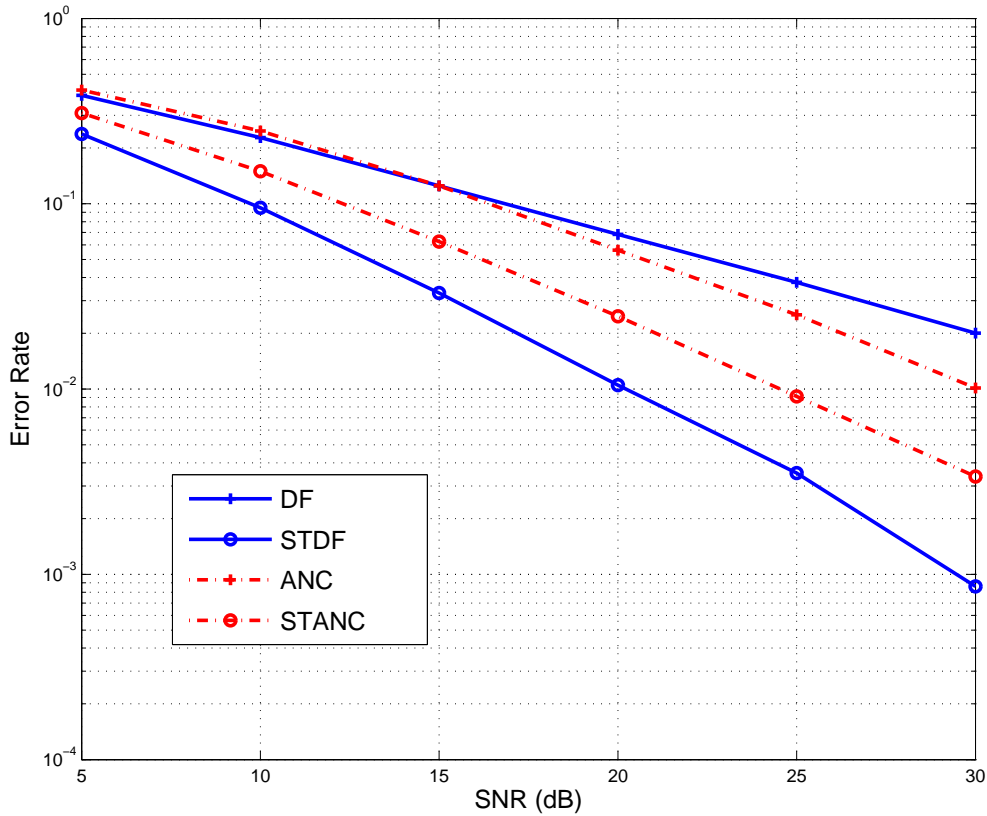


Fig. 5.2: Comparison of four schemes regarding system model A

5.2 System Model B: Two Sources With Direct Links

Consider cooperative system model B: multiple access relay channels with direct links. Two sources \mathcal{S}_1 , \mathcal{S}_2 communicate with destination \mathcal{D} via relay \mathcal{R} with direct links from sources to destination, as shown in Fig. 5.2. We also assume the sources \mathcal{S}_1 , \mathcal{S}_2 and the destination \mathcal{D} are equipped with single antenna, while relay \mathcal{R} is equipped with two antennas.

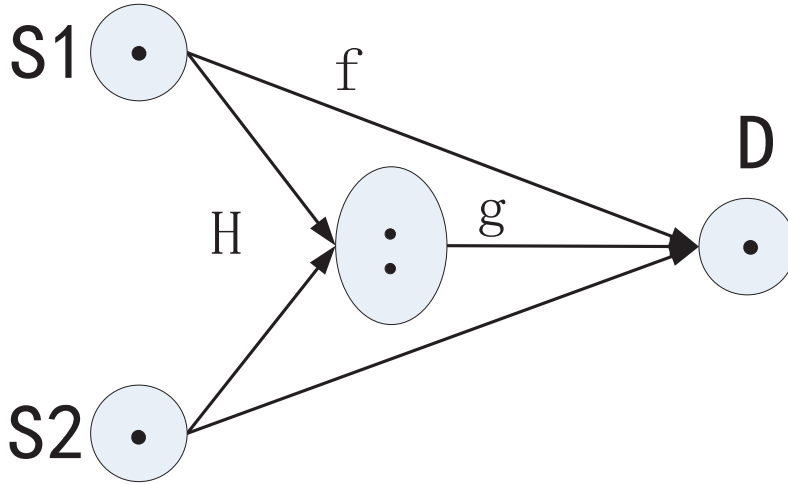


Fig. 5.3: System model B

One realization of the information transmission is performed in two time slots. We will describe in details the different four possible schemes, which all take two time slots for one transmission realization. Since we constrain the transmission is performed within two time slots, space-time coding cannot be directly applied to system model B directly.

5.2.1 Different Schemes for System Model B

(i) System Model B Scheme 1: Direct Transmission (DT)

In this scheme, we assume the relay will keep silent during all transmission realization and the sources will communicate to the destination one by one directly. \mathcal{S}_1 will transmit

in the first time slot; \mathcal{S}_2 will transmit in the second time slot.

$$\begin{aligned} y_{D1} &= \sqrt{E_x} f_1 x_1 + n_{D1}, \\ y_{D2} &= \sqrt{E_x} f_2 x_2 + n_{D2}, \end{aligned}$$

which can be combined to $\mathbf{y}_D = [y_{D1}, y_{D2}]^T$ as

$$\mathbf{y}_D = \sqrt{E_x} \underbrace{\begin{bmatrix} f_1 & 0 \\ 0 & f_2 \end{bmatrix}}_{\mathbf{F}} \underbrace{\begin{bmatrix} x_1 \\ x_2 \end{bmatrix}}_{\mathbf{x}} + \underbrace{\begin{bmatrix} n_{D1} \\ n_{D2} \end{bmatrix}}_{\mathbf{n}_D}, \quad (5.18)$$

or equivalently

$$\mathbf{y}_D = \sqrt{E_x} \mathbf{F} \mathbf{x} + \mathbf{n}_D. \quad (5.19)$$

f_i is the direct link channel coefficient between source \mathcal{S}_i to destination \mathcal{D} ; n_{Di} is the additive Gaussian noise at the i -th time slot. All channel coefficients are generated i.i.d. according to a normal distribution $\mathcal{N}(0, 1)$.

Hence the decoding procedure at destination \mathcal{D} will be

$$\hat{\mathbf{x}} = \arg \min_{\mathbf{x} \in \Omega_{\mathbf{x}}} \|\mathbf{y}_D - \sqrt{E_x} \mathbf{F} \mathbf{x}\|^2. \quad (5.20)$$

(ii) System Model B Scheme 2: Decode-and-Forward (DF)

In this scheme, two sources will transmit to relay \mathcal{R} and destination \mathcal{D} simultaneously in the first time slot, while in the second time slot relay \mathcal{R} will transmit the decoded signals to destination \mathcal{D} .

The received signal at destination \mathcal{D} at the end of first time slot is

$$y_{D1} = \sqrt{E_x} f_1 x_1 + \sqrt{E_x} f_2 x_2 + n_{D1}. \quad (5.21)$$

The received vector at relay \mathcal{R} with two antennas at the end of first time slot is

$$\mathbf{y}_R = \sqrt{E_x} \underbrace{\begin{bmatrix} h_{11} & h_{12} \\ h_{21} & h_{22} \end{bmatrix}}_{\mathbf{H}} \begin{bmatrix} x_1 \\ x_2 \end{bmatrix} + \begin{bmatrix} n_{R1} \\ n_{R2} \end{bmatrix}, \quad (5.22)$$

where h_{ri} is the channel coefficient between source node \mathcal{S}_i and relay antenna r ; n_{Ri} , $i = 1, 2$ is the additive Gaussian noise. Let

$$\mathbf{H} \triangleq [\mathbf{h}_1, \mathbf{h}_2]^T, \quad (5.23)$$

in other words, \mathbf{h}_i^T is the i -th row vector of matrix \mathbf{H} .

After receiving signals as (5.22), the relay will first decode for two sources

$$\hat{\mathbf{x}}_R = \begin{bmatrix} \hat{x}_{R1} \\ \hat{x}_{R2} \end{bmatrix} = \arg \min_{\mathbf{x} \in \Omega_{\mathbf{x}}} \|\mathbf{y}_R - \sqrt{E_x} \mathbf{H} \mathbf{x}\|^2. \quad (5.24)$$

Then, with two antennas and power constraint E_R , relay \mathcal{R} will transmit $[\hat{x}_{R1}, \hat{x}_{R2}]^T$.

The received signal at destination \mathcal{D} in the second time slot is,

$$y_{D2} = \sqrt{E_R} g_1 \hat{x}_{R1} + \sqrt{E_R} g_2 \hat{x}_{R2} + n_{D2}. \quad (5.25)$$

where g_r , $r = 1, 2$, is the channel coefficient between relay antenna r and destination \mathcal{D} .

Recall the received signals in the first time slot (5.21) and in the second time slot (5.25) at destination \mathcal{D} , we have

$$\begin{cases} y_{D1} = \sqrt{E_x} [f_1, f_2] \mathbf{x} + n_{D1}, \\ y_{D2} = \sqrt{E_R} [g_1, g_2] \hat{\mathbf{x}}_R + n_{D2}. \end{cases} \quad (5.26)$$

If we construct the matrix \mathbf{A}_1 as

$$\mathbf{A}_1 \triangleq \begin{bmatrix} \sqrt{E_x} f_1 & \sqrt{E_x} f_2 \\ \sqrt{E_R} g_1 & \sqrt{E_R} g_2 \end{bmatrix}, \quad (5.27)$$

then the decoding procedure will be

$$\hat{\mathbf{x}} = \arg \min_{\mathbf{x} \in \Omega_{\mathbf{x}}} \|\mathbf{y}_D - \mathbf{A}_1 \mathbf{x}\|^2. \quad (5.28)$$

(iii) System Model B Scheme 3: Digital Network Coding (DNC)

x_1	x_2	$x_1 + x_2$	$x_1 \oplus x_2$	$x_1 * x_2$
-1	-1	-2	-1	1
-1	1	0	1	-1
1	-1	0	1	-1
1	1	2	-1	1

Table 5.2: $x_1 \oplus x_2$ for BPSK modulation

In this scheme, two sources will also transmit to relay \mathcal{R} and destination \mathcal{D} simultaneously in the first time slot. Relay \mathcal{D} will decode for the two sources at the end of first time slot. The procedure is the same as (5.21)-(5.24). Then relay \mathcal{R} will calculate $\hat{x}_{R1} \oplus \hat{x}_{R2}$ ². For BPSK modulation, we will have the following relationship.

It is easily to conclude that

$$\hat{x}_{R1} \oplus \hat{x}_{R2} = -\hat{x}_{R1} * \hat{x}_{R2}. \quad (5.29)$$

According to digital network coding strategy, with two antennas and power constraint E_R , the relay will transmit $[\hat{x}_{R1} \oplus \hat{x}_{R2}, \hat{x}_{R1} \oplus \hat{x}_{R2}]^T$ in the second time slot,

$$\begin{aligned} y_{D2} &= \sqrt{E_R} [g_1, g_2] \begin{bmatrix} \hat{x}_{R1} \oplus \hat{x}_{R2} \\ \hat{x}_{R1} \oplus \hat{x}_{R2} \end{bmatrix} + n_{D2} \\ &= \sqrt{E_R} (g_1 + g_2)(-\hat{x}_{R1} * \hat{x}_{R2}) + n_{D2}. \end{aligned} \quad (5.30)$$

Recall the received signals in the first phase (5.21) and in the second phase (5.30) at destination \mathcal{D} , we have

$$\begin{cases} y_{D1} = \sqrt{E_x} f_1 x_1 + \sqrt{E_x} f_2 x_2 + n_{D1} \\ y_{D2} = \sqrt{E_R} (g_1 + g_2)(-\hat{x}_{R1} * \hat{x}_{R2}) + n_{D2}, \end{cases} \quad (5.31)$$

²The relay actually first demodulates \hat{x}_{Ri} to information bit \hat{b}_{Ri} , then calculate $\hat{b}_{R1} \oplus \hat{b}_{R2}$, and finally modulates them again. We simply denote the modulated $\hat{b}_{R1} \oplus \hat{b}_{R2}$ as $\hat{x}_{R1} \oplus \hat{x}_{R2}$.

and will decode $\hat{\mathbf{x}} = [\hat{x}_1, \hat{x}_2]^T$ as

$$\begin{aligned} \hat{\mathbf{x}} = \arg \min_{x_1, x_2} & \|y_{D1} - \sqrt{E_x} f_1 x_1 - \sqrt{E_x} f_2 x_2\|^2 \\ & + \|y_{D2} + \sqrt{E_R} (g_1 + g_2)(x_1 * x_2)\|^2. \end{aligned} \quad (5.32)$$

(iv) System Model B Scheme 4: Analog Network Coding (ANC)

In this scheme, relay \mathcal{R} will utilize analog network coding to process the received signals. First, after receiving \mathbf{y}_R of (5.22), relay \mathcal{R} constructs the signal vector $\mathbf{t} = [t_1, t_2]^T$ as follows,

$$\mathbf{t} = \begin{bmatrix} \beta_1 y_{R1} \\ \beta_2 y_{R2} \end{bmatrix} = \underbrace{\begin{bmatrix} \beta_1 & 0 \\ 0 & \beta_2 \end{bmatrix}}_{\mathbf{B}} (\sqrt{E_x} \mathbf{H} \mathbf{x} + \mathbf{n}_R), \quad (5.33)$$

where β_r , $r = 1, 2$ is the scaling factor at relay \mathcal{R} given by

$$\beta_r = \sqrt{\frac{1}{E\{|y_{Rr}|^2\}}} = \sqrt{\frac{1}{E_x \|\mathbf{h}_r\|^2 + 1}}. \quad (5.34)$$

Then, relay \mathcal{R} will transmit t_1, t_2 in the second time slot as follows,

$$\begin{aligned} y_{D2} &= \sqrt{E_R} [g_1, g_2] \begin{bmatrix} t_1 \\ t_2 \end{bmatrix} + n_{D2} \\ &= \sqrt{E_R} \sqrt{E_x} \mathbf{g}^T \mathbf{B} \mathbf{H} \mathbf{x} + \sqrt{E_R} \mathbf{g}^T \mathbf{B} \mathbf{n}_R + n_{D2}, \end{aligned} \quad (5.35)$$

where

$$\mathbf{g} \triangleq [g_1, g_2]^T, \quad (5.36)$$

is the channel vector between relay \mathcal{R} with two antennas to destination \mathcal{D} .

Combining the received signals in the first time slot (5.21) and in the second time slot (5.35) at destination \mathcal{D} , with $\mathbf{f} \triangleq [f_1, f_2]^T$, we have

$$\mathbf{y}_D = \underbrace{\sqrt{E_x} \begin{bmatrix} \mathbf{f}^T \\ \sqrt{E_R} \mathbf{g}^T \mathbf{B} \mathbf{H} \end{bmatrix}}_{\mathbf{A}_2} \mathbf{x} + \underbrace{\begin{bmatrix} n_{D1} \\ \sqrt{E_R} \mathbf{g}^T \mathbf{B} \mathbf{n}_R + n_{D2} \end{bmatrix}}_{\mathbf{z}}. \quad (5.37)$$

Model B	Time Slot 1	Time Slot 2
DT	$S1 : x_1$	$S2 : x_2$
DF	$S1 : x_1$ $S2 : x_2$	$R : \begin{bmatrix} \hat{x}_{R1} \\ \hat{x}_{R2} \end{bmatrix}$
DNC	$S1 : x_1$ $S2 : x_2$	$R : \begin{bmatrix} \hat{x}_{R1} \oplus \hat{x}_{R2} \\ \hat{x}_{R1} \oplus \hat{x}_{R2} \end{bmatrix}$
ANC	$S1 : x_1$ $S2 : x_2$	$R : \begin{bmatrix} t_1 \\ t_2 \end{bmatrix}$

Table 5.3: Different Schemes for System Model B

which can be decoded as

$$\hat{\mathbf{x}} = \arg \min_{\mathbf{x} \in \Omega_{\mathbf{x}}} \|\mathbf{y}_D - \mathbf{A}_2 \mathbf{x}\|^2. \quad (5.38)$$

The comparison of four schemes for system model B in three slots are shown in Table 5.3.

5.2.2 Experimental Studies

We present numerical results to evaluate the performance of all possible schemes for system model B. Let $E_x = E_R$, i.e., the transmission power constraint at sources and relay are equivalent. With the average of 100000 randomly generated channel realizations, the error rate comparison of all possible schemes for system model B is given in Fig. 5.4. All schemes are under two time slots constraint. Interestingly, we find that the schemes

of DNC and ANC both give inferior performance to the simply DF scheme, which means, when relay is equipped with multiple antennas, simply transmit decoded messages onto different antennas outperforms mixing signals as in DNC and ANC schemes.

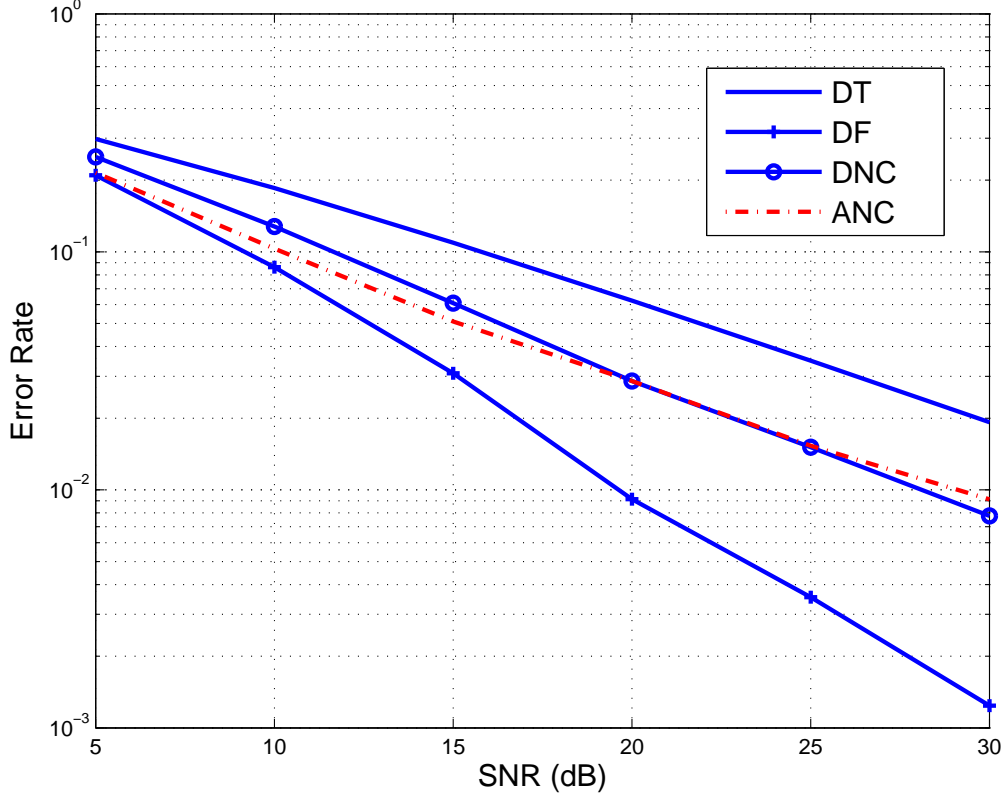


Fig. 5.4: Comparison of four schemes regarding system model B

5.3 System Model C: Three Sources with Direct Links

Consider the system model setting with three sources $\mathcal{S}_1, \mathcal{S}_2, \mathcal{S}_3$ communicating with destination \mathcal{D} via a relay \mathcal{R} , with direct links from sources to destination, as shown in Fig. 5.5. We assume sources $\mathcal{S}_1, \mathcal{S}_2, \mathcal{S}_3$ and destination \mathcal{D} are equipped with single antenna, while relay \mathcal{R} is equipped with two antennas.

We will discuss several possible transmission strategies for this system model. One realization of the information transmission will be performed within three time slots for

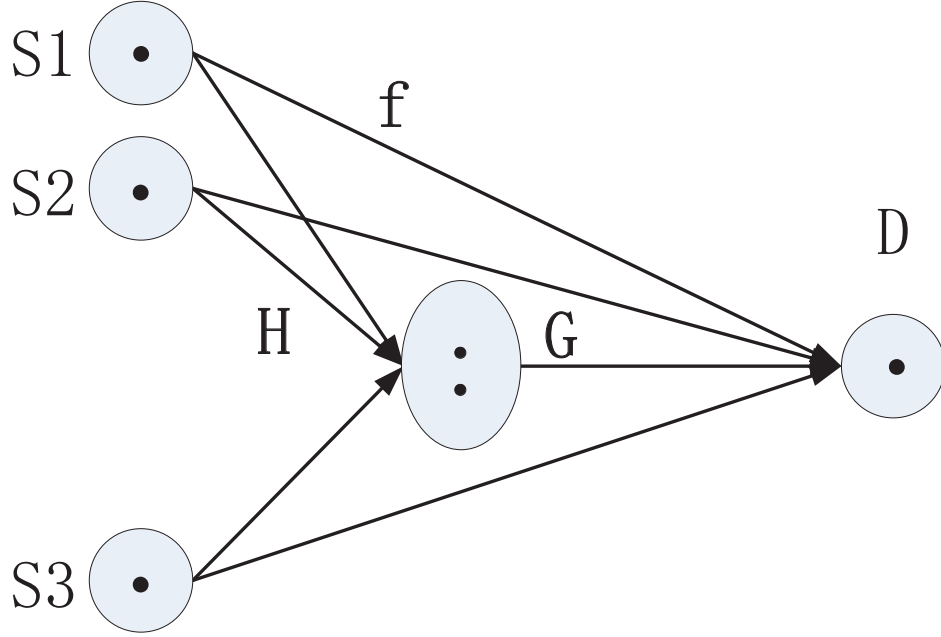


Fig. 5.5: System model C

all those strategies.

5.3.1 Different Schemes for System Model C

(i) System Model C Scheme 1: Direct transmission (DT)

In this scheme, we assume the relay will keep silent during all transmission realization and the sources will communicate to the destination one by one, which also takes three time slots. In the first time slot, \mathcal{S}_1 will transmit; in the second time slot, \mathcal{S}_2 will transmit and \mathcal{S}_3 will transmit in the third time slot.

Let f_i be the direct link channel coefficient between source \mathcal{S}_i to destination \mathcal{D} ; x_i be the transmit signal from node \mathcal{S}_i which satisfies the power constraint

$$E\{|x_i|^2\} \leq P_x. \quad (5.39)$$

n_{D_i} be the additive Gaussian noise that follows normal distribution.

Then, the received signals at destination \mathcal{D} during three time slots are

$$y_{D1} = f_1 x_1 + n_{D1}, \quad (5.40)$$

$$y_{D2} = f_2 x_2 + n_{D2}, \quad (5.41)$$

$$y_{D3} = f_3 x_3 + n_{D3}, \quad (5.42)$$

which can be combined to

$$\mathbf{y}_{DT} = \begin{bmatrix} y_{D1} \\ y_{D2} \\ y_{D3} \end{bmatrix} = \underbrace{\begin{bmatrix} f_1 & 0 & 0 \\ 0 & f_2 & 0 \\ 0 & 0 & f_3 \end{bmatrix}}_{\mathbf{A}_{DT}} \underbrace{\begin{bmatrix} x_1 \\ x_2 \\ x_3 \end{bmatrix}}_{\mathbf{x}} + \underbrace{\begin{bmatrix} n_{D1} \\ n_{D2} \\ n_{D3} \end{bmatrix}}_{\mathbf{z}_{DT}}. \quad (5.43)$$

Note that \mathbf{x} is the transmit data vector of three sources $\mathbf{x} \triangleq [x_1, x_2, x_3]^T$ and

$$\mathbf{x} \in \Omega_{\mathbf{x}}, \quad (5.44)$$

where $\Omega_{\mathbf{x}}$ is the data vector alphabet set. Hence the decoding procedure for DT scheme will simply be

$$\hat{\mathbf{x}}_{DT} = \arg \min_{\mathbf{x} \in \Omega_{\mathbf{x}}} \|\mathbf{y}_{DT} - \mathbf{A}_{DT} \mathbf{x}\|^2. \quad (5.45)$$

The sum rate at destination \mathcal{D} for DT scheme will be

$$R_{DT} = \frac{1}{3} \log \det (\mathbf{I}_3 + P_x \mathbf{A}_{DT} \mathbf{A}_{DT}^H). \quad (5.46)$$

The one-third factor above is the natural consequence of time sharing.

(ii) System Model C Scheme 2: Analog Network Coding (ANC)

Regarding this scheme, in the first phase all source nodes transmit simultaneously to relay \mathcal{R} and destination \mathcal{D} in one time slot; while the second phase is the transmission from relay \mathcal{R} to destination \mathcal{D} during the remaining two time slots.

At the end of first phase, the received signal at destination \mathcal{D} through direct links is

$$\begin{aligned}
y_D^{[1]} &= f_1 x_1 + f_2 x_2 + f_3 x_3 + n_D^{[1]} \\
&= [f_1, f_2, f_3] \begin{bmatrix} x_1 \\ x_2 \\ x_3 \end{bmatrix} + n_D^{[1]} \\
&= \mathbf{f}^T \mathbf{x} + n_D^{[1]},
\end{aligned} \tag{5.47}$$

where superscript $\{\cdot\}^{[1]}$ denotes the first phase; the direct link channel vector $\mathbf{f} \in \mathbb{C}^3$ is defined as

$$\mathbf{f} \triangleq [f_1, f_2, f_3]^T. \tag{5.48}$$

Additive Gaussian noise is denoted as $n_D^{[1]}$ and follows normal distribution.

The received signal at relay \mathcal{R} at the end of first phase is

$$\begin{aligned}
\mathbf{y}_R &= \begin{bmatrix} y_{R1} \\ y_{R2} \end{bmatrix} \\
&= \underbrace{\begin{bmatrix} h_{11} & h_{12} & h_{13} \\ h_{21} & h_{22} & h_{23} \end{bmatrix}}_{\triangleq \mathbf{H}} \begin{bmatrix} x_1 \\ x_2 \\ x_3 \end{bmatrix} + \mathbf{n}_R,
\end{aligned} \tag{5.49}$$

or equivalently

$$\mathbf{y}_R = \mathbf{H}\mathbf{x} + \mathbf{n}_R, \tag{5.50}$$

where $\mathbf{y}_R = [y_{R1}, y_{R2}]^T$ is the received vector at relay with two antennas; $\mathbf{n}_R = [n_{R1}, n_{R2}]^T$ is the additive Gaussian noise vector at relay; h_{ri} is the channel coefficient between source node \mathcal{S}_i and relay antenna r .

If we denote the channel vector of all sources to relay antenna r as

$$\mathbf{h}_r = [h_{r1}, h_{r2}, h_{r3}]^T \in \mathbb{C}^3, \tag{5.51}$$

the overall channel matrix between all sources and relay \mathcal{R} is

$$\mathbf{H} = [\mathbf{h}_1, \mathbf{h}_2]^T. \tag{5.52}$$

All channel coefficients and additive noise elements are generated i.i.d. according to a normal distribution $\mathcal{CN}(0, 1)$.

In the second phase, first, relay \mathcal{R} constructs the following signal vector \mathbf{t} based on the received signals on each antenna (y_{R1} and y_{R2}),

$$\mathbf{t} = \begin{bmatrix} t_1 \\ t_2 \end{bmatrix} = \begin{bmatrix} \beta_1 y_{R1} \\ \beta_2 y_{R2} \end{bmatrix} = \underbrace{\begin{bmatrix} \beta_1 & 0 \\ 0 & \beta_2 \end{bmatrix}}_{\triangleq \mathbf{B}} (\mathbf{H}\mathbf{x} + \mathbf{n}_R). \quad (5.53)$$

where β_r , $r = 1, 2$ is the scaling factor to meet the per-antenna power constraint P_R at relay \mathcal{R} given by

$$\begin{aligned} \beta_r &= \sqrt{\frac{P_R}{E\{|y_{Rr}|^2\}}} \\ &= \sqrt{\frac{P_R}{P_x \|\mathbf{h}_r\|^2 + 1}}. \end{aligned} \quad (5.54)$$

Then, relay \mathcal{R} will transmit t_1 and t_2 in two time slots as follows,

$$\begin{bmatrix} y_D^{[2]}(1), y_D^{[2]}(2) \end{bmatrix} = [g_1, g_2] \begin{bmatrix} t_1 & 0 \\ 0 & t_2 \end{bmatrix} + [n_D^{[2]}(1), n_D^{[2]}(2)], \quad (5.55)$$

where superscript $\{\cdot\}^{[2]}$ denotes the first phase; g_r , $r = 1, 2$, is the channel coefficient between relay antenna r and destination \mathcal{D} .

Equivalently, equation (5.55) can be written as

$$\begin{aligned} \mathbf{y}_D^{[2]} &= \begin{bmatrix} y_D^{[2]}(1) \\ y_D^{[2]}(2) \end{bmatrix} = \begin{bmatrix} g_1 & 0 \\ 0 & g_2 \end{bmatrix} \begin{bmatrix} t_1 \\ t_2 \end{bmatrix} + \mathbf{n}_D^{[2]} \\ &= \mathbf{G}_0 \mathbf{t} + \mathbf{n}_D^{[2]}, \end{aligned} \quad (5.56)$$

where matrix \mathbf{G}_0 is defined as

$$\mathbf{G}_0 \triangleq \begin{bmatrix} g_1 & 0 \\ 0 & g_2 \end{bmatrix}, \quad (5.57)$$

and $\mathbf{n}_D^{[2]} = [n_D^{[2]}(1), n_D^{[2]}(2)]^T$.

Plug in \mathbf{t} of (5.53) into equation (5.56), we will have the received signal at destination \mathcal{D} at the end of the second phase as

$$\mathbf{y}_D^{[2]} = \mathbf{G}_0 \mathbf{B} \mathbf{H} \mathbf{x} + \mathbf{G}_0 \mathbf{B} \mathbf{n}_R + \mathbf{n}_D^{[2]}. \quad (5.58)$$

Recall the received signals in the first phase as equation (5.47) and in the second phase as equation (5.58) at destination \mathcal{D} for this scheme, we have

$$\begin{cases} y_D^{[1]} = \mathbf{f}^T \mathbf{x} + n_D^{[1]}, \\ \mathbf{y}_D^{[2]} = \mathbf{G}_0 \mathbf{B} \mathbf{H} \mathbf{x} + \mathbf{G}_0 \mathbf{B} \mathbf{n}_R + \mathbf{n}_D^{[2]}. \end{cases} \quad (5.59)$$

Then, after one transmission realization, we can combine received signals at destination \mathcal{D} during two phases (three time slots), based on which to decode the data vector \mathbf{x} , as follows,

$$\mathbf{y}_{ANC} = \begin{bmatrix} y_D^{[1]} \\ \mathbf{y}_D^{[2]} \end{bmatrix} = \underbrace{\begin{bmatrix} \mathbf{f}^T \\ \mathbf{G}_0 \mathbf{B} \mathbf{H} \end{bmatrix}}_{\triangleq \mathbf{A}_{ANC}} \mathbf{x} + \underbrace{\begin{bmatrix} n_D^{[1]} \\ \mathbf{G}_0 \mathbf{B} \mathbf{n}_R + \mathbf{n}_D^{[2]} \end{bmatrix}}_{\triangleq \mathbf{z}_{ANC}}. \quad (5.60)$$

Hence the decoding procedure for ANC scheme will be

$$\hat{\mathbf{x}}_{ANC} = \arg \min_{\mathbf{x} \in \Omega_{\mathbf{x}}} \|\mathbf{y}_{ANC} - \mathbf{A}_{ANC} \mathbf{x}\|^2. \quad (5.61)$$

Let \mathbf{K}_{ANC} be the covariance matrix of effective noise vector \mathbf{z}_{ANC} at destination, i.e.,

$$\begin{aligned} \mathbf{K}_{ANC} &\triangleq \mathbb{E} \{ \mathbf{z}_{ANC} \mathbf{z}_{ANC}^H \} \\ &= \begin{bmatrix} 1 & \mathbf{0}_2^T \\ \mathbf{0}_2 & \mathbf{G}_0 \mathbf{B} \mathbf{B}^H \mathbf{G}_0^H + \mathbf{I}_2 \end{bmatrix}, \end{aligned} \quad (5.62)$$

where $\mathbb{E}\{\cdot\}$ is the expectation operation; $\mathbf{0}_2 = [0, 0]^T$ is the all-zero column vector in two dimension.

The sum rate at destination \mathcal{D} for ANC scheme will be

$$R_{ANC} = \frac{1}{3} \log \det (\mathbf{I}_3 + P_x \mathbf{A}_{ANC} \mathbf{A}_{ANC}^H \mathbf{K}_{ANC}^{-1}). \quad (5.63)$$

(iii) System Model C Scheme 3: Space-Time Analog Network Coding with Alamouti (STANC-Alamouti)

In this scheme, the first transmission phase will be the same as in ANC scheme. In other words, at the end of first phase, the received signal at the destination \mathcal{D} will be as equation (5.47) and the received signals at the relay \mathcal{R} will be as equation (5.50).

After constructing the signal vector \mathbf{t} as equation (5.53), relay \mathcal{R} will combine analog network coding with Alamouti scheme. According to Alamouti scheme, after obtaining $\mathbf{t} = [t_1, t_2]^T$, relay \mathcal{R} will transmit $[t_1, t_2]^T$ in the second time slot and $[-t_2^*, t_1^*]^T$ in the third time slot.

Denote the corresponding received signals at destination \mathcal{D} in the second phase (with two time slots) as $y_D^{[2]}(1)$ and $y_D^{[2]}(2)$, then

$$\begin{bmatrix} y_D^{[2]}(1) \\ y_D^{[2]}(2) \end{bmatrix} = [g_1, g_2] \begin{bmatrix} t_1 & -t_2^* \\ t_2 & t_1^* \end{bmatrix} + [n_D^{[2]}(1), n_D^{[2]}(2)]. \quad (5.64)$$

Destination \mathcal{D} arranges the received signals into a vector $\mathbf{y}_D^{[2]} = [y_D^{[2]}(1), -y_D^{[2]}(2)^*]^T$, which can be rewritten as

$$\begin{aligned} \mathbf{y}_D^{[2]} &= \begin{bmatrix} y_D^{[2]}(1) \\ -y_D^{[2]}(2)^* \end{bmatrix} = \begin{bmatrix} g_1 & g_2 \\ -g_2^* & g_1^* \end{bmatrix} \begin{bmatrix} t_1 \\ t_2 \end{bmatrix} + \mathbf{n}_D^{[2]} \\ &= \mathbf{G}_1 \mathbf{t} + \mathbf{n}_D^{[2]}, \end{aligned} \quad (5.65)$$

where matrix \mathbf{G}_1 is defined as

$$\mathbf{G}_1 \triangleq \begin{bmatrix} g_1 & g_2 \\ -g_2^* & g_1^* \end{bmatrix}, \quad (5.66)$$

and $\mathbf{n}_D^{[2]} = [n_D^{[2]}(1), -n_D^{[2]}(2)^*]^T$.

Plug in \mathbf{t} of (5.53) into equation (5.56), we will have the received signal at destination \mathcal{D} at the end of the second phase as

$$\mathbf{y}_D^{[2]} = \mathbf{G}_1 \mathbf{B} \mathbf{H} \mathbf{x} + \mathbf{G}_1 \mathbf{B} \mathbf{n}_R + \mathbf{n}_D^{[2]}. \quad (5.67)$$

Recall the received signals in the first phase as equation (5.47) and in the second phase as equation (5.67) at destination \mathcal{D} for this scheme, we have

$$\begin{cases} y_D^{[1]} = \mathbf{f}^T \mathbf{x} + n_D^{[1]}, \\ \mathbf{y}_D^{[2]} = \mathbf{G}_1 \mathbf{B} \mathbf{H} \mathbf{x} + \mathbf{G}_0 \mathbf{B} \mathbf{n}_R + \mathbf{n}_D^{[2]}. \end{cases} \quad (5.68)$$

Finally, after one transmission realization, we combine received signals at destination \mathcal{D} based on which to decode the data vector \mathbf{x} , during two phases (three time slots) as

$$\mathbf{y}_{STANC} = \begin{bmatrix} y_D^{[1]} \\ \mathbf{y}_D^{[2]} \end{bmatrix} = \underbrace{\begin{bmatrix} \mathbf{f}^T \\ \mathbf{G}_1 \mathbf{B} \mathbf{H} \end{bmatrix}}_{\triangleq \mathbf{A}_{STANC}} \mathbf{x} + \underbrace{\begin{bmatrix} n_D^{[1]} \\ \mathbf{G}_1 \mathbf{B} \mathbf{n}_R + \mathbf{n}_D^{[2]} \end{bmatrix}}_{\triangleq \mathbf{z}_{STANC}}. \quad (5.69)$$

The decoding procedure can be expressed as

$$\hat{\mathbf{x}}_{STANC} = \arg \min_{\mathbf{x} \in \Omega_{\mathbf{x}}} \|\mathbf{y}_{STANC} - \mathbf{A}_{STANC} \mathbf{x}\|^2. \quad (5.70)$$

Let \mathbf{K}_{STANC} be the covariance matrix of effective noise vector \mathbf{z}_{STANC} at destination, i.e.,

$$\begin{aligned} \mathbf{K}_{STANC} &\triangleq \mathbb{E} \{ \mathbf{z}_{STANC} \mathbf{z}_{STANC}^H \} \\ &= \begin{bmatrix} 1 & \mathbf{0}_2^T \\ \mathbf{0}_2 & \mathbf{G}_1 \mathbf{B} \mathbf{B}^H \mathbf{G}_1^H + \mathbf{I}_2 \end{bmatrix}. \end{aligned} \quad (5.71)$$

The sum rate at destination \mathcal{D} for STANC scheme will be

$$R_{STANC} = \frac{1}{3} \log \det (\mathbf{I}_3 + P_x \mathbf{A}_{STANC} \mathbf{A}_{STANC}^H \mathbf{K}_{STANC}^{-1}). \quad (5.72)$$

The comparison of different schemes within three slots are shown in Table 5.4.

System Model C	Time Slot 1	Time Slot 2	Time Slot 3
DT	$S_1 : x_1$	$S_2 : x_2$	$S_3 : x_3$
ANC	$S_1 : x_1$ $S_2 : x_2$ $S_3 : x_3$	$R : \begin{bmatrix} t_1 \\ 0 \end{bmatrix}$	$R : \begin{bmatrix} 0 \\ t_2 \end{bmatrix}$
STANC-Alamouti	$S_1 : x_1$ $S_2 : x_2$ $S_3 : x_3$	$R : \begin{bmatrix} t_1 \\ t_2 \end{bmatrix}$	$R : \begin{bmatrix} -t_2^* \\ t_1^* \end{bmatrix}$

Table 5.4: Different Schemes for System Model C

5.3.2 Experimental Studies

We present numerical results to evaluate the performance of all possible schemes for MARC system model. Let $P_x = P_R$, i.e., the transmission power constraint at sources and relay are equivalent. With the average of 100000 randomly generated channel realizations, we show in Fig. 5.6 the sum rate comparisons of three possible schemes. We can see that STANC outperforms the other two schemes unless the signal power is extremely low. The bit error rate simulation is shown in Fig. 5.7. Similar conclusions can be drawn.

5.4 System Model D: Four Sources with Direct Links

Consider the system model setting with four sources $\mathcal{S}_1, \mathcal{S}_2, \mathcal{S}_3$ and \mathcal{S}_4 communicating with destination \mathcal{D} via a relay \mathcal{R} with direct links from sources to destination, as shown in Fig. 5.9. We assume that the sources $\mathcal{S}_1, \mathcal{S}_2, \mathcal{S}_3, \mathcal{S}_4$ and the destination \mathcal{D} are equipped with single antenna, while relay \mathcal{R} is equipped with two antennas.

We will discuss several possible transmission strategies for this system model. One realization of the information transmission will be performed within four time slots for all those strategies.

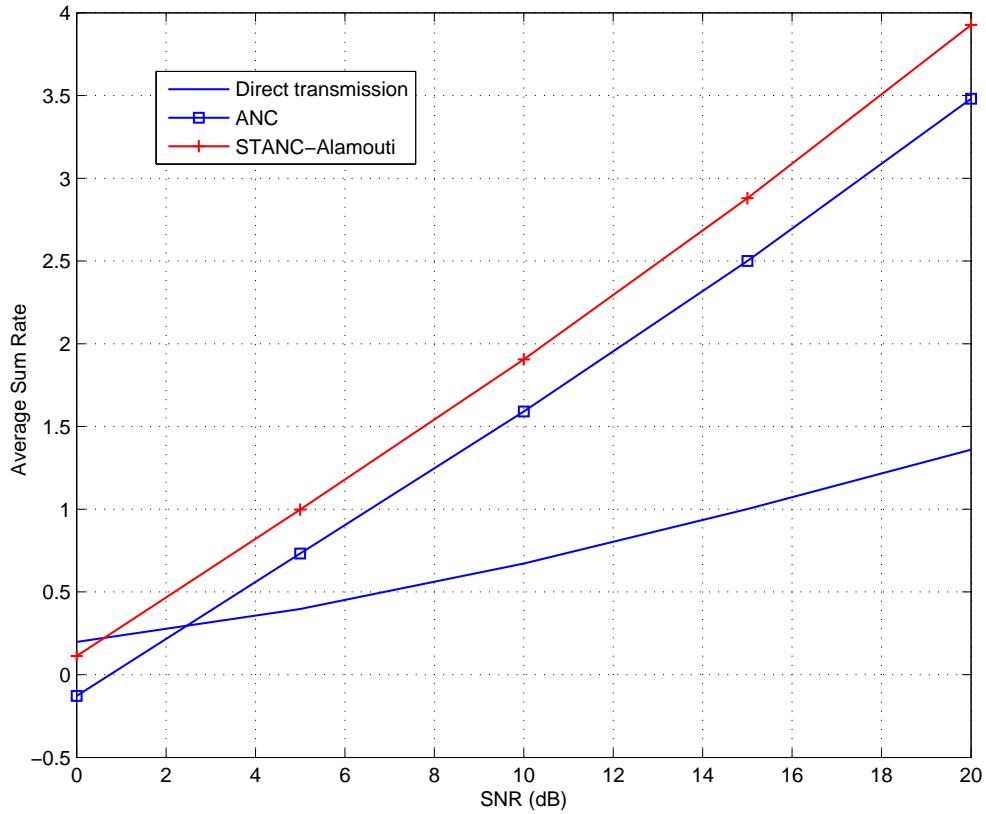


Fig. 5.6: Sum rate comparison for different schemes regarding system model C

5.4.1 Different Schemes for System Model D

(i) System Model D Scheme 1: Direct Transmission (DT)

In this scheme, we assume the relay will keep silent during all transmission realization and the sources will communicate to the destination one by one, which also takes four time slots. \mathcal{S}_1 will transmit in the first time slot; \mathcal{S}_2 will transmit in the second time slot, and so on. The transmit data vector of all source nodes is denoted by

$$\mathbf{x} = [x_1, x_2, x_3, x_4]^T, \quad (5.73)$$

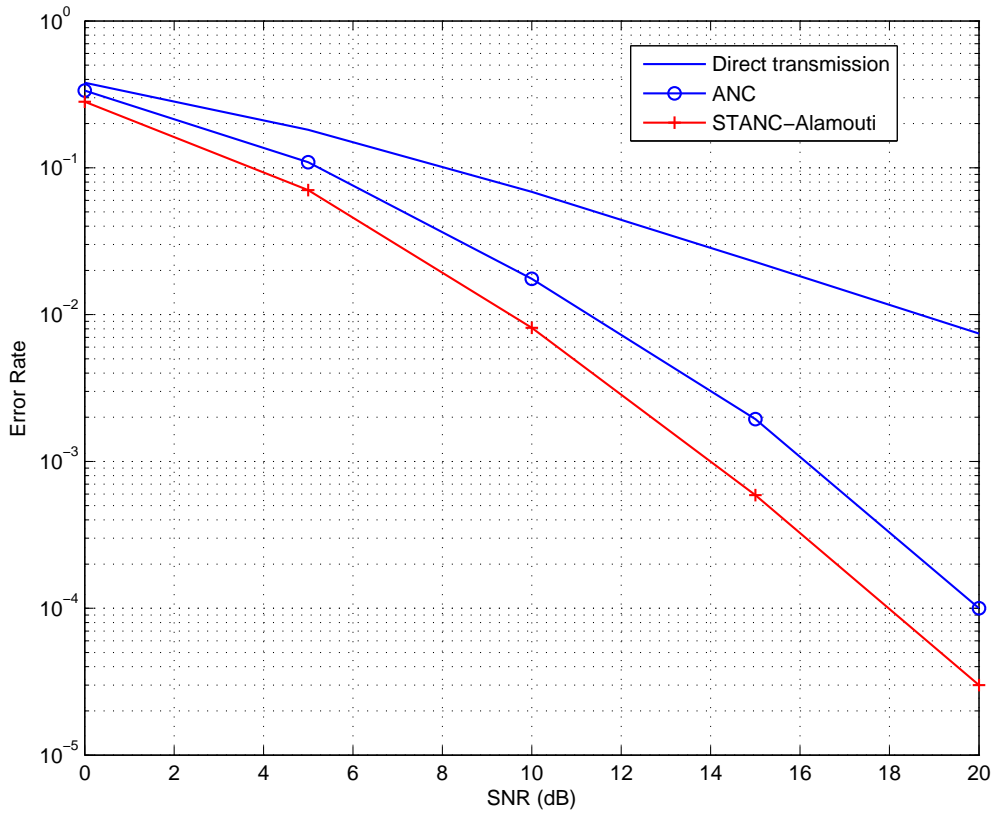


Fig. 5.7: BER comparison for different schemes regarding system model C

where $x_i \in \mathbb{R}$ is the transmit data symbol³ from node \mathcal{S}_i which has been normalized to $E\{|x_i|^2\} \leq 1$. E_x is the power constraint for data symbol transmission. Let $f_i \in \mathbb{R}$ be the direct link channel coefficient between source \mathcal{S}_i to destination \mathcal{D} , an independent Gaussian random variable with variance σ_f^2 . Additive Gaussian noise follows normal distribution $\mathcal{N}(0, 1)$.

Then, the received signals at the destination \mathcal{D} during the four time slots can be

³For source \mathcal{S}_i , x_i is the transmitted symbol after modulation based on the transmitted bit b_i , where $b_i \in \{0, 1\}$.

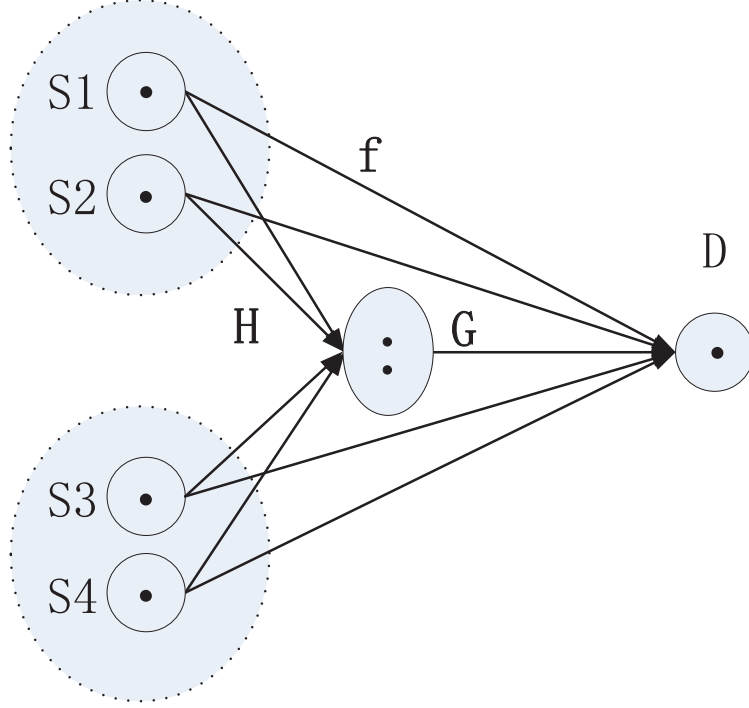


Fig. 5.8: System Model D

combined to $\mathbf{y}_D = [y_{D1}, y_{D2}, y_{D3}, y_{D4}]^T$ as

$$\mathbf{y}_D = \sqrt{E_x} \underbrace{\begin{bmatrix} f_1 & 0 & 0 & 0 \\ 0 & f_2 & 0 & 0 \\ 0 & 0 & f_3 & 0 \\ 0 & 0 & 0 & f_4 \end{bmatrix}}_{\mathbf{A}_{DT}} \underbrace{\begin{bmatrix} x_1 \\ x_2 \\ x_3 \\ x_4 \end{bmatrix}}_{\mathbf{x}} + \underbrace{\begin{bmatrix} n_{D1} \\ n_{D2} \\ n_{D3} \\ n_{D4} \end{bmatrix}}_{\mathbf{z}}, \quad (5.74)$$

or equivalently

$$\mathbf{y}_D = \mathbf{A}_{DT}\mathbf{x} + \mathbf{z}. \quad (5.75)$$

Note that \mathbf{x} is the transmit data vector of four sources and $\mathbf{x} \in \Omega_{\mathbf{x}}$, where $\Omega_{\mathbf{x}}$ is the data vector alphabet set. Hence the decoding procedure will simply be

$$\hat{\mathbf{x}} = \arg \min_{\mathbf{x} \in \Omega_{\mathbf{x}}} \|\mathbf{y}_D - \mathbf{A}_{DT}\mathbf{x}\|^2. \quad (5.76)$$

(ii) System Model D Scheme 2: Decode-and-Forward (DF)

In this scheme, one realization of the information transmission is performed in two phases. The first phase (with two time slots) is the transmission from sources to relay \mathcal{R} . We first separate the four sources into two groups. $\mathcal{S}_1, \mathcal{S}_2$ belong to one group and $\mathcal{S}_3, \mathcal{S}_4$ belong to another group. In the first time slot, sources \mathcal{S}_1 and \mathcal{S}_2 will transmit to the relay; while in the second time slot, sources \mathcal{S}_3 and \mathcal{S}_4 will transmit to the relay. The second phase (also with two time slots) is the transmission from relay \mathcal{R} to destination \mathcal{D} .

In the first phase, the received signals at destination \mathcal{D} at the end of first time slot and second time slot are

$$y_D^{[1]}(1) = \sqrt{E_x}f_1x_1 + \sqrt{E_x}f_2x_2 + n_D^{[1]}(1) \quad (5.77)$$

$$y_D^{[1]}(2) = \sqrt{E_x}f_3x_3 + \sqrt{E_x}f_4x_4 + n_D^{[1]}(2) \quad (5.78)$$

where the superscript $\{\cdot\}^{[1]}$ denotes the first phase. We can rewrite (5.77) and (5.78) into

$$\mathbf{y}_D^{[1]} = \sqrt{E_x} \underbrace{\begin{bmatrix} f_1 & f_2 & 0 & 0 \\ 0 & 0 & f_3 & f_4 \end{bmatrix}}_{\mathbf{F}} \begin{bmatrix} x_1 \\ x_2 \\ x_3 \\ x_4 \end{bmatrix} + \mathbf{n}_D^{[1]}, \quad (5.79)$$

where $\mathbf{y}_D^{[1]} = [y_D^{[1]}(1), y_D^{[1]}(2)]^T$; $\mathbf{n}_D^{[1]}$ is i.i.d. Gaussian noise with normal distribution.

The received signals at relay \mathcal{R} at the end of first time slot and second time slot are

$$\mathbf{y}_R^{(1)} = \sqrt{E_x} \begin{bmatrix} h_{11} & h_{12} \\ h_{21} & h_{22} \end{bmatrix} \begin{bmatrix} x_1 \\ x_2 \end{bmatrix} + \begin{bmatrix} n_{R1} \\ n_{R2} \end{bmatrix}, \quad (5.80)$$

$$\mathbf{y}_R^{(2)} = \sqrt{E_x} \begin{bmatrix} h_{13} & h_{14} \\ h_{23} & h_{24} \end{bmatrix} \begin{bmatrix} x_3 \\ x_4 \end{bmatrix} + \begin{bmatrix} n_{R3} \\ n_{R4} \end{bmatrix}, \quad (5.81)$$

where $\mathbf{y}_R^{(1)}$ is the received vector at relay with two antennas in the first time slot and $\mathbf{y}_R^{(2)}$ is the received vector at relay with two antennas in the second time slot; n_{Ri} , $i = 1, 2, 3, 4$ is the additive Gaussian noise; h_{ri} is the channel coefficient between source node \mathcal{S}_i and

relay antenna r , an independent Gaussian random variable with variance σ_h^2 . Additive noise elements are generated i.i.d. according to a normal distribution $\mathcal{N}(0, 1)$.

With equations (5.80) and (5.81), we can easily obtain

$$\begin{aligned}
\mathbf{y}_R &= \begin{bmatrix} \mathbf{y}_R^{(1)} \\ \mathbf{y}_R^{(2)} \end{bmatrix} = \begin{bmatrix} y_{R1} \\ y_{R2} \\ y_{R3} \\ y_{R4} \end{bmatrix} \\
&= \sqrt{E_x} \underbrace{\begin{bmatrix} h_{11} & h_{12} & 0 & 0 \\ h_{21} & h_{22} & 0 & 0 \\ 0 & 0 & h_{13} & h_{14} \\ 0 & 0 & h_{23} & h_{24} \end{bmatrix}}_{\mathbf{H}} \underbrace{\begin{bmatrix} x_1 \\ x_2 \\ x_3 \\ x_4 \end{bmatrix}}_{\mathbf{x}} + \underbrace{\begin{bmatrix} n_{R1} \\ n_{R2} \\ n_{R3} \\ n_{R4} \end{bmatrix}}_{\mathbf{n}_R},
\end{aligned} \tag{5.82}$$

or equivalently

$$\mathbf{y}_R = \sqrt{E_x} \mathbf{H} \mathbf{x} + \mathbf{n}_R, \tag{5.83}$$

which is the received signal at relay \mathcal{R} at the end of first transmission phase.

In the second phase, with the decode-and-forward (DF) scheme, relay \mathcal{R} will first decode for four sources

$$\hat{\mathbf{x}}_R = \begin{bmatrix} \hat{x}_{R1} \\ \hat{x}_{R2} \\ \hat{x}_{R3} \\ \hat{x}_{R4} \end{bmatrix} = \arg \min_{\mathbf{x} \in \Omega_{\mathbf{x}}} \|\mathbf{y}_R - \sqrt{E_x} \mathbf{H} \mathbf{x}\|^2. \tag{5.84}$$

Then, with two antennas and power constraint E_R , relay \mathcal{R} will transmit $[\hat{x}_{R1}, \hat{x}_{R2}]^T$ in the third time slot and transmit $[\hat{x}_{R3}, \hat{x}_{R4}]^T$ in the fourth time slot with two antennas.

The received signals at destination \mathcal{D} at the end of third time slot and fourth time

slot are

$$y_D^{[2]}(1) = \sqrt{E_R}g_1\hat{x}_{R1} + \sqrt{E_R}g_2\hat{x}_{R2} + n_D^{[2]}(1) \quad (5.85)$$

$$y_D^{[2]}(2) = \sqrt{E_R}g_1\hat{x}_{R3} + \sqrt{E_R}g_2\hat{x}_{R4} + n_D^{[2]}(2), \quad (5.86)$$

where the superscript $\{\cdot\}^{[2]}$ denotes the second phase. g_r , $r = 1, 2$, is the channel coefficient between relay antenna r and destination \mathcal{D} , an independent Gaussian random variable with variance σ_g^2 . Additive Gaussian noise elements are generated i.i.d. according to a normal distribution $\mathcal{N}(0, 1)$. We can rewrite (5.85) and (5.86) into

$$\mathbf{y}_D^{[2]} = \sqrt{E_R} \underbrace{\begin{bmatrix} g_1 & g_2 & 0 & 0 \\ 0 & 0 & g_1 & g_2 \end{bmatrix}}_{\mathbf{G}} \hat{\mathbf{x}}_R + \mathbf{n}_D^{[2]}. \quad (5.87)$$

With the received signals in the first phase (5.79) and in the second phase (5.87) at destination \mathcal{D} , we have

$$\left\{ \begin{array}{l} \mathbf{y}_D^{[1]} = \sqrt{E_x} \begin{bmatrix} f_1 & f_2 & 0 & 0 \\ 0 & 0 & f_3 & f_4 \end{bmatrix} \mathbf{x} + \mathbf{n}_D^{[1]} \\ \quad = \sqrt{E_x} \mathbf{F} \mathbf{x} + \mathbf{n}_D^{[1]}, \\ \\ \mathbf{y}_D^{[2]} = \sqrt{E_R} \begin{bmatrix} g_1 & g_2 & 0 & 0 \\ 0 & 0 & g_1 & g_2 \end{bmatrix} \hat{\mathbf{x}}_R + \mathbf{n}_D^{[2]} \\ \quad = \sqrt{E_R} \mathbf{G} \hat{\mathbf{x}}_R + \mathbf{n}_D^{[2]}. \end{array} \right. \quad (5.88)$$

If we construct the matrix \mathbf{A}_{DF} as

$$\mathbf{A}_{DF} \triangleq \begin{bmatrix} \sqrt{E_x} \mathbf{F} \\ \sqrt{E_R} \mathbf{G} \end{bmatrix}, \quad (5.89)$$

then the decoding procedure will be

$$\hat{\mathbf{x}} = \arg \min_{\mathbf{x} \in \Omega_{\mathbf{x}}} \|\mathbf{y}_D - \mathbf{A}_{DF} \mathbf{x}\|^2. \quad (5.90)$$

We note that in this DF scheme, the system model with four sources is actually equivalent to two separate multiple access relay channels (MARC) with two sources. Each separate MARC system is working in two time slots. For example, for a sub-system with sources \mathcal{S}_1 and \mathcal{S}_2 in Fig. 2, in the first time slot, \mathcal{S}_1 and \mathcal{S}_2 transmit simultaneously; in the second time slot, relay \mathcal{R} will forward the decoded \hat{x}_1 and \hat{x}_2 with two antennas.

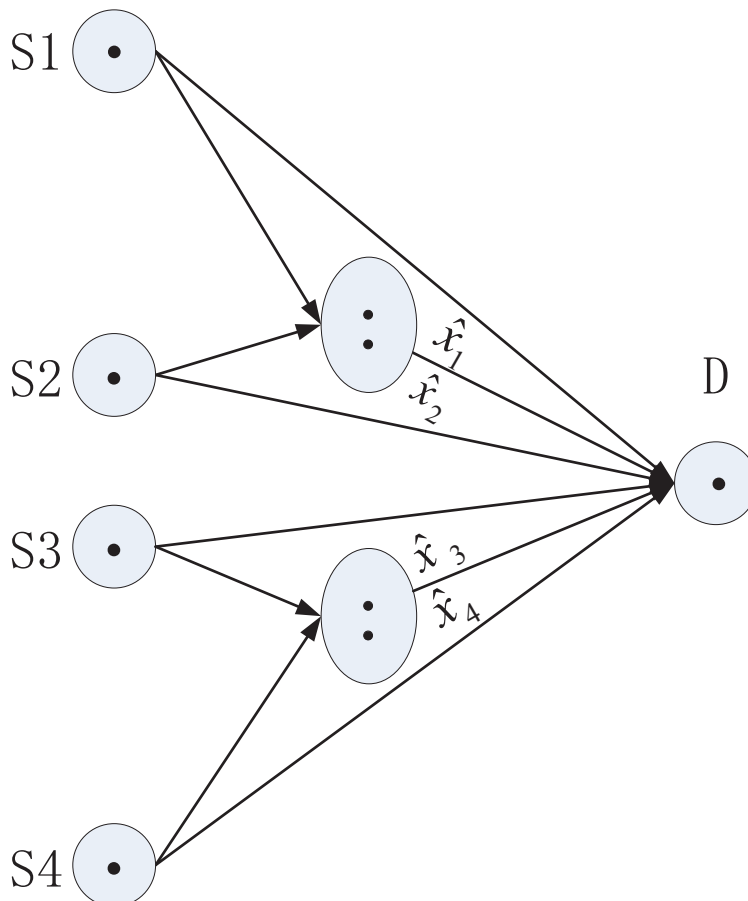


Fig. 5.9: The equivalent two separate MARC with two sources for DF

(iii) System Model D Scheme 3: Digital Network Coding (DNC)

In this scheme, the first transmission phase will be the same as in the decode-and-forward scheme. In other words, at the end of first phase, the received signals at the destination \mathcal{D} will be (5.79) and the received signals at the relay \mathcal{R} will be (5.82)-(5.83).

Then, relay \mathcal{R} will first decode for four sources the same way as the DF scheme,

equation (5.84) and formulate $\hat{x}_{R1} \oplus \hat{x}_{R2}, \hat{x}_{R3} \oplus \hat{x}_{R4}$ ⁴.

It can be denoted as

$$\hat{x}_{R1} \oplus \hat{x}_{R2} = -\hat{x}_{R1} * \hat{x}_{R2} \quad (5.91)$$

$$\hat{x}_{R3} \oplus \hat{x}_{R4} = -\hat{x}_{R3} * \hat{x}_{R4}. \quad (5.92)$$

According to digital network coding strategy, with two antennas and power constraint E_R , the relay will transmit $[\hat{x}_{R1} \oplus \hat{x}_{R2}, \hat{x}_{R1} \oplus \hat{x}_{R2}]^T$ and $[\hat{x}_{R3} \oplus \hat{x}_{R4}, \hat{x}_{R3} \oplus \hat{x}_{R4}]^T$ in the following two time slots,

$$\begin{aligned} [y_D^{[2]}(1), y_D^{[2]}(2)] &= \sqrt{E_R} [g_1, g_2] \begin{bmatrix} \hat{x}_{R1} \oplus \hat{x}_{R2} & \hat{x}_{R3} \oplus \hat{x}_{R4} \\ \hat{x}_{R1} \oplus \hat{x}_{R2} & \hat{x}_{R3} \oplus \hat{x}_{R4} \end{bmatrix} \\ &+ [n_D^{[2]}(1), n_D^{[2]}(2)], \end{aligned}$$

which can be arranged as

$$\mathbf{y}_D^{[2]} = \sqrt{E_R} \begin{bmatrix} g_1 + g_2 & 0 \\ 0 & g_1 + g_2 \end{bmatrix} \begin{bmatrix} \hat{x}_{R1} \oplus \hat{x}_{R2} \\ \hat{x}_{R3} \oplus \hat{x}_{R4} \end{bmatrix} + \mathbf{n}_D^{[2]}. \quad (5.93)$$

Recall the received signals in the first phase (5.79) and in the second phase (5.93) at destination \mathcal{D} , we have

$$\left\{ \begin{array}{l} \mathbf{y}_D^{[1]} = \sqrt{E_x} \begin{bmatrix} f_1 & f_2 & 0 & 0 \\ 0 & 0 & f_3 & f_4 \end{bmatrix} \mathbf{x} + \mathbf{n}_D^{[1]} = \mathbf{F}\mathbf{x} + \mathbf{n}_D^{[1]}, \\ \mathbf{y}_D^{[2]} = \sqrt{E_R} \begin{bmatrix} g_1 + g_2 & 0 \\ 0 & g_1 + g_2 \end{bmatrix} \begin{bmatrix} \hat{x}_{R1} \oplus \hat{x}_{R2} \\ \hat{x}_{R3} \oplus \hat{x}_{R4} \end{bmatrix} + \mathbf{n}_D^{[2]}. \end{array} \right. \quad (5.94)$$

we can easily see that, according to this DNC scheme, the system is actually equivalent to two separate multiple access relay channels (MARC) with two sources as in Fig. 3.

⁴The relay actually first demodulates \hat{x}_{Ri} to information bit \hat{b}_{Ri} , then calculate $\hat{b}_{R1} \oplus \hat{b}_{R2}, \hat{b}_{R3} \oplus \hat{b}_{R4}$, and finally modulates them again. We simply denote the modulated $\hat{b}_{R1} \oplus \hat{b}_{R2}, \hat{b}_{R3} \oplus \hat{b}_{R4}$ as $\hat{x}_{R1} \oplus \hat{x}_{R2}, \hat{x}_{R3} \oplus \hat{x}_{R4}$.

Each two sources MARC system is working in two time slots, while in the first time slot sources transmitting and in the second time slot the relay will forward the XOR symbol of the decoded messages.

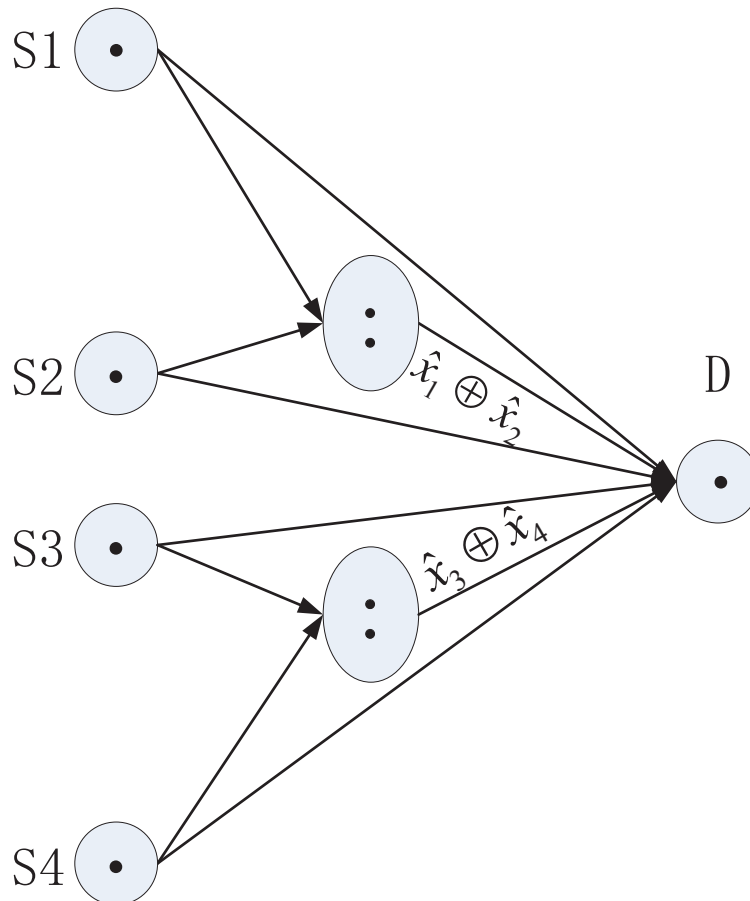


Fig. 5.10: The equivalent two separate MARC with two sources for DNC

The decoding procedure can also be processed according to those two separate MARC system. For sources \mathcal{S}_1 and \mathcal{S}_2 , we have

$$\begin{cases} y_D^{[1]}(1) = \sqrt{E_x}f_1x_1 + \sqrt{E_x}f_2x_2 + n_D^{[1]}(1) \\ y_D^{[2]}(1) = \sqrt{E_R}(g_1 + g_2)(-\hat{x}_{R1} * \hat{x}_{R2}) + n_D^{[2]}(1), \end{cases} \quad (5.95)$$

and will decode $[\hat{x}_1, \hat{x}_2]^T$ as

$$\begin{aligned} \begin{bmatrix} \hat{x}_1 \\ \hat{x}_2 \end{bmatrix} &= \arg \min_{x_1, x_2} \|y_D^{[1]}(1) - \sqrt{E_x} f_1 x_1 - \sqrt{E_x} f_2 x_2\|^2 \\ &\quad + \|y_D^{[2]}(1) + \sqrt{E_R}(g_1 + g_2)(x_1 * x_2)\|^2. \end{aligned} \quad (5.96)$$

For sources \mathcal{S}_3 and \mathcal{S}_4 we can decode in a similar way,

$$\begin{aligned} \begin{bmatrix} \hat{x}_3 \\ \hat{x}_4 \end{bmatrix} &= \arg \min_{x_3, x_4} \|y_D^{[1]}(2) - \sqrt{E_x} f_3 x_3 - \sqrt{E_x} f_4 x_4\|^2 \\ &\quad + \|y_D^{[2]}(2) + \sqrt{E_R}(g_1 + g_2)(x_3 * x_4)\|^2. \end{aligned} \quad (5.97)$$

(iv) System Model D Scheme 4: Digital Network Coding with Alamouti space time coding (DNC-Alamouti)

In this scheme, the first transmission phase will also be the same as in the decode-and-forward scheme. In other words, at the end of first phase, the received signals at the destination \mathcal{D} will be (5.79) and the received signals at the relay \mathcal{R} will be (5.82)-(5.83).

Then, relay \mathcal{R} will first decode for four sources the same way as the DF scheme, equation (5.84) and formulate $\hat{x}_{R1} \oplus \hat{x}_{R2}$ and $\hat{x}_{R3} \oplus \hat{x}_{R4}$. The transmission from relay \mathcal{R} will follow the Alamouti space time coding. In the third time slot, the relay will transmit $[\hat{x}_{R1} \oplus \hat{x}_{R2}, \hat{x}_{R3} \oplus \hat{x}_{R4}]^T$ and in the fourth time slot, the relay will transmit $[-(\hat{x}_{R3} \oplus \hat{x}_{R4})^*, (\hat{x}_{R1} \oplus \hat{x}_{R2})^*]^T$. Denote the corresponding received signals at destination \mathcal{D} in the second phase (with two time slots) as $y_D^{[2]}(1)$ and $y_D^{[2]}(2)$, then

$$\begin{bmatrix} y_D^{[2]}(1) \\ y_D^{[2]}(2) \end{bmatrix} = \sqrt{E_R}[g_1, g_2] \begin{bmatrix} \hat{x}_{R1} \oplus \hat{x}_{R2} & -(\hat{x}_{R3} \oplus \hat{x}_{R4})^* \\ \hat{x}_{R3} \oplus \hat{x}_{R4} & (\hat{x}_{R1} \oplus \hat{x}_{R2})^* \end{bmatrix} + [n_D^{[2]}(1), n_D^{[2]}(2)] \quad (5.98)$$

After receiving signals from relay \mathcal{R} in the second phase, destination \mathcal{D} arranges the received signals into a vector $\mathbf{y}_D^{[2]} = [y_D^{[2]}(1), -y_D^{[2]}(2)^*]^T$, which can be rewritten as

$$\mathbf{y}_D^{[2]} = \begin{bmatrix} y_D^{[2]}(1) \\ -y_D^{[2]}(2)^* \end{bmatrix} = \sqrt{E_R} \begin{bmatrix} g_1 & g_2 \\ -g_2^* & g_1^* \end{bmatrix} \begin{bmatrix} \hat{x}_{R1} \oplus \hat{x}_{R2} \\ \hat{x}_{R3} \oplus \hat{x}_{R4} \end{bmatrix} + \mathbf{n}_D^{[2]}, \quad (5.99)$$

where $\mathbf{n}_D^{[2]} = [n_D^{[2]}(1), -n_D^{[2]}(2)^*]^T$.

Recall the received signals in the first phase (5.79) and in the second phase (5.99) at destination \mathcal{D} , we have

$$\left\{ \begin{array}{l} \mathbf{y}_D^{[1]} = \sqrt{E_x} \begin{bmatrix} f_1 & f_2 & 0 & 0 \\ 0 & 0 & f_3 & f_4 \end{bmatrix} \mathbf{x} + \mathbf{n}_D^{[1]} = \mathbf{F}\mathbf{x} + \mathbf{n}_D^{[1]}, \\ \mathbf{y}_D^{[2]} = \sqrt{E_R} \begin{bmatrix} g_1 & g_2 \\ -g_2^* & g_1^* \end{bmatrix} \begin{bmatrix} \hat{x}_{R1} \oplus \hat{x}_{R2} \\ \hat{x}_{R3} \oplus \hat{x}_{R4} \end{bmatrix} + \mathbf{n}_D^{[2]}. \end{array} \right. \quad (5.100)$$

Equivalently, the received signals at destination during the two phases can be written as

$$\left\{ \begin{array}{l} y_{D1} = \sqrt{E_x}f_1x_1 + \sqrt{E_x}f_2x_2 + n_{D1} \\ y_{D2} = \sqrt{E_x}f_3x_3 + \sqrt{E_x}f_4x_4 + n_{D2} \\ y_{D3} = -\sqrt{E_R}g_1(\hat{x}_{R1} * \hat{x}_{R2}) - \sqrt{E_R}g_2(\hat{x}_{R3} * \hat{x}_{R4}) + n_{D3} \\ y_{D4} = \sqrt{E_R}g_2^*(\hat{x}_{R1} * \hat{x}_{R2}) - \sqrt{E_R}g_1^*(\hat{x}_{R3} * \hat{x}_{R4}) + n_{D4}, \end{array} \right.$$

where $[y_{D1}, y_{D2}, y_{D3}, y_{D4}] = [(\mathbf{y}_D^{[1]})^T, (\mathbf{y}_D^{[2]})^T]$ and $[n_{D1}, n_{D2}, n_{D3}, n_{D4}] = [(\mathbf{n}_D^{[1]})^T, (\mathbf{n}_D^{[2]})^T]$.

The correspondent decoding procedure will be

$$\begin{aligned} \hat{\mathbf{x}} = \arg \min_{x_1, x_2, x_3, x_4} & \|y_{D1} - \sqrt{E_x}f_1x_1 - \sqrt{E_x}f_2x_2\|^2 + \|y_{D2} - \sqrt{E_x}f_3x_3 - \sqrt{E_x}f_4x_4\|^2 \\ & + \|y_{D3} + \sqrt{E_R}g_1(\hat{x}_{R1} * \hat{x}_{R2}) + \sqrt{E_R}g_2(\hat{x}_{R3} * \hat{x}_{R4})\|^2 \\ & + \|y_{D4} - \sqrt{E_R}g_2^*(\hat{x}_{R1} * \hat{x}_{R2}) - \sqrt{E_R}g_1^*(\hat{x}_{R3} * \hat{x}_{R4})\|^2. \end{aligned} \quad (5.101)$$

(v) System Model D Scheme 5: Analog Network Coding (ANC)

In this scheme, relay \mathcal{R} will utilize analog network coding to process the received signals. First, after receiving \mathbf{y}_R of (5.82)-(5.83), relay \mathcal{R} constructs the following signal

vector

$$\mathbf{t} = \begin{bmatrix} t_1 \\ t_2 \\ t_3 \\ t_4 \end{bmatrix} = \begin{bmatrix} \beta_1 y_{R1} \\ \beta_2 y_{R2} \\ \beta_3 y_{R3} \\ \beta_4 y_{R4} \end{bmatrix} = \underbrace{\begin{bmatrix} \beta_1 & 0 & 0 & 0 \\ 0 & \beta_2 & 0 & 0 \\ 0 & 0 & \beta_3 & 0 \\ 0 & 0 & 0 & \beta_4 \end{bmatrix}}_{\mathbf{B}} (\sqrt{E_x} \mathbf{H} \mathbf{x} + \mathbf{n}_R), \quad (5.102)$$

where β_r , $r = 1, 2, 3, 4$ is the scaling factor at relay \mathcal{R} given by

$$\beta_r = \sqrt{\frac{1}{E\{|y_{Rr}|^2\}}} = \sqrt{\frac{1}{E_x \|\mathbf{h}_r\|^2 + 1}}. \quad (5.103)$$

Note that \mathbf{h}_r^T is the r -th row vector of matrix \mathbf{H} in (5.82), i.e.,

$$\mathbf{H} = [\mathbf{h}_1, \mathbf{h}_2, \mathbf{h}_3, \mathbf{h}_4]^T. \quad (5.104)$$

Then, relay \mathcal{R} will transmit t_1, t_2, t_3 and t_4 in two time slots as follows,

$$[y_D^{[2]}(1), y_D^{[2]}(2)] = \sqrt{E_R} [g_1, g_2] \begin{bmatrix} t_1 & t_3 \\ t_2 & t_4 \end{bmatrix} + [n_D^{[2]}(1), n_D^{[2]}(2)], \quad (5.105)$$

which can be arranged as

$$\begin{aligned} \mathbf{y}_D^{[2]} &= \begin{bmatrix} y_D^{[2]}(1) \\ y_D^{[2]}(2) \end{bmatrix} \\ &= \sqrt{E_R} \underbrace{\begin{bmatrix} g_1 & g_2 & 0 & 0 \\ 0 & 0 & g_1 & g_2 \end{bmatrix}}_{\mathbf{G}} \begin{bmatrix} t_1 \\ t_2 \\ t_3 \\ t_4 \end{bmatrix} + \mathbf{n}_D^{[2]} \\ &= \sqrt{E_R} \sqrt{E_x} \mathbf{G} \mathbf{B} \mathbf{H} \mathbf{x} + \sqrt{E_R} \mathbf{G} \mathbf{B} \mathbf{n}_R + \mathbf{n}_D^{[2]}. \end{aligned} \quad (5.106)$$

Combining the received signals in the first phase (5.79) and in the second phase (5.106) at destination \mathcal{D} , we have

$$\mathbf{y}_D = \underbrace{\sqrt{E_x} \begin{bmatrix} \mathbf{F} \\ \sqrt{E_R} \mathbf{G} \mathbf{B} \mathbf{H} \end{bmatrix}}_{\mathbf{A}_{ANC}} \mathbf{x} + \underbrace{\begin{bmatrix} \mathbf{n}_D^{[1]} \\ \sqrt{E_R} \mathbf{G} \mathbf{B} \mathbf{n}_R + \mathbf{n}_D^{[2]} \end{bmatrix}}_{\mathbf{z}}. \quad (5.107)$$

Model D	Time Slot 1	Time Slot 2	Time Slot 3	Time Slot 4
DT	S1: x_1	S2: x_2	S3: x_3	S4: x_4
DF	S1 : x_1 S2 : x_2	S3 : x_3 S4 : x_4	R : $\begin{bmatrix} \hat{x}_{R1} \\ \hat{x}_{R2} \end{bmatrix}$	R : $\begin{bmatrix} \hat{x}_{R3} \\ \hat{x}_{R4} \end{bmatrix}$
DNC	S1 : x_1 S2 : x_2	S3 : x_3 S4 : x_4	R : $\begin{bmatrix} \hat{x}_{R1} \oplus \hat{x}_{R2} \\ \hat{x}_{R1} \oplus \hat{x}_{R2} \end{bmatrix}$	R : $\begin{bmatrix} \hat{x}_{R3} \oplus \hat{x}_{R4} \\ \hat{x}_{R3} \oplus \hat{x}_{R4} \end{bmatrix}$
DNC-Alamouti	S1 : x_1 S2 : x_2	S3 : x_3 S4 : x_4	R : $\begin{bmatrix} \hat{x}_{R1} \oplus \hat{x}_{R2} \\ \hat{x}_{R3} \oplus \hat{x}_{R4} \end{bmatrix}$	R : $\begin{bmatrix} -(\hat{x}_{R3} \oplus \hat{x}_{R4})^* \\ (\hat{x}_{R1} \oplus \hat{x}_{R2})^* \end{bmatrix}$
ANC	S1 : x_1 S2 : x_2	S3 : x_3 S4 : x_4	R : $\begin{bmatrix} t_1 \\ t_2 \end{bmatrix}$	R : $\begin{bmatrix} t_3 \\ t_4 \end{bmatrix}$

Table 5.5: Different Schemes for System Model D

which can be decoded as

$$\hat{\mathbf{x}} = \arg \min_{\mathbf{x} \in \Omega_{\mathbf{x}}} \|\mathbf{y}_D - \mathbf{A}_{ANC}\mathbf{x}\|^2. \quad (5.108)$$

The comparison of those five discussed schemes are shown in Table 5.5.

5.4.2 Experimental Studies

We present numerical results to evaluate the performance of different schemes for the system model C. Let $E_x = E_R$, i.e., the transmission power constraint at sources and relay are equivalent. First, we setup that the channels have equal channel gain, i.e., $\sigma_f^2 = \sigma_h^2 = \sigma_g^2 = 1$. With the average of 100000 randomly generated channel realizations, we show in Fig. 4 the error rate of the transmission signal vector \mathbf{x} defined in (5.73) for five possible schemes. All schemes are under four time slots constraint. We can observe that direct transmission (DT) gives poor performance since relay helps in other schemes. Also, simply decode-and-forward (DF) gives the best performance and superior to digital network coding (DNC), DNC with Alamouti space time coding and analog

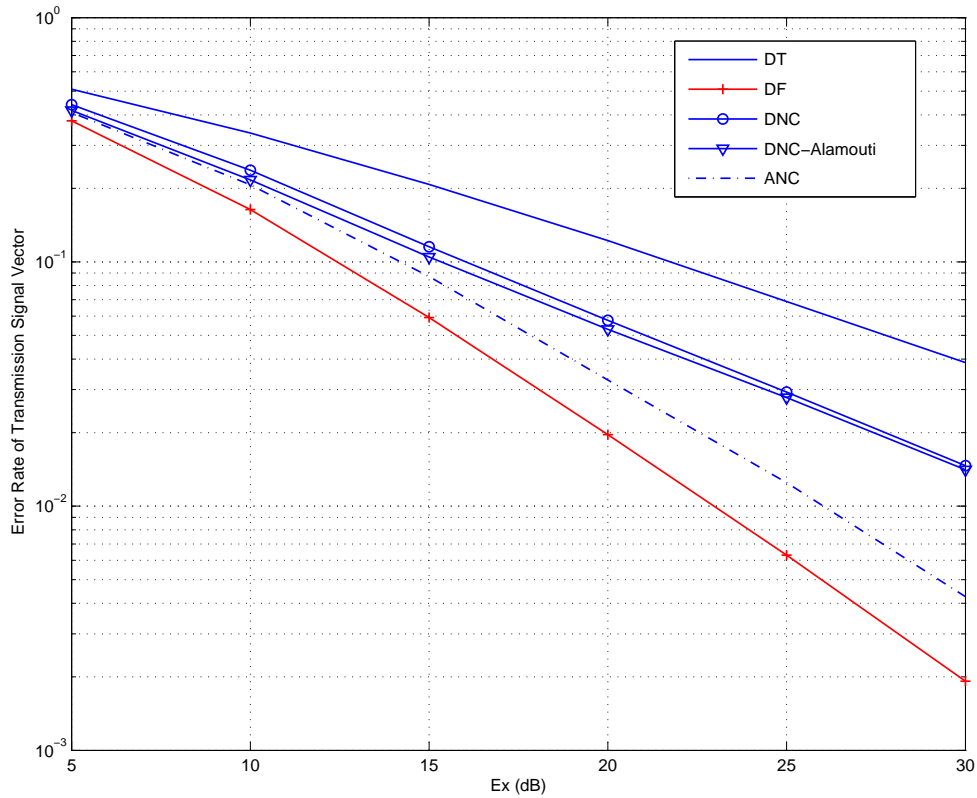


Fig. 5.11: Comparison of five schemes regarding system model D, $\sigma_f^2 = \sigma_h^2 = \sigma_g^2 = 1$

network coding (ANC). A rough explanation about this may be that in the DF case, each relay antenna has a clean decoded signal to transmit, while in schemes with network coding each relay antenna is transmitting a mixed decoded signals, which degrades the performance.

Then, we investigate the performance of all possible schemes with some extreme channel gain setup. For example, if the direct links from sources to destination have the worst channel with $\sigma_f^2 = 0.1$, $\sigma_h^2 = \sigma_g^2 = 1$, we show the error rate of the transmission signal vector comparisons in Fig. 5. We can see that DF still gives best performance, while DT, DNC and DNC-Alamouti schemes suffers more since they rely on the information transmitted on the direct links more.

Another extreme channel gain setup is that the links between the sources and the relay have the worst conditions amongst all, i.e., $\sigma_h^2 = 0.1$, $\sigma_f^2 = \sigma_g^2 = 1$. In this case, the

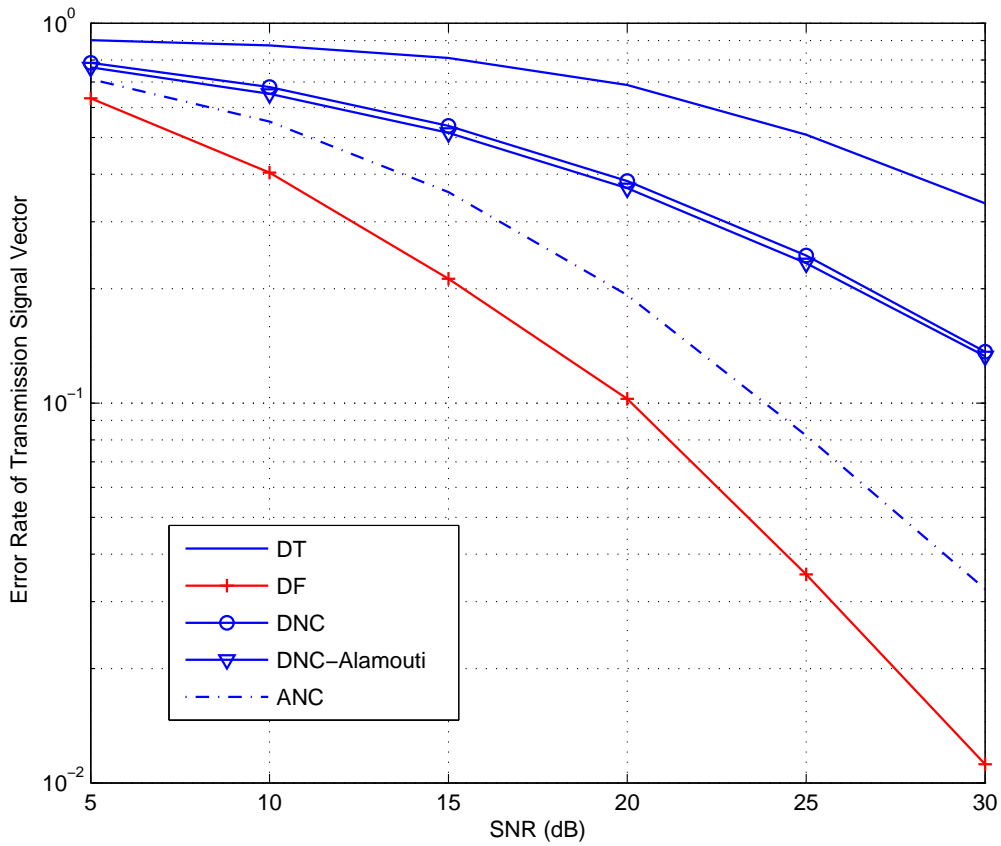


Fig. 5.12: Comparison of five schemes regarding system model D: $\sigma_f^2 = 0.1$, $\sigma_h^2 = \sigma_g^2 = 1$,

relay cannot help much since it cannot get enough accurate information. Hence, from the simulation result in Fig. 6, we can see that DT gives the best performance.

5.5 Conclusions

In this chapter, we consider four wireless cooperative system models: system model A as two sources multiple access relay channel without direct links; system model B as two sources multiple access relay channel with direct links; system model C as three sources multiple access relay channel with direct links; system model D as four sources multiple access relay channel with direct links. The relays are equipped with multiple antennas for all models. For each system model, we consider different possible relay transmission

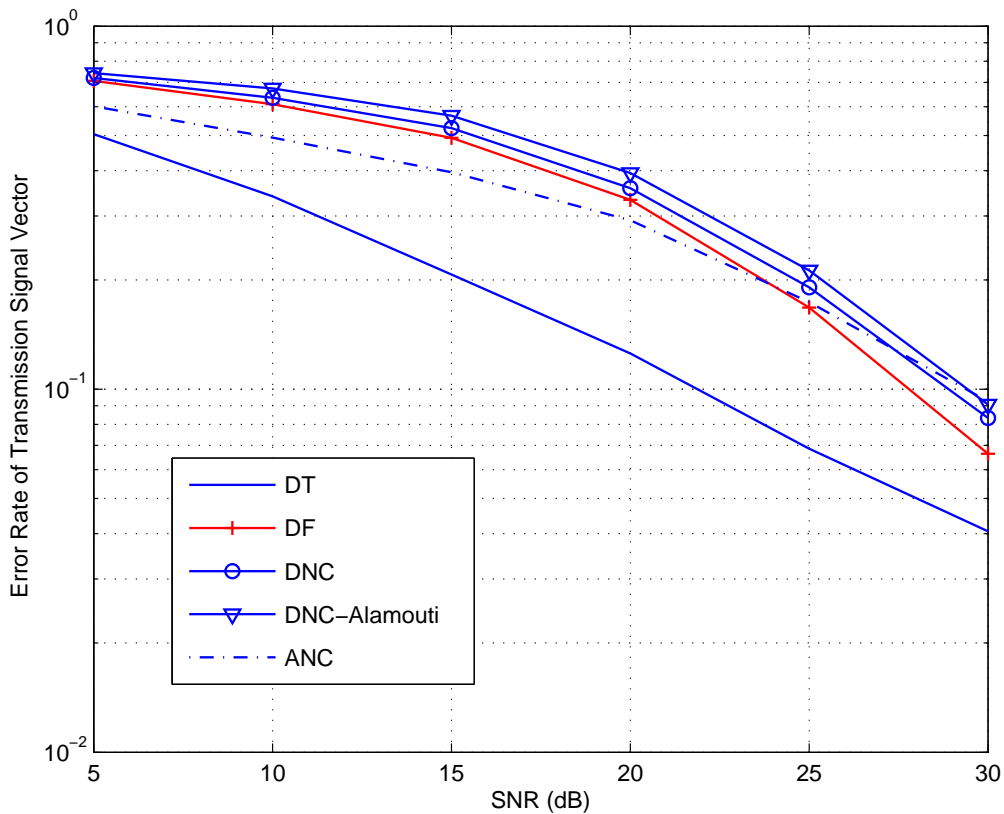


Fig. 5.13: Comparison of five schemes regarding system model D: $\sigma_h^2 = 0.1$, $\sigma_f^2 = \sigma_g^2 = 1$

schemes, including possibly combining network coding and space-time coding techniques.

We find that under three time slots constraint, space-time decode-and-forward (STD-F) gives superior performance than decode-and-forward (DF), analog network coding (ANC) and space-time analog network coding (STANC) schemes for system model A; while under two time slots constraint, the simply decode-and-forward (DF) scheme outperforms the direct transmission, physical layer network coding (PLNC) and analog network coding (ANC) schemes for system model B.

Regarding system model C, with three time constraints, traditional relay transmission schemes are not directly applicable. We discuss DT, ANC and STANC-Alamouti schemes. Simulation studies show that STANC with alamouti scheme outperform other schemes regarding sum rate and bit error rate performance at the destination.

Regarding system model D, we investigate several schemes for the system model under

four time slots transmission constraint, describe in details those different schemes and compare the error rate performance. Interestingly, simulation studies show that those schemes with network coding have not better performance than the traditional schemes, which indicates that network coding is not favorable for the system model if traditional schemes can also be implemented with the same time slots constraint.

Bibliography

- [1] **L. Wei** and W. Chen, “Compute-and-forward network coding design over multi-source multi-relay channels”, *IEEE Trans. Wireless Communications*, vol. 11, no. 9, pp. 3348-3357, Sept. 2012.
- [2] **L. Wei** and W. Chen, “Efficient compute-and-forward network codes search for two-way relay channel”, *IEEE Commun. Letters*, vol. 16, no. 8, pp. 1204-1207, Aug. 2012.
- [3] **L. Wei** and W. Chen, “Optimal binary/quaternary adaptive signature design for code-division multiplexing”, *IEEE Trans. Wireless Communications*, accepted, 2012.
- [4] **L. Wei** and D. A. Pados, “Optimal orthogonal carriers and sum-SINR/sum-capacity of the multiple-access vector channel”, *IEEE Trans. Communications*, vol. 60, no. 5, pp. 1188-1192, May 2012.
- [5] **L. Wei** and W. Chen, “Optimal upward scaling of minimum-TSC binary signature sets”, *IEEE Commun. Letters*, vol. 16, no. 2, pp. 168-171, Feb. 2012.
- [6] **L. Wei**, S. N. Batalama, D. A. Pados and B. W. Suter, “Adaptive binary signature design for code division multiplexing”, *IEEE Trans. Wireless Communications*, vol. 7, no. 7, pp. 2798-2804, July 2008.
- [7] **L. Wei**, S. N. Batalama, D. A. Pados, and B. W. Suter, “Upward scaling of minimum-TSC binary signature sets”, *IEEE Commun. Letters*, vol. 11, no. 11, pp. 889-891, Nov. 2007.

- [8] Y. Yu, W. Chen and **L. Wei**, “Design of convergence-optimized non-binary LDPC codes over binary erasure channel”, *IEEE Wireless Commun. Letters*, vol. 1, no. 4, pp. 336-339, Aug. 2012.
- [9] Y. Wei, Y. Yang, **L. Wei** and W. Chen, “Comments on A new parity-check stopping criterion for turbo decoding”, *IEEE Commun. Letters*, vol. 16, no. 10, pp. 1664-1667, Oct. 2012.
- [10] Y. Wei, Y. Yang, M. Jiang, W. Chen and **L. Wei**, “Joint shortening and puncturing optimization for structured LDPC codes”, *IEEE Commun. Letters*, vol. 16, no. 12, Dec. 2012.
- [11] **L. Wei** and W. Chen, “Integer-forcing linear receiver design with slowest descent method”, *IEEE Trans. Wireless Communications*, major revision.
- [12] K. Xie, W. Chen and **L. Wei**, “Increasing security degree of freedom in multi-user and multi-eve systems”, *IEEE Trans. Info. Forensics and Security*, accepted, 2012.
- [13] **L. Wei** and W. Chen, “Space-time analog network coding for multiple access relay channels”, *IEEE Wireless Commun. and Networking Conf. (WCNC)*, accepted, Shanghai, China, April 2013.
- [14] **L. Wei** and W. Chen, “A study on network coding in multiple access relay channels with multiple antenna relay”, submitted to *IEEE International Conf. on Commun. (ICC)*, Budapes, Hungary, June 2013.
- [15] **L. Wei** and W. Chen, “Optimal binary/quaternary adaptive signature design for code-division multiplexing”, in *Proc. IEEE GLOBECOM*, Anaheim, CA, Dec. 2012.
- [16] **L. Wei** and W. Chen, “Integer-forcing linear receiver design over MIMO channels”, in *Proc. IEEE GLOBECOM*, Anaheim, CA, Dec. 2012.
- [17] **L. Wei** and W. Chen, “Network coding in wireless cooperative networks with multiple antenna relays”, in *Proc. IEEE International Conference on Wireless Communications and Signal Processing (WCSP)*, Yellow Mountain City, China, Oct. 2012.

- [18] **L. Wei**, W. Chen and Y. Wei, “Linear transceiver and receiver design methods for multiuser MIMO channels”, in *Proc. IEEE International Conference on Wireless Communications and Signal Processing (WCSP)*, Yellow Mountain City, China, Oct. 2012.
- [19] **L. Wei**, D. A. Pados, S. N. Batalama, and M. J. Medley, “Sum-SINR/Sum-capacity optimal multisignature spread-spectrum steganography”, in *Proc. SPIE Defense and Security*, Orlando, FL, Mar. 2008.
- [20] **L. Wei**, S. N. Batalama, D. A. Pados, and B. W. Suter, “Cooperative transmission over code division multiplexing channels”, in *Proc. IEEE MILCOM*, Orlando, FL, Oct. 2007.
- [21] **L. Wei**, S. N. Batalama, D. A. Pados, and B. W. Suter, “Code division controlled-MAC in wireless sensor networks by adaptive binary signature design”, in *Proc. SPIE Defense and Security*, Orlando, FL, April, 2007.
- [22] **L. Wei**, S. N. Batlama, D. A. Pados, and B. W. Suter, “SINR-optimized binary search”, in *Proc. IEEE GLOBECOM*, San Francisco, CA, Nov. 2006.
- [23] **L. Wei**, S. N. Batalama, D. A. Pados, and B. W. Suter, “Adaptive binary signature design for code division multiplexing”, in *Proc. IEEE MILCOM*, Washington, D. C., Oct. 2006.
- [24] R. Ahlswede, N. Cai, S. R. Li and R. W. Yeung, “Network information flow”, *IEEE Trans. Info. Theory*, vol. 46, no. 4, pp. 1204-1216, July 2000.
- [25] S. R. Li, R. Ahlswede and N. Cai, “Linear network coding”, *IEEE Trans. Info. Theory*, vol. 49, no. 2, pp. 371-381, Feb. 2003.
- [26] R. Koetter and M. Medard, “An algebraic approach to network coding”, *IEEE/ACM Trans. Networking*, vol. 11, no. 5, pp.782-795, Oct. 2003.
- [27] S. Jaggi, P. Sanders, P. A. Chou, M. Effros, S. Egner, K Jain and L. Tolhuizen, “Polynomial time algorithms for multicast network code construction”, *IEEE Trans. Info. Theory*, vol. 51, no.6, June. 2005.

- [28] T. Ho, R. Koetter, M. Medard, D. R. Karger, M. Effros, J. Shi and B. Leong, “A random linear network coding approach to multicast”, *IEEE Trans. Info. Theory*, vol. 52, no. 10, pp. 4413-4430, Oct. 2006.
- [29] S. Zhang, S. Liew and P. P. Lam, “Physical-layer network coding”, in *Proc. IEEE MobiComm*, pp. 358-365, Los Angeles, USA, Sept. 2006.
- [30] T. Wang and G. B. Giannakis, “Complex field network coding for multiuser cooperative communications”, *IEEE J. Sel. Areas Commun.*, vol. 26, no. 2, pp. 561-571, Apr. 2008.
- [31] S. Katti, S. Gollakota, and D. Katabi, “Embracing wireless interference: Analog network coding”, in *Proc. ACM SIGCOMM*, Kyoto, Japan, pp. 397-408, Aug. 2007.
- [32] S. Katti, H. Rahul, W. Hu, D. Katabi, M. Medard and J. Crowcroft, “XORs in the air: Practical wireless network coding”, in *Proc. ACM SIGCOMM*, Pisa, Italy, pp. 243-254, Sept. 2006.
- [33] P. A. Chou, Y. Wu and K. Jain, “Practical network coding”, *Allerton Conf. Commun. Control, Computing*, Oct. 2003.
- [34] Y. Wu, P. A. Chou and S. Kung, “Information exchange in wireless networks with network coding and physical-layer broadcast”, Microsoft Research, Redmond, WA, Tech. Rep. MSR-TR-2004-78, Aug. 2004.
- [35] C. Fragouli, D. Katabi, A. Markopoulou, M. Medard and H. Rahul, “Wireless network coding: Opportunities & Challenges”, in *Proc. IEEE MILCOM*, Orlando, FL, Oct. 2007.
- [36] R. Zamir, “Lattices are everywhere”, in *Proceedings of the 4th Annual Workshop on Info. Theory and its Applications*, La Jolla, CA, Feb. 2009.
- [37] F. Oggier and E. Viterbo, “Algebraic number theory and code design for rayleigh fading channels”, in *Foundations and Trends in Commun. and Info. Theory*, vol. 1, pp. 333-415, 2004.

- [38] R. Zamir, S. Shamai, and U. Erez, “Nested linear/lattice codes for structured multiterminal binning”, *IEEE Trans. Info. Theory*, vol. 48, no. 6, pp. 1250-1276, June 2002.
- [39] U. Erez and R. Zamir, “Achieving $(1/2)\log(1+\text{SNR})$ on the AWGN channel with lattice encoding and decoding”, *IEEE Trans. Info. Theory*, vol. 50, no. 10, pp. 2293-2314, Oct. 2004.
- [40] H. E. Gamal, G. Caire and M. O. Damen, “Lattice coding and decoding achieve the optimal diversity-multiplexing tradeoff of MIMO channels”, *IEEE Trans. Info. Theory*, vol. 50, pp. 968-985, June 2004.
- [41] U. Fincke and M. Pohst, “Improved methods for calculating vectors of short length in a lattice, including a complexity analysis,” *Math. Comput.*, vol. 44, pp. 463-471, Apr. 1985.
- [42] E. Viterbo and J. Boutros, “A universal lattice code decoder for fading channels,” *IEEE Trans. Info. Theory*, vol. 45, no. 5, pp. 1635-1642, July 1999.
- [43] O. Damen, A. Chkeif, and J. C. Belfiore, “Lattice code decoder for space-time codes,” *IEEE Commun. Letters*, vol. 4, no. 5, pp. 161-163, May 2000.
- [44] M. O. Damen, H. El Gamal and G. Carie, “On maximum-likelihood detection and the search for the closest lattice point,” *IEEE Trans. Info. Theory*, vol. 49, no. 10, pp. 2389-2402, Oct. 2003.
- [45] M. Wilson, K. Narayanan, H. Pfister and A. Sprintson, “Joint physical layer coding and network coding for bidirectional relaying,” *IEEE Trans. Info. Theory*, vol. 56, pp. 5641-5654, Nov. 2010.
- [46] B. Hassibi, A. Sezgin, M. Khajehnejad and A. Avestimehr, “Approximate capacity region of the two-pair bidirectional gaussian relay network,” in *IEEE Inter. Symp. Info. Theory*, pp. 2018-2022, Seoul, Korea, June, 2009.

- [47] I. Baik and S. Y. Chung, "Network coding for two-way relay channels using lattices," in *IEEE Inter. Conf. Commun.*, pp. 3898-3902, Beijing, China, May 2008.
- [48] B. Nazer and M. Gastpar, "Compute-and-forward: harnessing interference through structured codes", *IEEE Trans. Info. Theory*, vol. 57, no. 10, pp. 6463-6486, Oct. 2011.
- [49] B. Nazer and M. Gastpar, "Reliable physical layer network coding", *IEEE Proceedings*, vol. 99, no. 3, pp. 438-460, Mar. 2011.
- [50] A. Osmane and J. C. Belfiore, "The compute-and-forward protocol: implementation and practical aspects", *IEEE Commun. Lett.*, submitted. Available online: <http://arxiv.org/abs/1107.0300>.
- [51] C. Feng, D. Silva, and F. R. Kschischang, "Design criteria for lattice network coding", *IEEE 45th Annual Conf. Info. Sci. & Sys.*, Baltimore, USA, Mar. 2011.
- [52] M. Nokleby and B. Aazhang, "Lattice coding over the relay channel", *IEEE Inter. Conf. Commun.*, Kyoto, Japan, June 2011.
- [53] C. Feng, D. Silva and F. R. Kschischang, "An algebraic approach to physical-layer network coding", *IEEE Inter. Symp. Info. Theory*, Austin, TX, USA, June. 2010.
- [54] J. C. Belfiore and M. A. V. Castro, "Managing interference through space-time codes, lattice reduction and network coding", in *proc. IEEE Info. Theory Workshop*, Dublin, Ireland, Aug. 2010.
- [55] J. Zhan, U. Erez, M. Gastpar and B. Nazer, "MIMO compute-and-forward," in *IEEE Inter. Symp. Info. Theory*, pp. 2848-2852, Seoul, Korea, June 2009.
- [56] D. Tse and P. Viswanath, *Fundamentals of wireless communications*. New York, NY, USA: Cambridge University Press, 2005.
- [57] K. J. R. Liu, A. K. Sadek, W. Su and A. Kwasinski, *Cooperative Communications and Networking*. Cambridge Univ. Press, 2009.

- [58] J. Zhan, B. Nazer, U. Erez and M. Gastpar, “Integer-forcing linear receivers”, in *IEEE Inter. Symp. Info. Theory*, pp. 1022-1026, Austin, Texas, June 2010.
- [59] J. Zhan, B. Nazer, U. Erez and M. Gastpar, “Integer-forcing linear receivers: a new low-complexity MIMO architecture”, in *IEEE Veh. Tech. Conf.*, Ottawa, Canada, Sept. 2010.
- [60] P. Spasojevic and C. N. Georghiades, “The slowest descent method and its application to sequence estimation”, *IEEE Trans. Commun.*, vol. 49, no. 9, pp. 1592-1604, Sept. 2001.
- [61] F. Simoens, D. V. Welden, H. Wymeersch and M. Moeneclaey, “Low complexity MIMO detection based on the slowest descent method”, *IEEE Commun. Lett.*, vol. 11, no. 5, pp. 429-431, May 2007.
- [62] Y. S. Cho, J. Kim, W. Y. Yang and C. G. Kang, “MIMO-OFDM wireless communications with matlab”, John Wiley & Sons Pte Ltd, ISBN: 978-0-470-82561-7, 2010.
- [63] K. R. Kumar, G. Caire, and A. L. Moustakas, “Asymptotic performance of linear receivers in MIMO fading channels”, *IEEE Trans. Info. Theory*, vol. 55, no. 10, pp. 4398-4418, Oct. 2009.
- [64] S. A. Hejazi and B. Liang, “Throughput analysis of multiple access relay channel under collision model”, in *Proc. IEEE INFOCOM*, San Diego, CA, Mar. 2010.
- [65] S. Yao nad M. Skoglund, “Analog network coding mappings in gaussian multiple-access relay channel”, *IEEE Trans. Commun.*, vol. 58, no. 7, pp. 1973-1983, July 2010.
- [66] M. E. Soussi, A. Zaidi and L. Vanderdorpe, “Iterative sum-rate optimization for multiple access relay channels with a compute-and-forward relay”, in *Proc. IEEE ICC*, Ottawa, Canada, June 2012.

- [67] M. E. Soussi, A. Zaidi and L. Vanderdorpe, “Resource allocation for multiple access relay channel with a compute-and-forward relay”, in *Proc. IEEE International Symp. Wireless Commun. Systems*, Aachen, Germany, Nov. 2011.
- [68] S. M. Alamouti, “A simple transmit diversity technique for wireless communications,” *IEEE J. Sel. Areas Commun.*, vol. 16, no. 8, Oct. 1998.
- [69] C. Yuen, W. H. Chin, Y. L. Guan, W. Chen and T. Tee, “Bi-directional multi-antenna relay communications with wireless network coding”, in *proc. IEEE 67th Veh. Tech. Conf.*, Singapore, May 2008.
- [70] D. Xu, Z. Bai, A. Waadt, G. H. Bruck and P. Jung, “Combining MIMO with network coding”, in *proc. IEEE ICC*, Cape Town, South Africa, May, 2010.
- [71] A. Amah and A. Klein, “Non-regenerative multi-way relaying: space-time analog network coding and repetition”, *IEEE Commun. Lett.*, vol. 15, no. 12, Dec. 2011.

Publications During Postdoc in SJTU

Journal Papers

1. **L. Wei** and W. Chen, “Optimal binary/quaternary adaptive signature design for code-division multiplexing”, *IEEE Trans. Wireless Communications*, accepted, 2012.
2. **L. Wei** and W. Chen, “Compute-and-forward network coding design over multi-source multi-relay channels”, *IEEE Trans. Wireless Communications*, vol. 11, no. 9, pp. 3348-3357, Sept. 2012.
3. **L. Wei** and W. Chen, “Efficient compute-and-forward network codes search for two-way relay channel”, *IEEE Commun. Letters*, vol. 16, no. 8, pp. 1204-1207, Aug. 2012.
4. **L. Wei** and D. A. Pados, “Optimal orthogonal carriers and sum-SINR/sum-capacity of the multiple-access vector channel”, *IEEE Trans. Communications*, vol. 60, no. 5, pp. 1188-1192, May 2012.
5. **L. Wei** and W. Chen, “Optimal upward scaling of minimum-TSC binary signature sets”, *IEEE Commun. Letters*, vol. 16, no. 2, pp. 168-171, Feb. 2012.
6. K. Xie, W. Chen and **L. Wei**, “Increasing security degree of freedom in multi-user and multi-eve systems”, *IEEE Trans. Info. Forensics and Security*, accepted, 2012.
7. Y. Yu, W. Chen and **L. Wei**, “Design of convergence-optimized non-binary LDPC codes over binary erasure channel”, *IEEE Wireless Commun. Letters*, vol. 1, no. 4, pp. 336-339, Aug. 2012.
8. Y. Wei, Y. Yang, **L. Wei** and W. Chen, “Comments on A new parity-check stopping criterion for turbo decoding”, *IEEE Commun. Letters*, vol. 16, no. 10, pp. 1664-1667, Oct. 2012.

9. Y. Wei, Y. Yang, M. Jiang, W. Chen and **L. Wei**, “Joint shortening and puncturing optimization for structured LDPC codes”, *IEEE Commun. Letters*, vol. 16, no. 12, Dec. 2012.
10. **L. Wei** and W. Chen, “Integer-forcing linear receiver design with slowest descent method”, *IEEE Trans. Wireless Communications*, major revision.

Conference Papers

11. **L. Wei** and W. Chen, “A study on network coding in multiple access relay channels with multiple antenna relay”, submitted to *IEEE International Conf. on Commun. (ICC)*, Budapes, Hungary, June 2013.
12. **L. Wei** and W. Chen, “Space-time analog network coding for multiple access relay channels”, *IEEE Wireless Commun. and Networking Conf. (WCNC)*, accepted, Shanghai, China, April 2013.
13. **L. Wei** and W. Chen, “Optimal binary/quaternary adaptive signature design for code-division multiplexing”, in *Proc. IEEE GLOBECOM*, Anaheim, CA, Dec. 2012.
14. **L. Wei** and W. Chen, “Integer-forcing linear receiver design over MIMO channels”, in *Proc. IEEE GLOBECOM*, Anaheim, CA, Dec. 2012.
15. **L. Wei** and W. Chen, “Network coding in wireless cooperative networks with multiple antenna relays”, in *Proc. IEEE International Conference on Wireless Communications and Signal Processing (WCSP)*, Yellow Mountain City, China, Oct. 2012.
16. **L. Wei**, W. Chen and Y. Wei, “Linear transceiver and receiver design methods for multiuser MIMO channels”, in *Proc. IEEE International Conference on Wireless Communications and Signal Processing (WCSP)*, Yellow Mountain City, China, Oct. 2012.

Research Projects and Patents Information

参与科研项目

- 1 项目名称 : 无线协作通信中的网络编码技术研究

项目描述 : 中国博士后科学基金第51批面上资助

起止时间 : 2011年3月-2013年2月

经费 : 5 万

主持或参加 : 主持
- 2 项目名称 : 无线协作通信中的网络编码技术研究

项目描述 : 华为重点高校重点教授合作框架

起止时间 : 2011年3月-2012年12月

经费 : 150万

主持或参加 : 主要参加人
- 3 项目名称 : 高移动性宽带无线通信网络重点理论基础研究

项目描述 : 国家973项目

起止时间 : 2012年1月-2013年2月

经费 : 462万

主持或参加 : 参加人

专利信息

1. 魏莉莉, 陈文, 魏越军, 金莹, “一种计算转发网络编码的方法和装置”, 中国发明专利, CN 201210030171.X, Feb. 10, 2012.
2. 陈文, 魏莉莉, 魏越军, 金莹, “一种双向中继传输中采用计算转发的网络编码方法”, 中国发明专利, CN 201210188787.X, June 8, 2012.